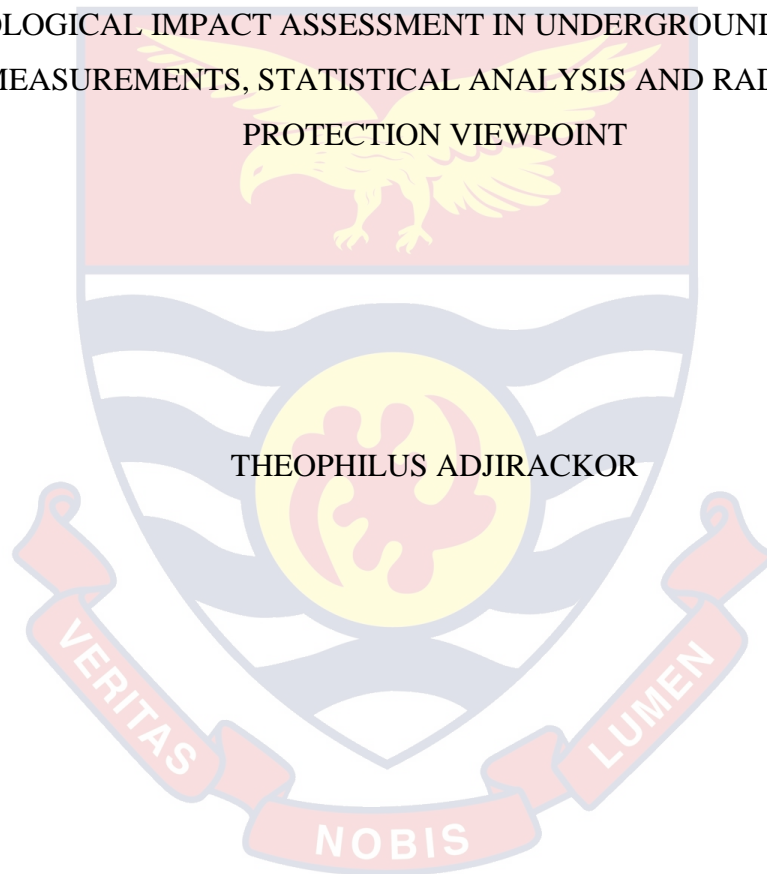
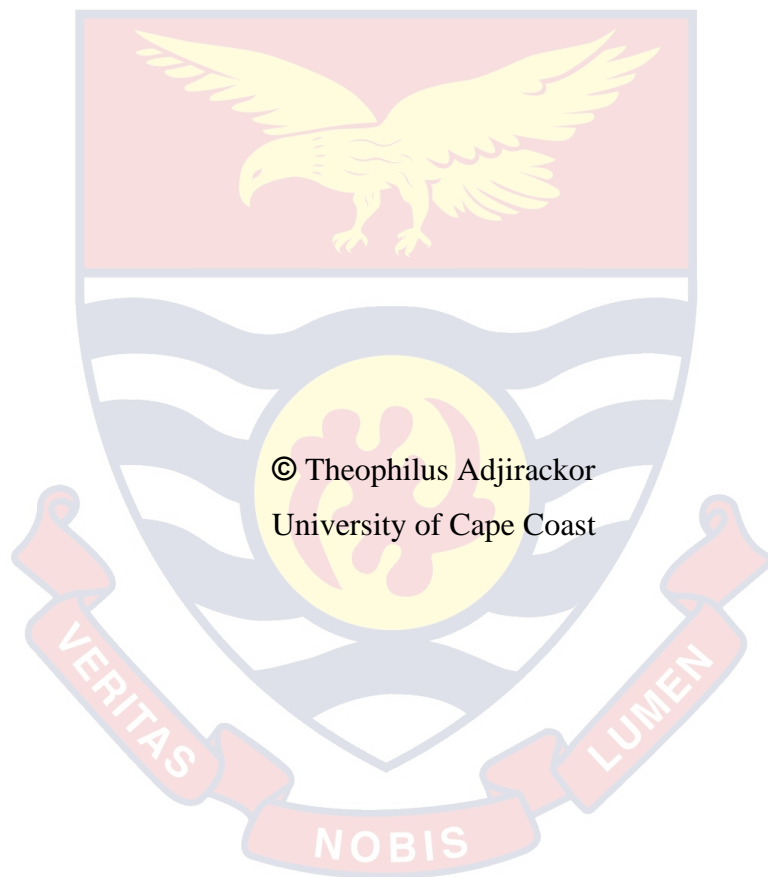


UNIVERSITY OF CAPE COAST

RADIOLOGICAL IMPACT ASSESSMENT IN UNDERGROUND GOLDMINE:
MEASUREMENTS, STATISTICAL ANALYSIS AND RADIATION
PROTECTION VIEWPOINT

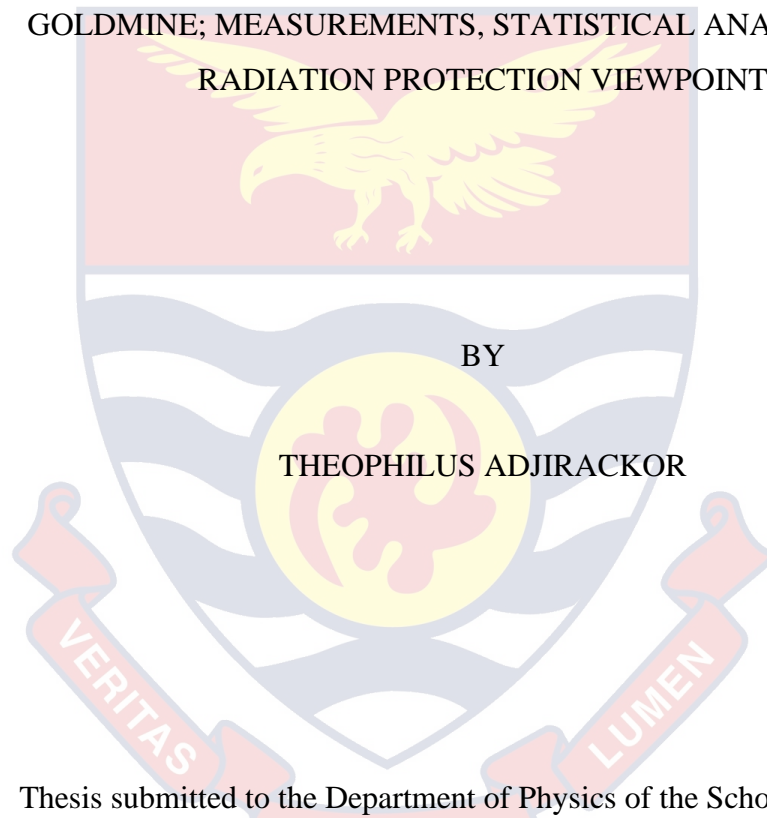


2020



UNIVERSITY OF CAPE COAST

RADIOLOGICAL IMPACT ASSESSMENT IN UNDERGROUND
GOLDMINE; MEASUREMENTS, STATISTICAL ANALYSIS AND
RADIATION PROTECTION VIEWPOINT



BY

THEOPHILUS ADJIRACKOR

Thesis submitted to the Department of Physics of the School of Physical Sciences, College of Agriculture and Natural Sciences, University of Cape Coast, in partial fulfilment of the requirements for the award of Doctor of Philosophy degree in Physics

OCTOBER, 2020

DECLARATION

Candidate's Declaration

I hereby declare that this thesis is the result of my own original research and that no part of it has been presented for another degree in this University or elsewhere.

.....

Date:

Theophilus Adjirackor
(Candidate)

Supervisors' Declaration

We hereby declare that the preparation and presentation of the thesis were supervised in accordance with the guidelines on supervision of thesis laid down by the University of Cape Coast.

.....

Date:

Prof. Emmanuel Ofori Darko
(Principal Supervisor)

.....

Date:

Dr. Frederick Sam
(Co-Supervisor)

ABSTRACT

Measurements of indoor radon concentrations, environmental factors, soil and rock samples were collected monthly over a period of one year in 10 different levels in an underground goldmine to determine the radiological impact on workers. The detectors were installed in batches within four quarters. The measurements were carried out using LR115 solid state nuclear track detectors. Statistical models were applied in the prediction and analysis of the radon concentration at various depths. The results show that the activity concentration of radon in the underground mine ranges from a minimum of 2 Bqm⁻³ to a maximum of 284 Bqm⁻³ with a mean value of 58.51 Bqm⁻³. The highest radon concentration was observed in the second quarter when the season was warm and the lowest radon concentration was observed in the first quarter when the season was colder. The exposure rate, annual effective dose and excess lung cancer risk were below the acceptable limit. A positive relationship was observed between dry bulb temperature, relative humidity and radon concentration while a negative relationship was observed between barometric pressure, air quantity, wet bulb temperature, wet kata temperature and radon concentration. Statistical analysis of the results indicate that all the relationships were insignificant. Principal component analysis deduced three main factors that influences the indoor radon concentration of which wet bulb temperature was statistically significant. The hazard indices, exposure rate, excess lung cancer risk and annual effective dose from the rock and soil samples possess no radiological hazard if used for building materials. Even though radon concentration increases with increased depth, the assumption of the time series model confirmed a reduced radon concentration with adequate ventilation.

KEYWORDS

Correlation

Environmental Factors

Naturally Occurring Radioactive Materials

Radon

Regression

Underground Mine



ACKNOWLEDGEMENT

I would like to thank the Newmont Ghana Gold Company Limited for giving me an opportunity to assess the Subika underground gold mine. My sincere thanks also go to the Physics Department, UCC for their guidance, support and the opportunity given to me to undertake my studies. My unalloyed appreciation goes to my two supervisors Prof. Emmanuel Ofori Darko and Dr. Frederick Sam for their intellectual support and contribution to a successful completion of this study.



DEDICATION

To my late father Mr. Joseph Adjirackor.



TABLE OF CONTENTS

DECLARATION	II
ABSTRACT	III
KEYWORDS	IV
ACKNOWLEDGEMENT	V
DEDICATION	VI
TABLE OF CONTENTS	VII
LIST OF TABLES	XII
LIST OF FIGURES	XV
LIST OF ACRONYMS	XVII
LIST OF ABBREVIATIONS	XVIII
CHAPTER ONE: INTRODUCTION	
Background to the Study	1
Statement of the Problem	4
Objective of the Study	7
General Objective	7
Specific Objectives	7
Research Questions	7
Significance of the Study	8
Scope and Limitation of the Study	9
Organization of the Study	10
Chapter Summary	10
CHAPTER TWO: LITERATURE REVIEW	
Theoretical Framework	12
Definition of Radon	12

Physical and Chemical Properties of Radon	13
An Introduction to Radon Decay and Ionizing Radiation	13
Radon Decay	14
Alpha Decay	15
Beta Decay	16
Gamma Decay	16
Radon Decay Constant and Half Life	17
Behaviour of Decay Products	20
Behaviour of Unattached Radon Progeny	22
Behaviour of Attached Radon Daughters	23
Health Effects of Radon Exposure	23
Sources of Natural Radiation.	25
Natural Radiation Sources	26
Man-Made Radiation Sources	27
Biological Effects of Radiation	28
Radiation Dosimetry	29
Basic Radiation Quantity and Unit Exposure	29
Absorbed Dose	29
Equivalent and Effective Dose	31
Radiation Protection and Dose Limit	33
Radon Risk Assessment	37
Radon Measurement Methods	38
Passive Techniques	38
Active Techniques	39
Solid State Nuclear Track Detection (SSNTD) and their Applications (Passive Technique)	39
Etching Mechanisms and Track Revelation	40
Chemical Etching	42

Track Counting and Evaluation	43
Scanner Image Acquisition	44
Detection of Gamma Radiation	45
Interaction of Gamma Radiation with Matter	45
Compton Scattering	46
Pair Production	47
Empirical Framework	47
Radon in Mines	48
Chapter Summary	52
CHAPTER THREE: METHODOLOGY	
Introduction	54
Description of Study Area	54
Location, Geology and Sampling Points of the Underground Mine	54
Geographical Positions of Sampling Areas.	56
Deployment of Detectors at the Sampling Points	61
Track Revelation	62
Image Acquisition and Counting of Tracks	63
Determination of the Annual Effective Dose and Lung Cancer Risk	64
Radiation Dose Estimation	64
Soil and Rock Samples	65
Sample Preparation	66
Soil and Rock	66
Calibration of Gamma Spectrometry System	68
Energy Calibration	69
Efficiency Calibration	70
Minimum Detectable Activity	72
Radiological Impact Assessment of Soil and Rock Samples	72
Estimation of Hazard Indices	72

Exposure Rate and Annual Effective Dose Equivalent at 1m from a Radioactive Source	75
Exposure Rate (<i>ER</i>)	75
Dose rate (<i>DR</i>) and its Relation with Exposure (<i>ER</i>)	75
Estimation of Annual Dose Rate	75
Excess Lifetime Cancer Risk (<i>ELCR</i>)	77
Effect of Environmental Factors on Radon Concentration in the Underground Goldmine	77
Hypothesis	78
Statistical Modelling	78
Assumptions for the Model	79
Chapter Summary	80
CHAPTER FOUR: RESULTS AND DISCUSSION	
Radon Concentration in the Underground Goldmine	82
Radiological Impact Assessment of Indoor Radon	89
Regression Analysis	97
Time Series Model	111
Activity Concentration of Radionuclides in Rock and Soil Samples	120
Chapter Summary	130
CHAPTER FIVE: SUMMARY, CONCLUSIONS AND RECOMMENDATIONS	
Overview	131
Summary	131
Conclusions	132
Recommendations	135
REFERENCES	137
APPENDICES	152

APPENDIX A: RADON CONCENTRATIONS OF FIRST TO FOURTH QUARTER	152
APPENDIX B: EFFECT OF ENVIRONMENTAL FACTORS ON RADON CONCENTRATION	156
APPENDIX C: ACTIVITY CONCENTRATION FOR ROCK AND SOIL SAMPLES	158



LIST OF TABLES

Table	Page
1 Uranium Series	19
2 Thorium Series	19
3 Radiation Weighting Factors for Different Ionizing Radiations	31
4 Tissue Weighting Factors	32
5 ICRP 60 Recommended Effective Dose Limits	36
6 Radon Concentrations at Locations for First Quarter	82
7 Radon Concentrations at Locations for Second Quarter	83
8 Radon Concentrations at Locations for Third Quarter	85
9 Radon Concentrations at Locations for Fourth Quarter	86
10 ICRP 115 and Task Group Reference Levels	89
11 Annual Radon Concentration ($Bq\ m^{-3}$)	90
12 Comparison of Radon Concentrations to International Standards and Published Work	91
13 Annual Radon Exposure ($WLM\ y^{-1}$), Annual Effective Dose ($mSv\ y^{-1}$) and Excess Lifetime Cancer Risk (%)	92
14 Comparison of Annual Radon daughter Exposure ($WLM\ y^{-1}$) to Protection Standards and Guidance for Occupational Exposure to Radon Progeny	93
15 Comparison of Annual Effective Dose and Excess Life Time Cancer Risk to International Standards and Published.	95
16 Descriptive Statistics of Variables	96
17 Model Summary	97
18 ANOVA ^a	98

19	Coefficients ^a	99
20	Multicollinearity of Independent Variables	102
21	Collinearity Diagnostics of variables	103
22	Cluster Analysis	105
23	Principal Component Analysis	106
24	Weight of Each Component	107
25	Factor Analysis	108
26	PCA Regression Coefficients	109
27	Time Series Moving Averages	112
28	Seasonal Index	114
29	Deseasonalised and Radon Concentration	115
30	Depth from Reference Level	117
31	Deseasonalised Radon Concentration at Various Depth.	117
32	Trend Regression Coefficient	118
33	Trend Model Summary	118
34	Trend ANOVA	119
35	Activity Concentration of Radionuclides at Various Levels	121
36	Comparison of Activity Concentration Ra-226, Th-232 and K-40 in Soil and Rock Samples with Worldwide Average and other Published Work	122
37	Descriptive Statistics of Activity Concentration Distribution in Soil and Rock Samples	123
38	External Hazard Indices of Rock and Soil Samples (H_{EX})	124
39	Internal Hazard Indices of Rock and Soil Samples (H_{IN})	125

40	Radium Equivalent Activity and External Level in Rock and Soil Samples	126
41	Annual Dose Parameters	127
42	Correlation Matrix Between Ra-222, Rn-226, Th-232 and K-40	129



LIST OF FIGURES

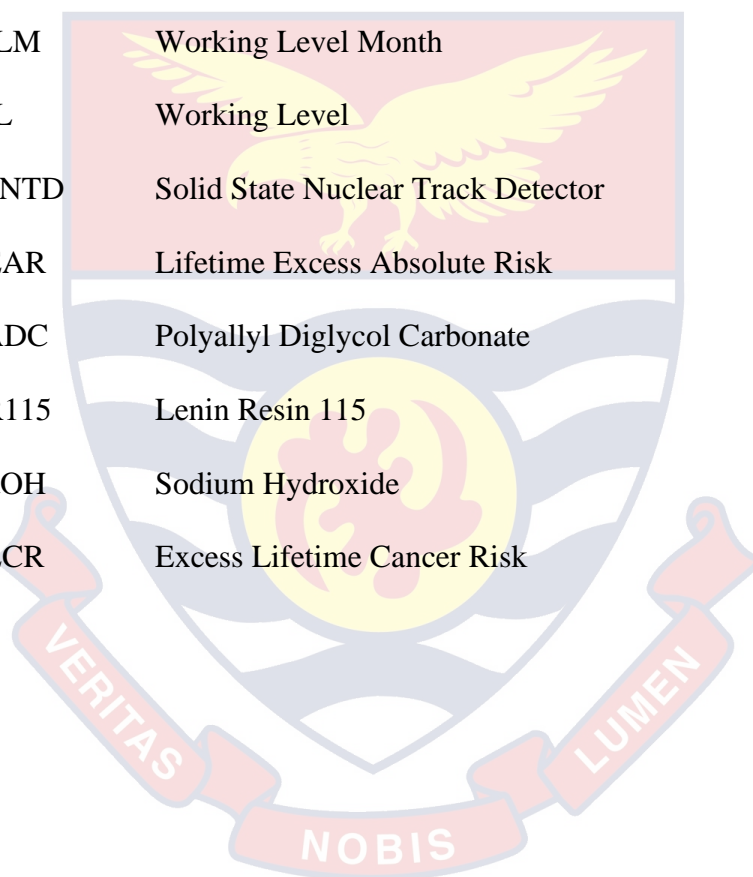
Figure		Page
1	Radon Exposure Pathway	3
2	Average Annual Exposure to Ionizing	25
3	Dose Response Curve	34
4	Track Revelation	41
5	Simple Schematic Diagram of Thin and Thick Detector.	42
6	Theory of Etching	43
7	LR-115 Detector Images Obtained from Scanner	45
8	Interaction Mechanisms of X and Gamma-Rays with Matter as a Function of Photon Energy and Atomic Number	46
9	Compton Scattered Gamma Photon	46
10	Pair Production Process	47
11	Sampling Area 1 (S1): Level 800 EMP	56
12	Sampling Area 2 (S2): Level 810 YOD	56
13	Sampling Area 3 (S3): Level 840 YOD	57
14	Sampling Area 4 (S4): Level 880 YOD	57
15	Sampling Area 5 (S5): Level 790 EXPL	58
16	Sampling Area 6 (S6): Level 820 SKY ACCN	58
17	Sampling Area 7 (S7): Level 960 YOD	59
18	Sampling Area 8 (S8): Level 1000 SKY DEC	59
19	Sampling Area 9 (S9): Level 920 YOD	60
20	Sampling Area 10 (S10): Level 1000 YOD	60
21	Installation of Radon Detectors	62
22	Air Dried Detectors	63

23	Detectors Scanner Coupled to a Laptop	64
24	Energy Calibration Curve for 1000 ml Marinelli Geometry	69
25	Efficiency Calibration Curve for 1L Marinelli Beaker Geometry	71
26	Principal Component Analysis Scree Plot	106
27	A Graph of Radon Concentration and Deseasonalised Radon	116



LIST OF ACRONYMS

OECD	Organization for Economic Cooperation and Development
ImageJ	Image Processing and Analysis in Java
IAEA	International Atomic Energy Agency
WHO	World Health Organization
NCRP	National Council on Radiation Protection and Measurements
DCF	Dose Conversion Factor
WLM	Working Level Month
WL	Working Level
SSNTD	Solid State Nuclear Track Detector
LEAR	Lifetime Excess Absolute Risk
PADC	Polyallyl Diglycol Carbonate
LR115	Lenin Resin 115
NaOH	Sodium Hydroxide
ELCR	Excess Lifetime Cancer Risk



LIST OF ABBREVIATIONS

^{220}Rn	Thoron-220
^{235}U	Uranium-235
^{238}U	Uranium-238
^{232}Th	Thorium-232
^{222}Rn	Radon-222
^{226}Ra	Radium-226
C_R	Radon Concentration
F	Equilibrium Factor
n	Occupancy Factor
H	Hours in Year
F_R	Risk Coefficient for Radon
I_α	Alpha Index
C_{Ra}	Radium Concentration
E_A	Surface/Area Exhalation
E_M	Mass Exhalation
D_E	Effective Dose
DCF	Dose Conversion Factor
E_R	Exposure to Radon Daughters
Bq/m^3	Becquerel Per Cubic Meter
μSv	Micro Sievert
Bq/kg	Becquerel Per Kilogram
mSv	Milli Sievert

CHAPTER ONE

INTRODUCTION

Background to the Study

Environment around us always contains small amounts of Naturally Occurring Radioactive Materials (NORMs), which have existed since the formation of the earth. NORMs availability in the environment is generally, at levels that, are not potentially harmful to human health. A major concern arises when the levels are elevated as a result of human practices, such as mining and natural hazards, such as earth quakes (Ahmed & El-Arabi, 2005).

In nature, mining involves the production of large quantities of waste, which may contaminate soils over a large area, thereby negatively impacting the environment and human health (Munyaradzi et al., 2018). Mining is one of the major causes of elevation of NORMs concentrations on the earth's surface causing health risks to humans, especially when inhaled or ingested (Rowland, 1993). The most important NORMs in radiation protection are radionuclides from the Uranium-238 (^{238}U) and Thorium-232 (^{232}Th) decay series. Potassium-40 (^{40}K), a non-series radionuclide, also contributes significantly to human exposure in the environment (Ziajahromi et al., 2015). Therefore, the knowledge of ^{238}U , ^{232}Th and ^{40}K activity concentrations is important in the evaluation of absorbed doses that can lead to the estimation of their radiological hazard to the population.

Thorium and Uranium are both sources of radon and they are common, naturally-occurring elements that are found in low concentrations in rock and soil. Radon is naturally occurring radioactive noble gas produced from the

radioactive decay of the element Radium, which is itself a decay product of either Uranium or Thorium.

There are three radioisotopes of radon naturally present in the environment: Radon-222 from the uranium-238 decay series, Radon-220 from Thorium-232 decay series and Radon-219 from Uranium-235 decay series. Radon-219 is of low radiological significance because of its short half-life of 4 seconds and Uranium-235 represents a small percentage (0.3%) of the activity of natural occurring Uranium (Biira, Kisolo, & D'ujanga, 2014).

While the concentration of thorium-232 in the environment are comparable or higher than that of uranium-238, the relatively shorter half-life (56 seconds) of Radon-220 compared to radon-222 with half-life (3.82 days), makes Radon- 222 more important. This is so because Radon-222 can migrate over much greater distances after production than Radon-220.

Therefore Radon-222 produced in the soil and the decay products as shown in figure 1, is the principal source of radon concentration in buildings or walls of mines and in both indoor and outdoor air, while radon-220 is of concern from a radiation protection view point if the concentration of thorium-232 is high (A. Nero Jr, 1985; A. V. Nero Jr, 1990).

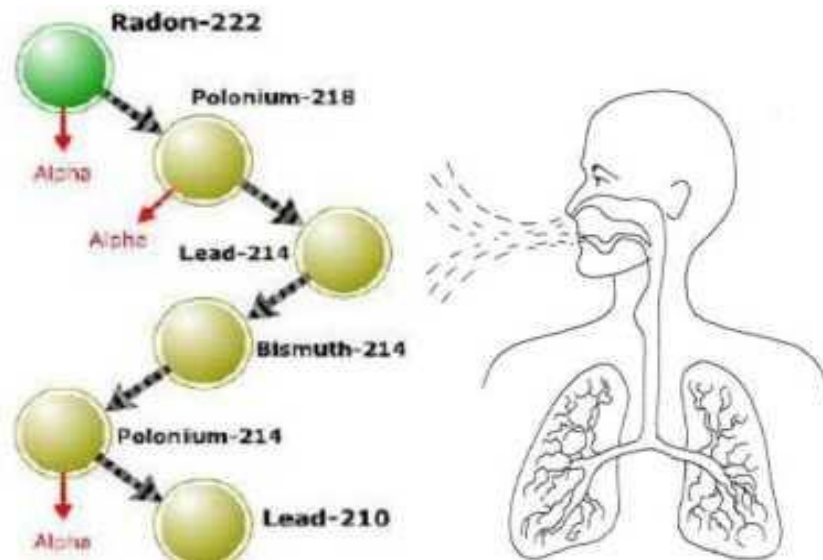


Figure 1: Radon Exposure Pathway

Source: (Podstawczyńska, 2015)

This current study is based on measurement and analysis of naturally occurring radioactive materials and indoor radon concentration in underground goldmine in the Western Region of Ghana. The study includes radiological impact assessment, effects of environmental factors on radon concentration in the underground goldmine as well as estimating the radiation doses that people who have access to these underground goldmines are exposed to. For a long time, researches have shown that exposure to certain levels of concentration of radiation from radon is harmful to biological life, including humans (Council, 1999a). In some cases, high concentration of radon gas has been identified to be a precursor to lung cancer among persons exposed to high doses of radon. People at risk include miners and workers in Caves, tour guides, and any other persons that has used the underground goldmine for a long period. However, while the harmful effect of radon is generally accepted, information on concentration of radon in underground goldmines in Ghana is very scanty.

There is therefore a need to study specific underground goldmine with the aim of measuring and documenting the actual level of concentration of radon in order to estimate the actual risk of radon exposure of workers in underground goldmine. Measures can then be taken to reduce the risk if necessary. This study focuses specifically on underground Goldmine with a view to assess the radiological impact of Radon gas and naturally occurring radioactive materials of underground goldmine workers.

There has been concern about the effects of radon exposure to people especially miners, in Ghana. There is however, a lack of information about radon concentrations in underground goldmines in Ghana. Database of radon concentration in particular in Caves and underground mines are very scanty and in some cases absent. This study is therefore a contribution towards the national data base of Concentration of Radon and other naturally occurring radioactive materials for the Regulatory Authorities.

Statement of the Problem

The underground mine environment is complex and variable. Radon, after being exhaled, decays to a more stable radionuclides: ^{218}Po , ^{214}Pb , ^{214}Bi and ^{214}Po (Cousins et al., 2011). These radionuclides attach to the aerosol particles in the air, forming what is termed attached radon progeny. The fraction of radon progeny that does not attach to the aerosol particle in the air is termed the unattached state. In both cases, concentrations of these radon decay products increase rapidly with residence time of the air in the mine. If inhaled, both attached and unattached radon progenies may be deposited in the lung, especially in the upper respiratory tract, and irradiate the lung tissue as they decay. The entry of radioactive aerosol into the respiratory tract depends on

their size; larger particles stop in the nasal cavity, while smaller aerosols reach the lungs (Planinic et al., 1999). Epidemiological studies have revealed a strong correlation between lung cancer and exposure to radon (Yoon et al., 2016). It was identified as a human lung carcinogen in 1986 by the World Health Organization – WHO. High concentration of radon is found in poorly ventilated structures and if the radon input from its sources is high, such as mines, caves, cellars, ancient tombs and air tight houses. The inhaled radon passes from lungs into the blood and body tissues and may irradiate different soft tissue causing cancers such as lung cancer, kidney cancer and prostatic cancer. Radon has also been linked with melanoma and some childhood cancers. There is also a positive association between coronary heart disease and radon exposures where an elevated risk of mortality from coronary heart disease was observed among miners with accumulative radon exposure exceeding 1000 Working Level Month (WLM) (Bajwa & Virk, 1997; Hussein, 2008).

There are currently four goldmines in Ghana operating underground. Apart from the Obuasi underground goldmine, which some work has been done (Darko et al, 2005, A. B Andam 1991), there has not been any radiological impact assessment on the rest. Preliminary investigations indicate that the ventilation is poor, which makes it conducive to high radon levels. Some workers have complained about the quality of air inside the underground goldmine. It is therefore important to understand how much risk these workers may be exposed to and, therefore, how the risk can be avoided and minimized.

Despite increased interest and concern of the international scientific community on the importance of monitoring radon and its impact on public health, Ghana has not yet carried out any systematic studies on radon levels on a

national scale. There are therefore no national regulations for residential and occupational radon protection. However, studies on the concentration levels of radon and its progeny in goldmines, industries (work places) and dwellings in Ghana are limited. This means that the average radon concentration levels and effective dose exposure to the entire population are not yet established. It is important to monitor this gas and its products in underground mines in order to assess the radiological hazards of the exposed workers. The knowledge of the radon distribution and its origin in mines is essential according to radiation-protection standards. In Ghana, studies on radon have been carried out over the past two decades. These studies have been independent and uncoordinated and have focused only on a few areas of interest (Darko et al, 2005, A. B Andam 1991, Insiyah Akoto et al, 2017). The Subika underground goldmine is a new underground mine where there has been no radiological impact assessment. This means that the average radon concentration levels and effective dose to the entire population are not yet established.

To address this concern, the researcher aims to assess the radon and its progeny concentrations in the Subika underground goldmine to obtain reference data and information for regulatory authorities and other stakeholders to prepare the national regulations and standards for miners. This study is part of the Radon Project which is being conducted by the Ghana Atomic Energy Commission (GAEC) and the Nuclear Regulatory Authority (NRA). The set of data will contribute to limit occupational radiation exposure of workers and to obtain information and parameters to prepare the Ghana regulatory standards for miners.

Objective of the Study

The objectives of the study are grouped into two. These are general objective and specific objectives.

General Objective

This study is aimed at assessing the level of indoor radon and naturally occurring radioactive materials in underground goldmine in Ghana.

Specific Objectives

The specific objectives are as follows;

1. To measure indoor radon and other natural radioactivity concentration in Subika underground goldmine.
2. To estimate the radiation doses due to ^{222}Ra and its progeny to the Subika underground workers.
3. To determine the effect of environmental factors on radon concentration in the Subika underground goldmines.
4. To determine radon concentration at different depths in the Subika underground goldmine using trend analysis.
5. To assess the radiological impact of Naturally Occurring Radioactive materials in the Subika underground goldmine.
6. Recommend remediation measures in case adverse effects are observed.

Research Questions

1. What are the levels of indoor radon and other natural radioactivity in the underground goldmine?
2. What are the radiation doses due to ^{222}Ra and its progeny to the underground workers?

3. What are the effects of environmental factors on radon concentration in the underground goldmines?
4. What are the radon concentrations at different depths in the underground goldmine?
5. What are the radiological impacts of Naturally Occurring Radioactive materials in the underground goldmine?

Significance of the Study

The findings will help decision makers, Ghana Nuclear Regulatory Authority (NRA), Minerals Commission, Environmental Protection Agency (EPA Ghana), Geological Survey Department and Ghana Standards Authority in developing a national radon policy for Goldmines and to make recommendations from radiation protection view point to stakeholders on the need for further investigation, development and implementation of protection strategies to ensure protection of workers and the public.

In this regard, the occurrence of radiological hazards and consequences associated with indoor radon and NORM which may pose serious health implications to workers, the public and the environment, can be assessed and prevention and mitigation measures undertaken where appropriate.

It will also provide a basis for further detailed assessment of radiation exposures from NORMs in the mining industries in Ghana.

The necessary awareness through this study will be created for management of these facilities so that workers are appropriately protected from the harmful effect of radon gas and other associated natural radioactivity and the public radiation protective measures

This research will also serve as a useful data for Regulatory Bodies, Environmental Protection Agency, Minerals Commission and the Ghana Nuclear Regulatory Authority. This study is also important to minimize, and in some cases eliminate future problems that are associated with Radon gas and NORMs in the mining industry in Ghana.

Scope and Limitation of the Study

The work is intended to cover measurement of the indoor radon series and their daughter products as well as naturally occurring radioactive materials in a newly constructed underground goldmine in the western region of Ghana.

Measurements of ^{222}Rn for mapping need to be done on a large scale but due to lack of regulations on radiological environmental monitoring from the Ghana Nuclear Regulatory Authority (NRA) and the Ghana Environmental Protection Agency (EPA) made it very difficult for the mining companies to grant authorization and access to the underground goldmine for the monitoring. Due to this challenge a purposive sampling of underground goldmine was done to be a representative. The mine was chosen purposively since it was a virgin underground mine that no activity or monitoring has never taken place, hence the radiological safety assessment of this mine will be of utmost importance to the workers who will be exposed to the naturally occurring radioactive materials and the results obtained will be set as a base line for the mining regulatory authorities as well as the Ghana Nuclear Regulatory Authority for regulating underground mining in the country.

Time and financial constraints of monitoring all underground goldmines, searching for information from relevant sources and combining academic work

and the research work with our professional work could not be overlooked when it comes to considering the limitations of the study.

Organization of the Study

This section describes the content of chapters and sections.

Chapter one consists of the introduction, background of study, problem statement, objective of the study, research questions, hypothesis, significance of the study and organization of the study. Chapter two reviews literature with more highlight on theories and works done related to the topic and a conceptual framework for statistical analysis on the effect of environmental factors on radon concentration in underground goldmines.

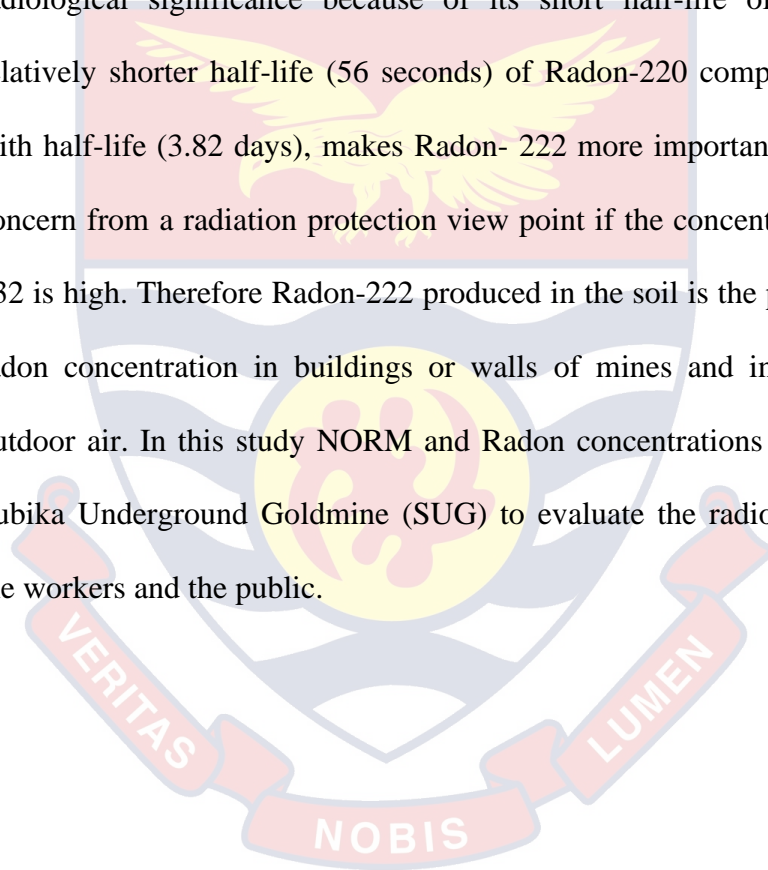
Chapter three discuss the methodological framework used for sampling, sample preparation and analyses. The chapter discusses the types and sources of data, sampling techniques, population size and procedures for collection and analysis of data. Chapter four entails the analysis of data and generated results from the analysis. Chapter five emphasize the findings of the research study and draws conclusion. Answers to specific objectives of the research are discussed in this chapter and recommendations are made based on the findings and analysis of data obtained from the field.

Chapter Summary

Naturally Occurring Radioactive Materials (NORMs) originate from radionuclides in the earth (from terrestrial origin) and the atmosphere (from cosmic rays). The most important NORMs in radiation protection are radionuclides from the earth, notably- Uranium-238 (^{238}U), Thorium-232 (^{232}Th) decay series and Potassium-40 (^{40}K). Their availability in the environment is generally at levels that are not potentially harmful to human

health. A major concern arises when the levels are elevated as a result of human practices such as mining or natural hazards such as earth quakes.

Radon is a NORM and part of the natural decay series of uranium (U) and thorium (Th) found in all soils and rocks to a varying concentration. There are three radioisotopes of radon naturally present in the environment: Radon-222 from the uranium-238 decay series, Radon-220 from thorium-232 decay series and Radon-219 from uranium-235 decay series. Radon-219 is of low radiological significance because of its short half-life of 4 seconds. The relatively shorter half-life (56 seconds) of Radon-220 compared to radon-222 with half-life (3.82 days), makes Radon-222 more important. Radon-220 is of concern from a radiation protection view point if the concentration of thorium-232 is high. Therefore Radon-222 produced in the soil is the principal source of radon concentration in buildings or walls of mines and in both indoor and outdoor air. In this study NORM and Radon concentrations were measured in Subika Underground Goldmine (SUG) to evaluate the radiological impact on the workers and the public.



CHAPTER TWO

LITERATURE REVIEW

Introduction

This chapter highlight on theories of radon gas, naturally occurring radioactive materials, radiation protection and statistical instruments in the study (Theoretical Framework), works done related to radon and naturally occurring radioactive materials both in Ghana and worldwide (Empirical Framework) and diagrammatic and Operational definitions of dependent and independent variables in the study (Conceptual Framework).

Theoretical Framework

Definition of Radon

Radon (chemical symbol, Rn) is a naturally occurring radioactive gaseous element that is emitted by radioactive material in the earth's crust (J. D. Appleton, 2013; Nemangwele, 2005). The most abundant isotope, ^{222}Rn is produced by the breakdown of uranium in the soil, rocks, and water. Radon is found naturally in certain geological formations such as Cave limestone where ^{238}U occurs naturally. Radon has numerous different isotopes, but ^{220}Rn , and ^{222}Rn are most common. ^{222}Rn is the decay product of ^{226}Ra . ^{222}Rn and its parent, ^{226}Ra , are part of the long decay chain of ^{238}U . Since uranium is found everywhere in the earth's crust, ^{226}Ra and ^{222}Rn are present in almost all rocks, soil, and water. ^{222}Rn is the greatest source (69%) of absorbed dose due to natural radiation (Apraku, 2013). If the gas is inhaled into the lungs, its decay and more importantly the decay of the radon daughters that enter the lung can increase the chance of getting lung cancer (Keith et al., 2013; Nazaroff &

Nero, 1988). The term radon will be used to refer to ^{222}Rn in this thesis, in accordance with usual practice.

Physical and Chemical Properties of Radon

Radon is a colourless, tasteless, radioactive noble gas, which means it is essentially inert. It has a half-life of 3.82 days and decays by alpha emission. The alphas have energy of 5.5 MeV. Radon has all the properties of other noble gases. Its atomic number is 86. Radon has a high melting point of -71°C and a boiling point of -62.7°C . It has first ionization energy of $1037\text{ kJ}\cdot\text{mol}^{-1}$ and a density of $9.99\times 10^{-3}\text{ g}\cdot\text{cm}^{-3}$ at 200°C (Durrani, 1997; Righi & Bruzzi, 2006).

An Introduction to Radon Decay and Ionizing Radiation

Ionizing radiation is any of the various forms of radiant energy that causes ionization when they interact with matter. The most common types are alpha radiation, beta radiation and gamma or X-rays, the latter consisting of high-energy photons. Radon is an alpha emitter found in the decay chain of uranium and radium. Radon and its progeny may cause harmful health effects after being inhaled.

Ionizing radiation can overcome the binding energy of electrons in an atom. Electromagnetic waves (gamma rays) are released from the nuclei of radioactive atoms undergoing decay. The energy possessed by these particles and rays are capable of damaging living tissues at the molecular level (for example DNA) by breaking chemical bonds (R. Njinga et al., 2019; R. L. Njinga et al., 2016).

^{238}U and its progeny in the soil are an important source of background radiation. Due to the high concentration of ^{222}Rn and low ventilation levels in underground mines and Caves, it is necessary to measure radiation dose in order to monitor the effects of nuclear radiation on biological tissue. In this thesis we are mostly interested in alpha radiation because ^{222}Rn and two of its daughters are alpha emitters. The main concern is the inhalation of radon and these daughters by underground workers, since the high energy alphas can damage cells.

Alpha radiation from polonium isotopes produce radiologically significant dose. Alpha particles deposit their energy within body tissue. The concentration of radon decay product in air is ordinarily not given in terms of individual decay product concentration, but it is given by a combined collection that is normalized to the amount of alpha decay energy. Finally, the result from the mixture of radon decay product that is present is called Equilibrium-Equivalent Decay Product Concentration (EEDC).

EEDC is the amount of each decay product necessary collectively or have the same Potential Alpha Energy Concentration (PAEC) that is actually present.

Radon Decay

In 1895, Wilhelm Roentgen discovered X-rays. Henri Becquerel in 1896 was using natural fluorescent mineral to study the properties of X-rays, which led to the discovery of radioactivity (Radvanyi & Villain, 2017). The term radioactivity was coined by Marie Curie and her husband, Pierre, when investigating the phenomena relating to the discovery of radioactive decay (Strohmeier, 2011).

Decay rates depend on the type of interaction and on the amount of energy released. There are three common types of radioactive decay, alpha, beta, and gamma. The difference between them is the particles emitted by the nucleus during the decay process. All three types occur in the ^{222}Rn series.

Alpha Decay

In alpha decay, the nucleus emits an alpha particle (Zhong-Zhou et al., 2003). An alpha particle is essentially a helium nucleus; it is a group of two protons and two neutrons. A helium nucleus is very stable (Hosseini et al., 2018). An example of an alpha decay involves ^{222}Rn :



The process of transforming one element to another is known as transmutation. Alpha particles do not travel far in air before being absorbed (Müller, 2017). An alpha particle is a positively charged particle emitted in the radioactive decay of some unstable atoms. It consists of two protons and two neutrons (it is essentially the nucleus of a helium atom) and is thus heavier and slower-moving than other decay emissions (Smith, 2010). Alpha particles do not penetrate far into a material and can be stopped quite easily; however, they are capable of breaking chemical bonds (which can cause chemical or biological damage) when they strike a molecule because of their size, mass and charge. (Penetration distance of alpha particles depends upon the energy with which they are emitted and the material through which they are passing). Thus, while alpha particles can be stopped by thin barriers such as a piece of paper or skin, alpha emitters are mostly damaging if they are ingested or inhaled into the lungs. Uranium (^{238}U), Radium (^{226}Ra) and Radon (^{222}Rn) are typical alpha-particle emitters (Smith, 2010).

Beta Decay

A beta particle is an electron, or a positron. If an electron is involved, the number of neutrons in the nucleus decreases by one and the number of protons increases by one. An example of such a process in the ^{222}Rn decay chain is:



In terms of safety, beta particles are much more penetrating than alpha particles, but much less than gamma particles. Beta particles can have either a negative charge or a positive charge and they have the same very small mass (1/2000 the mass of a neutron) regardless of charge (Smith, 2010). A negatively charged beta particle is called an electron, and a positively charged beta particle is called a positron. Beta particles can penetrate farther than alpha particles (Its penetration distance depends upon the energy of beta particle and material used); however, they can be stopped fairly easily by a sheet of aluminium.

Gamma Decay

The third class of radioactive decay is gamma decay, in which the nucleus changes from a higher-level energy state to a lower level. The third type of radiation leads to the formation of gamma rays. When alpha and beta decay lead to the formation of a new nucleus, the latter can be in the excited form, it has more energy than usual. This surplus energy is lost by the emission of a gamma ray. This radiation is characterized by a long-range emission, being then neutral. Typical energies range from a few to 3000 keV. An example is the decay of ^{152}Dy to de-excited ^{152}Dy by emission of a photon

These three different kinds of radiation represent a danger for human health in different ways, but they all cause damage primarily by losing energy passing through matter. The energy is lost by ionization, which can cause in

biological tissue chemical reactions, leading to destruction of cells or changes in the functions. Ionization power highly depends on the speed at which particles are travelling (Chancellor et al., 2018; Durante et al., 2019).

Radon Decay Constant and Half Life

The decay processes occurring inside the mine are important in this study. It is impossible to predict when a specific atom would disintegrate to form another.

The radioactive decay law is derived from two simple assumptions. The number of decays N in a time t , the number of radioactive nuclei present:

$$\frac{\Delta y}{\Delta x} = \lambda N \quad (3)$$

where $\lambda(s^{-1})$ is called the decay constant of a specific radioactive nucleus.

$$\lambda = -\frac{\Delta N}{\Delta \frac{t}{N}} \quad (4)$$

The above decay explains the nature of λ , which is the probability per unit time for the decay of an atom. The value of λ differs for each nuclide. The solution of equation (4) is called the exponential decay law of radioactivity.

It is given by

$$N(t) = N_0 e^{-\lambda t} \quad (5)$$

where N_0 is the original number of nuclei present at time $t = 0$. $N(t)$ is the activity after disintegration of the original nuclei. There is a statistical time $T_{1/2}$ after which half of the number of nuclei will have decayed.

To get

$$T_{1/2} = \frac{N_{(t)}}{N_o} = \frac{1}{2}$$

Taking logarithms, it follows that $\log_e 2 = \lambda t$

so that the half-life is given by

$$T_{1/2} = \frac{\ln 2}{\lambda} \quad (6)$$

Decay Products of Radon (^{222}Rn)

Radon decay products is another name for the Radon progeny or Radon daughters. Radon decay products rather than Radon gas deliver the actual radiation dose to lung tissues (R. W. Field, 1999).

The Radon decay products are radioactive isotopes of Polonium, Bismuth, Lead, and thallium. Which are produced by decay of the Radon isotopes. These daughters of the radioactive gases are isotopes of heavy metals and are easily fixed to existing aerosol particles in the atmosphere. They decay by alpha particles and beta / gamma emission.

Radon decay products are divided into two groups: the "short-lived" Radon daughters ^{218}Po (3.05 min), ^{214}Pb (36.8 min), ^{214}Bi (19.7 min), ^{214}Po (164 μSv) with half – lives below 30 min, and the "long-lived" Radon decay products ^{218}Po (22.3 years), ^{210}Bi (5.01 days), ^{210}Po (138.4 days), as show in Table 1 and 2.

Table 1: Uranium Series

A/A	Nucleus	Half-live	Energy (Mev)	Radiation type
1	²³⁸ U	4.51x10 ⁵ Years	4.2 (75%)	α
2	²³⁴ U	2.47x10 ⁵ Years	4.77 (72%)	A
3	²³⁸ Ac	24Days	0.100,0.192 0.09	β γ
4	²³⁰ Th	8.0x10 Years	4.68 (76%)	A
5	²²⁶ Ra	1602Years	4.68 (95%)	A
6	²²² Rn	3.82Da s	5.49 (100)	A
7	²¹⁸ Po	3.05 min	6.00 (100%)	A
8	²¹⁴ Bi	19.7min	3.26,1.5,1.00	B
9	²¹⁴ Po	016 msec	7.69 (100%)	A
10	²¹⁰ Pb	22Years	0.015,0.065 0.065	β γ
11	²¹⁰ Bi	5Days	1.17	B
12	²¹⁰ Po	138 Days	5.30 (100%)	A
13	²⁰⁶ Pb		Stable	

Source: (Mohammed, 2013)

Table 2: Thorium Series

A/A	Nucleus	Half-live	Energy (Mev)	Radiation type
1	²³⁸ Th	1.4x10 ¹⁰ Years	3.95 (76%) 0.055	α γ
2	²²⁸ Ra	6.7Years	0.055	B
3	²²⁸ Ac	6.13Years	2.18,1.85, 1.11, 1.72	B
4	²²⁸ Th	1.91Years	5.68 (71%)	A
5	²²⁴ Ra	3.64Days	5.68 (94%)	A
6	²²⁰ Rn	55 s	6.29 (100%)	A
7	²¹⁶ Po	.015s	6.79 (100%)	A
8	²¹² Pb	10.6 hours	0.57, 0.33 0.3, 0.238, 0.178	β γ
9	²¹² Bi	60sec	2.23 (100%)	B
10	²¹² Po	304 ns	8.78 (100%)	A
11	²⁰⁸ Ta	301 min	1.8	B
12	²⁰⁸ Pb		Stable	

Source: (Mohammed, 2013)

Behaviour of Decay Products

The overall concentration of decay products is represented by the potential alpha energy concentration (PAEC). It depends on the concentration of the first three decay products (^{218}Po , ^{214}Pb and ^{214}Bi) and on the amount of polonium energy that obtained. The behaviour of Radon daughter is of high interest among scientists not only to satisfy a relationship between indoor Radon concentration and decay product concentration but also to provide a view of decay products exposures (Nazaroff & Nero, 1988).

The decay products can attach to aerosol particles, indoor walls, furniture and the human lung if the Radon is inhaled. After the decay of Radon, the daughters can deposit on surface before or after attachment to the particles. The health significance of the decay products is greatly influenced by their half-life decay modes and their behaviour after decay (Nazaroff & Nero, 1988).

- a. The initial Radon (^{222}Rn) atom.
- b. Is an electrically neutral gas atom which is unaffected by electric fields.

When Radon decays it emits an alpha-particle (alpha radiation) but at the same time the so-called daughter nucleus of atom, ^{218}Po , recoils.

- c. In doing so it cannot take all of its atomic electrons with it and as a result the daughter atom carries a net positive charge i.e. it is a positively charged ion. Chemically this is a ^{218}Po ion, an isotope of polonium. Within 10^{-6} seconds this ion attracts trace water molecules and gases in air growing to a size of ~ 10 nm.
- d. Such small particles are termed 'ultrafine aerosols'. Within one second the initial positive charge is lost, so resulting in a neutral aerosol.

- e. This aerosol may (or may not) then go on to attach itself to larger aerosols in room air of size range typically 0.1 to 0.2 μm . These are then said to be attached radon daughter'. These larger aerosols may pick up stray positive or negative charges, so their charge state (+ve, -ve, or neutral) can vary.
- f. Each ^{218}Po atom is itself alpha-radioactive and has a mean lifetime of 4.4 minutes. When this decay the above process (a) to (e) is repeated i.e. the daughter nucleus from the decay of ^{218}Po , an aerosol becoming a positively charge ^{214}Pb atom or ion.

The concentration of Radon in air is measured in units of picocuries per liter (pCi/L) or (Bq/m^3), with ($1\text{pCi}/\text{L} = 37\text{Bq}/\text{m}^3$). One Bq corresponds to one disintegration per second. The concentration of Radon daughters is measured in units of working level (WL). One WL correspond to 101.3 pCi/L of Radon equilibrium with its short-lived daughter in a typical indoor environmental (Bodansky et al., 1987).

Assume that ^{222}Rn and its decay products are removed only by radioactive decay, then radon and its decay products would be in a state of secular equilibrium, having the same (radioactive) activity. However, radon and its decay products are removed from air, not only by radioactive decay, but also by ventilation, which is driven by pressure differences caused by airflow (Pflitsch & Piasecki, 2003; Przylibski, 1999). A further difference between ^{222}Rn itself and the radon decay products is their chemical activity. The radon decay products can attach to airborne particles, and when inhaled, attach itself to the human respiratory tract. Radon decay products after being inhaled can be

deposited either directly in the lungs, or while attached to particles, stick to the lung.

Radon progeny are formed throughout the volume of the compartment by the radioactive decay of radon gas. Like radon, the progeny can leave by ex-filtration and by decay. Unlike radon, the progeny can attach themselves to aerosol particles or the walls.

The free progeny and the ones attached to particles need to be treated differently. The terms “unattached” and “attached” radon progeny are commonly used to distinguish between these two states of radon progeny.

Behaviour of Unattached Radon Progeny

After an atom of ^{222}Rn has decayed in the atmosphere, the first daughter product of ^{222}Rn , ^{218}Po becomes a positively charged ion. There will initially be excess electrons remaining, but these are stripped away by recoil, and one or more orbital electrons are lost as well.

Short-lived radon daughters are initially born in an atomic state but subjected to attachment to the aerosol particles and/or wall surface. Fractions of unattached radon daughter are considered to be an important parameter in estimating the dose to human respiratory organs through inhalation of radon daughters (Kojima & Abe, 1988).

In the Cave or underground mine atmosphere, the ratio of the respective activity concentrations of short-lived radon progeny to radon, changes rapidly with the age of the ventilating air as it flows through the Agency (2004). In relatively fresh air, the ratio is low, but it approaches unity in old (stagnant) air. Most radon progeny, in the form of small positive ions or neutral atoms clustered on water or other molecules in the air, become attached to atmospheric

aerosol particles of about $0.3 \mu\text{m}$ diameter and therefore, like the unattached progeny, are respirable.

Behaviour of Attached Radon Daughters

Air normally contains copious numbers of small solid or liquid particles called aerosol particles or aerosols. These particles range in size from almost atomic dimensions up to several micrometers in diameter (Nazaroff & Nero, 1988). Aerosol plays an important role in the behaviour of radon progeny in underground places such as Caves and underground mines.

Radon progeny whether attached or unattached tends to deposit on and stick to the surface exposed to the air. Since material removed from the air is no longer available to be breathed, surface deposition supplements ventilation as a means of reducing human exposure to radon progeny.

Health Effects of Radon Exposure

Radon gas presents a serious internal alpha radiation hazard to the lungs. It can decay to its daughters while in the lungs or its daughters can be inhaled after radon decays in the air. The daughters are solid particles and when they are inhaled they release radiation (alpha, beta) into the lungs, which can potentially cause cancerous cell growth (in the lungs) (Council, 1999a).

Radon is identified as the second leading cause of lung cancer, while tobacco smoke is the primary cause. It is calculated that in the United States of America, 5000 to 21000 deaths per year are caused by radon induced lung cancer (Guimond, 1988). The problem in isolating the effect of ^{222}Rn is that, the majority of the documented results were miners. Most of them are smokers and inside the mine they all inhaled dust containing radon and other pollutants.

Because radon and cigarette smoke both cause lung cancer, it is complicated to separate the effects of the two kinds of exposure.

The combination of smoking and radon exposure can greatly increase the risk of developing lung cancer. There exists evidence that, if a person smokes or lives with someone who smokes where radon levels exceed the acceptable levels, the risk of lung cancer is 1.2% higher than for those who have never smoked (Ann, 2000). The Biological Effect of Ionizing Radiation committee (Council, 1999a) further reported that, apart from the results of very limited in vitro and animal experiments, the only source of evidence on the combined effects of the two carcinogens (cigarette smoke and radon) was the data from 6 of the miner studies. Analysis of that data indicates a synergistic effect of the two exposures acting together, which was characterized as sub-multiplicative, i.e. less than the anticipated effect if the joint effect were the product of the risks from the two agents individually, but more than if the joint effect were the sum of the individual risk. The BEIR VI committee studies this multiplication although the committee could not precisely characterize the joint effect of smoking and radon exposure. The committee preferred the sub-multiplication relation because it was found to be more consistent with the available data.

The major conclusion by BEIR VI was that “radon is the second leading cause of lung cancer after smoking”. BEIR VI further realizes a statistical analysis of results from the latest epidemiologic follow-up of 11 cohorts of underground miners in the United States, which, in all, included about 2700 lung cancers among 68000 miners, representing nearly 1.2 million person years of observations.

Sources of Natural Radiation

Naturally occurring radioactive materials are common in the environment and in the human body. These materials are continuously emitting ionizing radiation. Ionizing radiation from outer space (cosmic radiation) bombards the earth constantly. Collectively, the ionizing radiation from these and similar sources is called background radiation. Human activities, such as making medical x-rays, generating nuclear power, testing nuclear weapons, and producing smoke detectors which contain radioactive materials, cause additional exposure to ionizing radiation. The sources of radiation can be classified into natural and man-made radiation.

The percentage of the average annual radiation exposure contributed by each major source is illustrated in Figure 2. About 82 percent is from nature, and 18 percent is from industrial, medical, and consumer sources. The values given in Figure 2 are averages for the United States. Actual values vary depending on where people live and how they spend their time (Fentiman & Hajek et al., 2017).

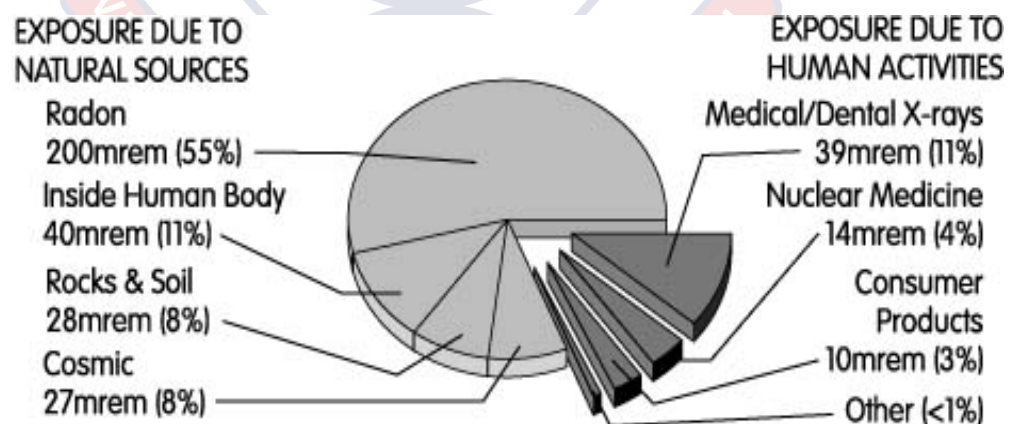


Figure 2: Average Annual Exposure to Ionizing Radiation (1Sv = 100rem)

Source: (Health & Services, 1999)

Natural Radiation Sources

Primordial Radionuclides Sources

Primordial radionuclides sources include naturally occurring radioactive materials that exist in rocks, soil, water, and vegetation. The major isotopes of concern for primordial radionuclides radiation are uranium and its decay products, such as thorium, radium, and Radon. Some of these materials are ingested with food and water, while others, such as Radon, are inhaled.

The dose from primordial radionuclides sources varies in different parts of the world. Locations with higher concentrations of uranium and thorium in their soil have higher dose levels (Thorne, 2003). These primordial radionuclides are left long time ago. They are typically long lived, with half-lives often on the order of hundreds of millions of years. Radionuclides that exist for more than 30 half – lives are not measurable (McAdam et al., 2017). The progeny or decay products of the long-lived radionuclides are also, in this heading. Here is some basic information on some common primordial radionuclides in table 4:

Cosmic Radiation

Charged particles from the sun and stars interact with the earth's atmosphere and magnetic field to produce a shower of radiation. The dose from cosmic radiation varies in different parts of the world due to differences in elevation and to the effects of the earth's magnetic field (Thorne, 2003).

Cosmic radiation is really divided into two types, primary and secondary.

Internal Radiation

Internal radiation comes from radioactive materials that occur naturally in the human body. Potassium and Carbon are the primary sources of internal radiation exposures.

Potassium is an essential mineral for life. The Potassium (^{40}K) isotope (0.01 percent of all potassium) is naturally radioactive. It enters the human body through the food chain. Carbon makes up about 23 percent, by weight, of the human body. Cosmic radiation creates Carbon (^{14}C), which is a small percentage of all carbon. Carbon enters the body both through the food chain and by breathing (Hashim et al., 2017).

Man-Made Radiation Sources

Natural and artificial radiation sources are identical in their nature and their effect. By far, the most significant source of man-made radiation exposure to the general public is from medical procedures, such as diagnostic X-rays, nuclear medicine, and radiation therapy. Some of the major isotopes would be ^{131}I , ^{99}Tc , ^{60}Co , ^{192}Ir , ^{137}Cs , and others.

In addition, members of the public are exposed to radiation from consumer products, such as tobacco (Polonium ^{210}Po), building materials, combustible fuels (gas, coal, etc.), ophthalmic glass, televisions, luminous watches and dials (tritium), airport X-ray systems, smoke detectors (americium), road construction materials, electron tubes, fluorescent lamp starters, lantern mantles (thorium), etc (Thorne, 2003).

Occupationally exposed individuals are exposed according to their occupations and to the sources with which they work. The exposure of these individuals to radiation is carefully monitored with the use of pocket-sized instruments called dosimeters. Some of the isotopes of concern would be cobalt (^{60}Co), caesium (^{137}Cs), americium (^{241}Am), and others (Thorne, 2003).

Examples of industries where occupational exposure is a concern include:

- i. Fuel Cycle
- ii. Industrial Radiography
- iii. Radiology Departments (Medical)
- iv. Radiation Oncology Departments
- v. Nuclear Power Plant
- vi. Nuclear Medicine Departments
- vii. National (government) and University Research Laboratories

It is known that the background level of radiation exposure, the NRC requires that its licensees limit man-made radiation exposure to individual members of the public to 100 mrem (1 mSv) per year, and limit occupational radiation exposure to adults working with radioactive material to 5,000 mrem (50 mSv) per year.

The exposure for an average person is about 360 millirems/year (360 mrem = 3.6mSv), 81 percent of which comes from natural sources of radiation. The remaining 19 percent results from exposure to man-made radiation sources.

Biological Effects of Radiation

When the human body is exposed to any radiation, either from external or internal sources, ionisation and excitation of atoms and molecules can be produced. Consequently, the interaction of radiation with biological organisms can result in the damage and death of living cells and/or the mutation of genetic material. The variation of the biological effects of radiation depends on types of radiation and its energy which is transferred to the irradiated parts of tissues and organs during the exposure time (Eisenbud & Gesell, 1997; Lilley, 2013; Noz & Maguire Jr, 2007). The quantification of the

amount of ionisation which occurred and the energy absorbed by particular cells associated with biological effectiveness can be considered in terms of radiation dosimetry.

Radiation Dosimetry

Basic Radiation Quantity and Unit Exposure

The 'roentgen' (R) is the unit to express the radiation exposure that can be defined as the amount of ionisation that X- or γ radiation produces in air. This unit accounts for the production of 1 esu of electrical charge of either sign in 1 cm³ or 0.001293 g of air at standard temperature and pressure (Turner, 2007). Since 1esu = 3.34 × 10⁻¹⁰ Coulomb(C) (Turner, 2007), the exposure unit can be expressed in the SI system as (Lilley, 2013; Noz & Maguire Jr, 2007; Turner, 2007) exposure unit is designated only for limited energy range X- or γ radiation interacting with air (Noz & Maguire Jr, 2007; Turner, 2007).

$$1R = 1 \frac{esu}{cm^3} = \frac{3.34 \times 10^{-10}}{0.001293 \times 10^{-3}} = 2.58 \times 10^{-4} \frac{C}{kg} \quad (7)$$

Absorbed Dose

One limitation of the exposure unit is that it does not reflect the biological significance of the radiation. A unit considering the quantity of energy absorption by any kind of ionising radiation in any kind of material was introduced. The absorbed dose is measured in units of 'gray' (Gy) where 1Gy equals to one joule of absorbed energy per one kilogram of irradiated The target (Cember, et al., 2008; Lilley, 2013; Noz & Maguire Jr, 2007). The absorbed dose can be expressed in another unit called the 'rad' (radiation absorbed dose). The rad is the original unit and is defined as an

absorbed energy of 100 *erg per gram* . It is related to the gray as follow (Cember et al., 2008; Rashed-Nizam et al., 2016; Turner, 2007):

$$\begin{aligned} 1J &= 10^7 \text{ ergs} \\ 1\text{Gy} &= \frac{1J}{\text{kg}} = \frac{10^7}{10^3} = \frac{10^4}{\text{g}} = 100\text{rad} \\ 1\text{rad} &= 0.001\text{Gy} = 1\text{centigray}(\text{cGy}) \end{aligned} \quad (8)$$

The total absorbed energy is not the only factor which determines the level of biological damage from the radiation. The type of radiation and its energy also have to be considered. In general, the biological effect of highly ionizing radiation in a tissue is more severe per unit absorbed dose than those of radiation which produce low ionization. For this reason, the term relative biological effectiveness (RBE) was introduced as a dimensionless quantity of the amount of absorbed dose of ionising radiation relative to that of X- or γ radiation of a particular energy to provide the same biological response (Cember et al., 2008; Lilley, 2013; Noz & Maguire Jr, 2007). Due to the difficulty in applying such complicated functions of energy, RBE has been normalized to a factor known, as the radiation weighting factor (wR) by the ICRP and NCRP (Cember et al., 2008; Noz & Maguire Jr, 2007). This factor is derived from the RBE over the range of energies for a particular type of radiation. A list of radiation weighting factors for various types of ionizing radiation is presented in Table 3.

Table 3: Radiation Weighting Factors for Different Ionizing Radiations

Type of Radiation	Energy range	Weighting factor, W_R
Photon, electrons, positrons and muons	All energies	1
Neutrons	< 10 keV	5
	> 10 keV to 100 keV	10
	> 100 keV to 2 MeV	20
	> 2 MeV to 20 MeV	10
	> 20 MeV	5
Photons	< 20 MeV	5
Alpha particles, fission fragments, non-relativistic heavy nuclei		20

Source: (1, 1991; Cember et al., 2008; Noz & Maguire Jr, 2007)*

Equivalent and Effective Dose

In order to determine the effect of the nature of the radiation by the weighting factor in Table 6, a unit called the equivalent dose (H_T) is specified. This is the amount of the dose ($D_{T,R}$) absorbed over a tissue or organ (T) due to radiation (R) and is given by (Cember et al., 2008; Eisenbud & Gesell, 1997; Lilley, 2013; Noz & Maguire Jr, 2007).

$$H_T = \sum_R W_R D_{T,R} \quad (9)$$

The 'sievert' (Sv) is used to express the equivalent dose when the absorbed dose is in units of gray (Gy); thus, one sievert is also equal to one joule per kilogram. An older unit of the equivalent dose is the 'rem' (radiation equivalent man) with the absorbed dose expressed in units of rad (Choppin et al., 2002), hence, 1 Sv equals to 100 rem (Choppin et al., 2002; Eisenbud & Gesell, 1997; Knoll, 2000; Lilley, 2013; Turner, 2007).

In addition to the radiation types and energy, the biological effect to radiation is concerned with the sensitivities of irradiated organs or tissues. The variation of radiation sensitivity of each organ is taken into account in the contribution of the equivalent dose in all tissues and organs of the body. The new terms the effective dose (E) and the tissue weighting factor (W_T) are introduced. The definition of the effective dose is the sum of the equivalent doses weighted by the tissue weighting factors for each tissue, as given in the following expression (Cember et al., 2008; Noz & Maguire Jr, 2007; Rashed-Nizam et al., 2016).

$$E = \sum_T W_T H_T \quad (10)$$

Considering equation 9 and 10

$$E = W_T \sum W_R D_{T,RT,R} \quad (11)$$

Table 4: Tissue Weighting Factors

Tissue or Organ	Tissue weighting factors, W_T
Gonads	0.20
Colon	0.12
Lung	0.12
Red bone marrow	0.12
Stomach	0.12
Bladder	0.05
Breast	0.05
Oesophagus	0.05
Liver	0.05
Thyroid	0.05
Skin	0.01
Bone surfaces	0.01
Remainder	0.05

Source: (1, 1991; Noz & Maguire Jr, 2007)

Table 4 lists the tissue weighting factors for tissues and organs of the human body. These factors were obtained from a reference population of equal numbers of men and women ranging in age. Because of the normalization of all tissue weighting factor values is unity, the effective dose equals a uniform equivalent dose over the whole body (Noz & Maguire Jr, 2007; Rashed-Nizam et al., 2016). The SI unit of effective dose is also the sievert (Sv).

Radiation Protection and Dose Limit

The magnitude of the radiation absorbed per year due to natural or background radiation may provide a basis for a health risk to human body.

Effect of radiation: Radiation causes ionizations in the molecules of living cells. These ionizations result in the removal of electrons from the atoms, forming ions or charged atoms. The ions formed then can go on to react with other atoms in the cell, causing damage.

At low doses, such as what we receive every day from background radiation, the cells repair the damage rapidly. At higher doses (up to 100 rem), the cells might not be able to repair the damage, and the cells may either be changed permanently or die. Cells changed permanently may go on to produce abnormal cells when they divide. In the right circumstance, these cells may become cancerous. This is the origin of our increased risk in cancer, as a result of radiation exposure (Indrajit, 2010; Parkin & Darby, 2011). Prolong exposure to the radiation would certainly cause health risks.

Since ionising radiation can damage biological organs in the human body, there have been many studies concerning the biological effects of radiation. The aims of these studies are to establish dose limits in order to protect radiation workers and members of the public from radiation exposure.

Much of the knowledge of radiation effects on humans has been obtained from a group of people who survived from the atomic bombs in Hiroshima and Nagasaki and those individuals who received radiation exposure from routine work or accidents (Cember et al., 2008; Eisenbud & Gesell, 1997; Lilley, 2013; Noz & Maguire Jr, 2007).

The relationship between biological effect and radiation exposure was studied by the Biological Effect of Ionising Radiation (BEIR) in agreement with the United Nations Scientific Committee on the Effect of Atomic Radiation (UNSCEAR) and the International Commission on Radiological Protection (ICRP), as shown in Figure 3. Initial reports used a linear relationship between the effect and the amount of exposure (shown in curve A) as a 'linear, no-threshold' hypothesis. Further studies also allowed the possible hypothesis of a different trend (curve B) with the radiation exposure at very low levels not significant to cause harmful effects; this is referred to as the 'threshold effect'. Curve C represents the hypothesis with the opposite effect, where absorbed doses of ionising radiation at low levels are more dangerous.

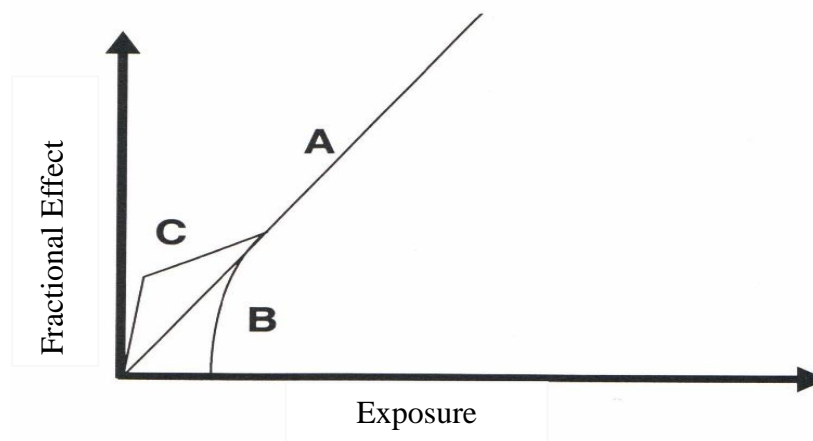


Figure 3: Dose Response Curve

Source: (Cember et al., 2008; Noz & Maguire Jr, 2007)

These curves show theoretical relationships between radiation exposure and the biological effect. Curve A shows the linear relationship that the effect and the exposure. The threshold effect represents the cut-off curve at the low levels of radiation exposure as shown in curve B. Curve C shows a possible increased effect at the low level of exposure (Noz & Maguire Jr, 2007).

The effect of radiation exposure can be classified into deterministic effects and stochastic effects (Cember et al., 2008; Eisenbud & Gesell, 1997; Noz & Maguire Jr, 2007; Rashed-Nizam et al., 2016). The effects which can be observed when organs of the body received a certain level of dose or threshold are called deterministic effects. Below this threshold, detrimental effects are not observed. The response of the effect is similar to curve B in Figure 3 The severity of the effect increases with the size of the dose (Cember et al., 2008; Rashed-Nizam et al., 2016). Stochastic effects occur randomly and the probability of occurrence is dependent of the size of dose (Cember et al., 2008; Noz & Maguire Jr, 2007). Cancer induction and genetic effects in future generation are thought to possibly result from these types of the effect. The expected relationship between the probability of the stochastic effect and the size of dose is along the lines of curve A in Figure 3.

To avoid unnecessary exposure causing the biological effects of radiation to radiation workers and the general public, all doses must be kept as low as reasonably achievable (ALARA) with the dose limits recommended by the ICRP (Cember et al., 2008). The recommendations of the ICRP for radiation protection standards are based on three general principles as follows (Cember et al., 2008; Rashed-Nizam et al., 2016):

1. Justification – any practice which does not produce sufficient benefit to the exposed individuals should not be adopted.
2. Optimisation – all exposures within a practice shall be kept as low as reasonably achievable (ALARA) considered with economic and social factors.
3. Dose limitation – individuals should receive exposure dose within the recommended limits.

In ICRP Publication 60, the recommended dose limits were set and estimated from the detrimental effect of the radiation which the prevention of deterministic effects and the limitation of stochastic effects were considered (1, 1991).

Table 5: ICRP 60 Recommended Effective Dose Limits

Application	Dose limit	
	Occupational	Public
Whole body	20 mSv ^a per year, averaged over a defined period of 5 years ^b	1 mSv ^a in a year
Annual equivalent dose in lens of the eye	150 mSv	15 mSv
Annual equivalent dose in skin	500 mSv	50 mSv

Source: (1, 1991; Cember et al., 2008; Noz & Maguire Jr, 2007).

For occupational exposure, the annual effective dose that the whole body is uniformly irradiated is limited to 20 mSv averaged over a defined period of 5 years to limit the probability of stochastic effects. The dose can be allowed to be over 20 mSv but cannot exceed 50 mSv in any single year. The dose limit of a member of the general public is set to be lower than a group of

radiation workers, at 1 mSv per year. To prevent deterministic effects, occupational equivalent dose limits of 500, 500 and 150 mSv per year are recommended for the skin, the hands and the feet, and the lens of the eye, respectively. The annual equivalent doses for individual members of the public are limited to be 15 mSv for the lens of the eye and 50 mSv for the skin (Cember et al., 2008; (Noz & Maguire Jr, 2007; Rashed-Nizam et al., 2016).

For non-uniform irradiation of the body, the tissue weighting factors of various organs as shown in Table 5 are used for determining the detrimental effects that contribute to each individual organ due to their different radiation sensitivities. The weighting factors of the several tissues and organs are relative to the whole body which has a value of unity (Noz & Maguire Jr, 2007; Rashed-Nizam et al., 2016).

The total weighted dose of all tissues and organs is equal to the effective dose as described by equation 11.

Radon Risk Assessment

Risk assessment is defined as the characterization of the potential adverse health effects of human exposures to environmental hazards (Board, 1983). Assessment of all types of hazards, including radiological hazards, requires all or some of the following components:

1. Hazard identification which is investigated to determine whether a particular hazard has a corresponding health effect.
2. Dose-response assessment, in which the relation between the magnitude of the dose and the probability that the health effect will occur is determined.
3. Exposure or dose assessment, which is the determination of the extent to which human will be exposed to the hazard.

4. Risk characteristic, which describes the nature and magnitude including uncertainties surrounding that risk (Board, 1983). It is the last component of risk characterisation that integrates the results of the previous three components into a risk model that includes one or more quantities estimates

Factors that affect the risk of lung cancer from radon exposure includes time since initiation of exposure, cigarette smoking, age, physical condition, genetic tendency either to resist or be affected by internal radiation exposure and geographic location. Building characteristics and environmental factors also affect indoor radon concentrations. Radon concentration are usually high in the lowest levels. Levels of radon indoors are mostly elevated in the rainy season than the dry season.

Radon Measurement Methods

The environmental radon concentration is a function of time and climatic conditions. To monitor radon, both active and passive techniques have been developed. Active methods are usually used for short-term measurements of radon and mostly battery powered. Passive methods are more suitable for the assessment of radon exposure over long time scales and can be used for large-scale surveys at a moderate cost (Ahn & LEE, 2005) and does not run on batteries. Below are some of the commonly used methods and the methods used for this thesis (SSNTD) will be discussed below:

Passive Techniques

Some of the passive techniques available are:

1. Charcoal Canister Technique
2. Solid State Nuclear Track Detectors (SSNTDs)

3. Electrets ion chamber (EICs)
4. Thermoluminescent Detectors (TLDs)

Active Techniques

Some of the available active techniques are:

1. Ionization Chamber
2. Scintillation Cell
3. Two Filter Method
4. Active Pylon Detectors /Continuous Monitoring
5. Surface Barrier Detector (SBD)
6. RAD7

Solid State Nuclear Track Detection (SSNTD) and their Applications (Passive Technique)

The present research was performed using SSNTDs. Solid State Nuclear Track Detectors (SSNTDs) are insulating solids both naturally occurring and man-made. When a heavily ionising charged particle passes through such insulating solids, it leaves a narrow trail of damage about 50 Å in diameter along its path. This is called 'Latent Track' as it cannot be seen with the naked eye. These latent tracks can be enlarged by etching with some chemicals such as sodium hydroxide and hydrofluoric acid, developed and viewed under an optical microscope by etching.

Advantages and Disadvantages of SSNTDs

SSNTDs are very sensitive, pose no great handling problems and are not fogged by exposure to light or affected by moderate degree of heating (Opoku-Ntim et al., 2019). Due to their durability and simplicity, they are particularly valuable for remote use, such as in high altitude balloon exposure to cosmic

rays and their robustness enable them to be used in personnel dosimetry. The reasons for its widespread use include the basic simplicity of its methodology and the low cost of its materials. Other important factors include the small geometry of the detectors, and their ability in certain cases to preserve their track record for almost infinite lengths of time (indeed, mineral grains in geological and planetary materials less than a millimeter across can, by suitable treatment, be made to reveal the billions of years old record of their radiation history).

One of the disadvantages of SSNTD is that it has some background radiation caused by radon particles in the air.

Etching Mechanisms and Track Revelation

Etching is the process of subjecting the exposed detectors to an etchant (that is, a polymer degrader rather than a solvent), for latent track to be visible under optical microscope. The speed at which the dissolved plastic material is removed from the remaining plastic sheet, is called “the etching rate”. For a track detector there are two kinds of etching rate. These are bulk or material etching rate V_B (μmh^{-1}) for the undamaged material and the track etching rate V_T (μmh^{-1}) at which the etching solution proceeds along the latent track. A track will obviously be enlarged by etching only if the rate of etching along the track, V_T , exceeds the rate at which the surface is etched, V_B . The track etching rate depends strongly on the energy loss of the ion.

The surface of the polymer is removed with a bulk etch rate V_B . As a result of the passage of a highly ionizing particle in a polymer (LR-115 type II), a chemically reactive damage trail may be produced, characterized by a different etching rate known as the track etch rate V_T . The volume around the

latent track will be attacked preferentially, so the trail of heavily charged particles and nuclear particles become visible as cylindrical or cone-shaped hole of 1 to 30 μm length as shown in Fig 4.

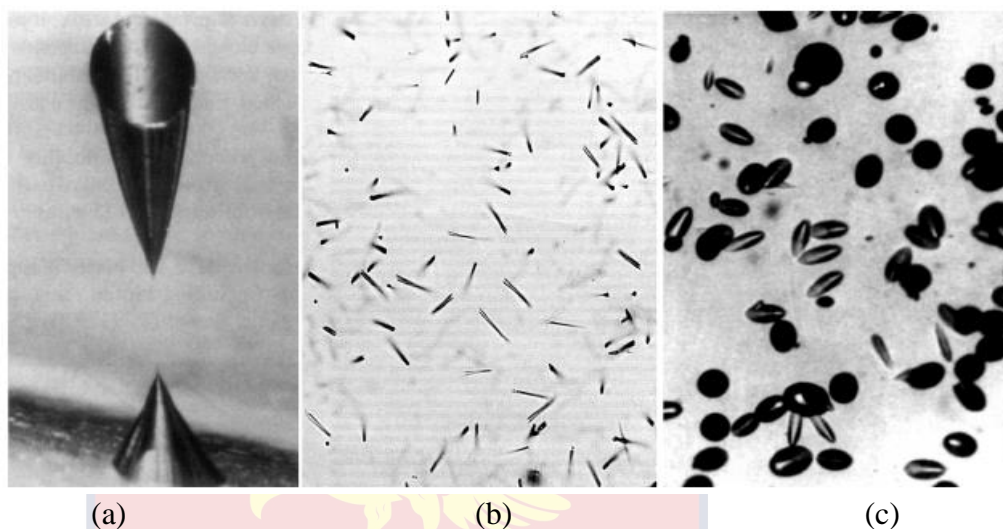


Figure 4: Track Revelation

Source: L'Annunziata (2012)

Figure 4: (a) Etched track of a cosmic ray (Argon) ion that penetrates an Apollo electrophoresis device made of Lexan (b) etched spontaneous-fission tracks (^{238}U) in Durango apatite; and (c) etched neutron-induced fission tracks (^{235}U) in obsidian glass.

The two forms of etching are chemical and electrochemical etching. This work will employ the chemical etching process and it is discussed below. The principle of the ECE method is to apply a high –frequency (several KHz) electric field ($\sim 30\text{-}50\text{ KVcm}^{-1}$) across two components of an etching cell, filled with a conducting etchable solution example NaOH and separated by a plastic detector containing etchable tracks on its surface. After a period of chemical pre-etching, which produce sharp tipped tracks, the electric field at the tip builds up to a value equalling the breakdown limit of the dielectric medium, i.e. the plastic detector.

Chemical Etching

A thermostatically controlled bath is normally used for chemical etching. For plastics, the most frequently etchant used is sodium hydroxide (NaOH) or potassium hydroxide (KOH). The concentrations usually range from molarities of 1- 12 (~ 6 M being the most popular). The temperature usually used ranges from ~ 40 °C to 70 °C. Sometimes ethyl alcohol is added to the etchant to increase sensitivity and speeding of etching. A large beaker is usually placed inside the temperature-controlled bath, and it is this beaker which contains the etching solution. Several detectors that are to be etched simultaneously are suspended by means of strings or wires making sure that they do not touch each other. The beaker is covered to reduce evaporation. According to different properties of the etched tracks, the detectors can be classified into two categories. (i) thin detectors where the majority of etched tracks are etched through holes; (ii) thick detectors where the residual foil thickness is greater than the etched-track depth. Simple schematic diagram of thin and thick detector is shown in Fig 5. In the diagram below a) represents the thin detector and b) represents the thick detector

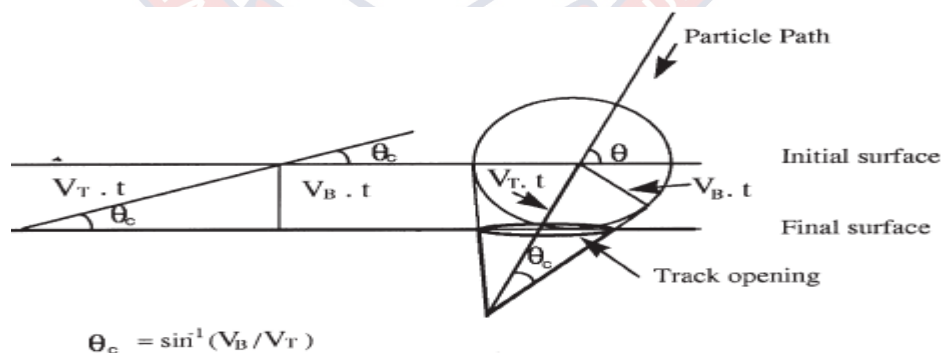


Figure 5: Simple Schematic Diagram of Thin and Thick Detector.

Source: (Griffith & Tommasino, 1990; Kpordzro, 2018)

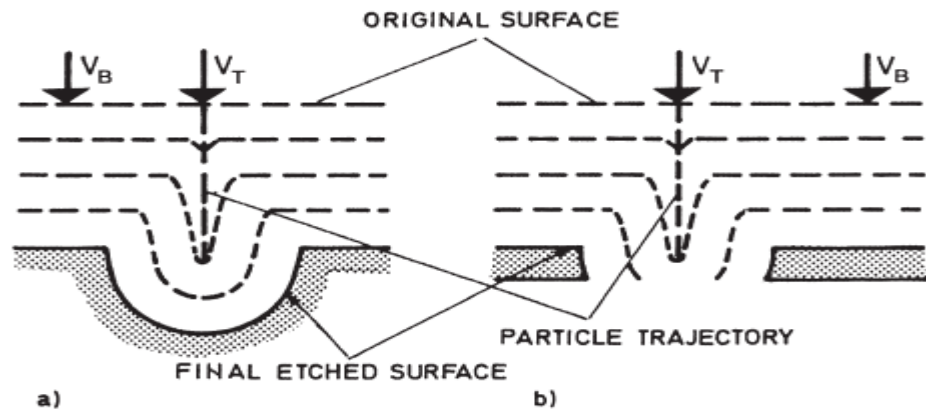


Figure 6: Theory of Etching

Source: (Griffith & Tommasino, 1990; Kpordzro, 2018)

In the figure 6, there is an angle θ_c for each medium and a given heavy ion such that by the time that the etchant travels a distance $V_B t$ vertically into the body of the detector, it reaches the end of the range of the particle proceeding along that “dip angle” θ_c at the same instant, i.e. $\frac{V_B t}{V_T t} = \sin \theta_c$.

Only tracks making dip angles with the detector surface, such that $\theta > \theta_c$, will thus leave observable track openings. The half cone angle of all such etch pits is

$$\text{also } \theta_c = \sin^{-1} \left(\frac{V_B}{V_T} \right) \text{ (Durrani, 1997).}$$

Track Counting and Evaluation

Various authors have designed and proposed image analysis methods to automatically count tracks. Advanced and automatic track counting systems based on new optical devices coupled with microprocessors have also been employed to count the tracks. In one such device, images of the tracks focused under the microscope, scanned through a camera to an image digitizer in the

PC. These digital images are subsequently analysed by a software called Image Pro Plus. The evaluation of SSNTD for track diameter and track density is done by various methods. Some of the methods are manual or ocular counting; spark counting and analysis with image analyzers. Previously, works done at the SSNTD Laboratory, counting was done using the spark counter which destroys detectors after sparking but with the new method of counting proposed by De Cicco, Pugliese, Roca, and Sabbarese (2013), detectors scanned and counted can be re-used for future works. This method has been used for this thesis and the method will be discussed.

Scanner Image Acquisition

The image acquisition is performed using a high-resolution commercial scanner. In this work the Epson Perfection V600 having 4800 x9600-dpi resolution and 48-bit for colour and 16-bit for grey maximum depth will be used. An important characteristic of the scanner is its double-lighting system. The films are inserted between two rigid transparent sheets on the scanner surface. This arrangement provides a reasonable uniform illumination of the films, reducing the formation of folds and/or bubbles.

The negative acquisition of the film image is carried out using 24-bit colour depth and 4800-dpi resolution. This choice produces an image that allows discerning appropriately tracks without requiring too much memory. A square area inside the exposed surface of the film is acquired.

Since the presence of tracks interferes with the thickness determination, two different acquisition setting modes are used for thickness determination and track counting. In particular, the automatic exposure selection, that makes tracks

more evident, is disabled for thickness determination (Figure 7a) in contrast to what is done for track counting (Figure 7b).

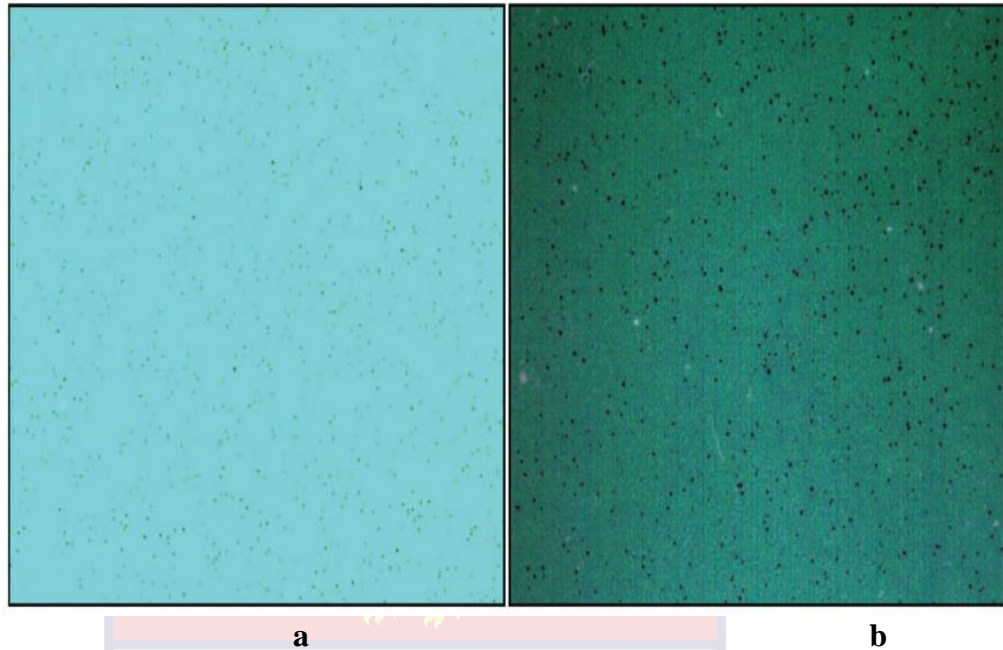


Figure 7: LR-115 Detector Images Obtained from Scanner

Source: (De Cicco et al., 2013)

Detection of Gamma Radiation

Interaction of Gamma Radiation with Matter

There are three main mechanisms with which gamma-rays interact with matter. The energy of the radiation affects which type of interaction it undergoes with more probability. The interactions and their energy dependence are:

- Photoelectric effect, dominant at low energies,
- Compton scattering, more probable at moderate energies,
- Pair production which occurs only at and above 1.022 MeV increasing in probability above this photon energy.

Figure 8 depicts the dependence of each of the three mechanisms on photon energy and material atomic number.

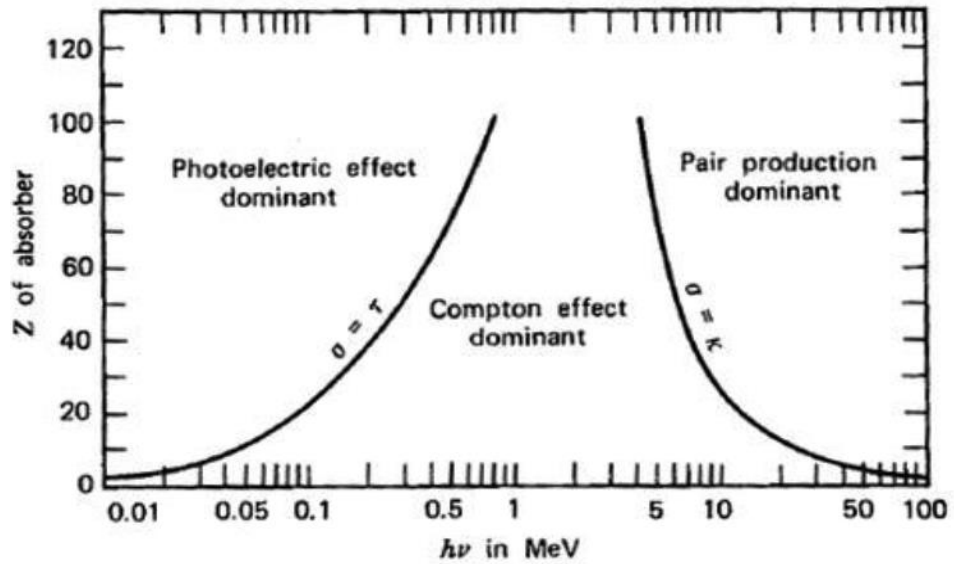


Figure 8: Interaction Mechanisms of X and Gamma-Rays with Matter as a Function of Photon Energy and Atomic Number

Source: (Knoll, 2000)

Compton Scattering

Compton scattering is an elastic scattering between a gamma photon and an electron. The electron, called the recoil electron, gains part of the photon energy and the photon is scattered with the rest of its energy in an angle theta, see Figure 9. The scattered photon energy ($h\nu'$) is given by

$$h\nu' = \frac{h\nu}{1 + \frac{h\nu}{m_0c^2}(1 - \cos\phi)} \quad (12)$$

where m_0c^2 is the rest mass energy of the recoil electron (= 0.511 MeV).

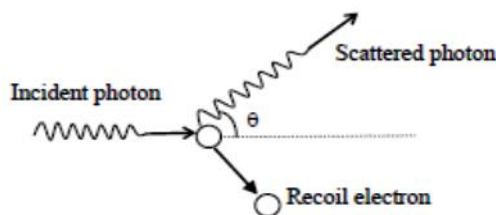


Figure 9: Compton Scattered Gamma Photon

Source: (Taylor, Dubson, & Zafiratos, 2004)

Pair Production

Pair production occurs when a gamma photon interacts with the Coulomb field of a nucleus. The photon disappears and its energy (E) is converted to an electron positron pair, Figure 10. The gamma photon must possess energy higher than 1022 keV, which is the combined rest mass of the electron and the positron ($=2m_0c^2$).

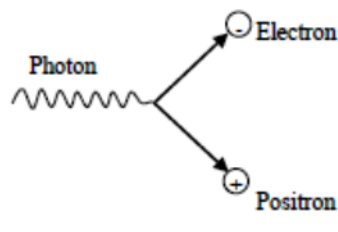


Figure 10: Pair Production Process

Source: (Taylor et al., 2004)

Excess energy over the pair rest mass appears as kinetic energy of the pair:

$$E = 2m_0c^2 + E_{e^-} + E_{e^+} \quad (13)$$

where E_{e^-} is the kinetic energy of the electron and E_{e^+} is the kinetic energy of the positron. Pair production is more probable for higher gamma energies, and it dominates the total interaction probability for photon energies above 5 MeV, see Figure 10.

Empirical Framework

Exposure to radon has been seen to pose a risk to the health of humans. One such risk is radon's association with lung cancer. Studies have shown that radon causes lung cancer, and is a threat to health because it tends to collect in places frequented by people such as mines and Caves [Lario et al., (2005)]. It has been identified as the largest source of exposure to naturally occurring radiation. Since the 1970s, the investigations of exposure of

radon radiation in underground mine and Caves systems in many parts of the world have taken place (Przylibski, 1999). Research has been conducted in amongst others, Poland, Australia, United States, Venezuela, Switzerland, Northern Spain, Italy, Hungary, Egypt, Ireland, Greece, Slovenia, Norway and many more (Colgan & Gutiérrez, 1996; Coskeran et al., 2002; Denman et al., 2005).

The results of the surveys show that a relatively high ($>1000 \text{ Bq.m}^{-3}$) radon concentration is present in Mines and Caves, giving rise to appreciable occupational exposures. This has implications for tour guides and underground workers, because of the increased risk of lung cancer associated with exposure to elevated radon levels (M. S. Field, 2007).

Radon in Mines

In an abandoned Uranium mine Podgorze in Kowary, the concentration of Radon was measured in two points (Fijałkowska–Lichwa, 2016). The measurements were performed with two SRDN-3 active systems from April to September 2011 in two galleries one operating as tourist route and the second one planned to be opened for touristic visits.

The concentration of Radon in the visiting gallery ranges from 3 kBq/m^3 to 1015 kBq/m^3 . In the other gallery the radon concentration varies from 6.7 kBq/m^3 to 1072 kBq/m^3 . With the help of a ventilation system, the Radon concentration was lowered to 5 kBq/m^3 in adit 19 and 20 kBq/m^3 in adit 19a, (Fijałkowska–Lichwa, 2016). The author concluded that the maximum values of Radon activity concentration in both adits of the disused uranium mine 'Podgorze' in Kowary ranged from 800 kBq/m^3 to a million Bq/m^3 . Such a range was observed every hour between April and late June 2011".

In Kosovo, the Radon concentration was investigated in Trepca underground mine by Sadik Bekteshi et al.,(Bekteshi et al., 2017). The Trepca mine is located in northern Kosovo and is one of the most ramified and deep mines in Kosovo. This mine is situated in the so-called Trepca Mineral Belt, being one of the largest leads and zinc ore areas in Europe. In this mine the Radon concentration was measured with a Continuous Radon Monitor CRM-510 using the method based on ionising chamber, recording data hourly up to 96 hours, and, also with a portable radon monitor PRM-145. In the second case, air sample of 0.7 dm³ were collected in special cells and measured after 3 hours, necessary time to reach the equilibrium of Radon and its progenies. The Radon concentration was measured in 2015 in two campaigns first from February to April and second from September to December. The Radon concentration in Trepca mine has an average activity of 286 Bq/m³ and a maximum activity of 691 Bq/m³. The authors observed that the average radon concentrations were found to range from 245 Bq/m³ (horizon V) to 441 Bq/m³ (horizon XI). Most enhanced values, up to 691 Bq/m³, occurred at mining locations in horizon XI". Also, the authors concluded the radon concentration measured in the Trepca mine in 2015 varies from 54 Bq/m³ to 691 Bq/m³. The average and median indoor radon concentrations were 286 Bq/m³ and 279 Bq/m³, respectively. Radon concentrations at all horizon sites were below the actionable level ranges for workplaces recommended by ICRP."

The Radiological Protection Institute of Ireland in spring 1993 conducted a preliminary investigation to establish the levels of radon and its decay products present in Irish show Caves. The Caves investigations included: Aillwee Cave, Ballyvaughan country Clare, Mitchelstown Cave, Burn court,

County Tipperary, Crag Cave, Castle Island, and Country Kerry. These Caves are located in carboniferous limestone in Ireland and attract thousands of visitors each year (Duffy, Madden, Mackin, McGarry, & Colgan, 1996; Nemangwele, 2005). In Aillwee Cave a high value of radon concentration (2040 Bq.m^{-3}) was found at the central part of the Cave around Mud hall and the Cascadee. In Mitchelstown Cave, the highest level of radon concentration was found namely 5590 Bq.m^{-3} . In Crag Cave, the average radon concentration of three Caves surveyed showed a highest recorded value of about 7400 Bq.m^{-3} in Tube, Kitchen and Crystal gallery. This value indicates that the potential for dangerous radon exposure is high.

The Australian National Health and Occupational Council (NHMRC) and the National Occupational Health and Safety Commission (NOHSC) have prepared jointly, recommendations and standards based on the ICRP recommendations, for application in the Australian context. Australia has over 60 tourist or show Caves, under the management of the various state departments, local authorities, or private groups. Preliminary measurements in some of these Caves have shown ^{222}Rn levels of 1000 Bqm^{-3} (Guides; Solomon et al., 1996).

ICRP 65 has produced guidelines and recommendations dealing with workplace exposure to elevated background radiation. An intervention level for ^{222}Rn of 1000 Bq.m^{-3} is proposed (Solomon et al., 1996) as the limit, which is associated with the risk of inhalation of radon and radon progeny. These ^{222}Rn levels show no risk to members of the public viewing the Caves, but may present a potential long-term health risk for the 200 or more full-time staff

spending extended periods conducting tours or carrying out maintenance within the Caves.

The NRPB demonstrated that several regions in the United Kingdom has elevated radon levels. The granite areas of Cornwall and Devon have been found to have substantially elevated levels of radon. The metamorphic aureole around the granite areas has also been identified as having a significant impact on indoor radon levels. Radon surveys in Caves in such areas face a number of difficult problems. These include the security of radon detectors and the difficulty of designing the placement of detectors necessary to determine, with reliability, the spatially complex pattern of radon concentration.

The radiation dose from the exposure to radon progeny can be derived from measurements of the Potential Alpha Energy Concentration (PAEC) combined with a Dose Conversion Factor (DCF or dose per unit intake) which reflects the radiation dose to the respiratory tract from the deposition of the inhaled progeny (Vogiannis & Nikolopoulos, 2015).

The International Commission for Radiological Protection (Ann, 2000) in its publication recommends the use of a single factor of 5 mSv per WLM, determined from uranium mining epidemiological studies, as the preferred method converting radon progeny exposure to effective dose (radon progeny conversion convention). Working Level Month (WLM) is an exposure to 1 working level for 170 hours (2,000 working hours per year/12 Month per year = approximately 170 hours per Month).

The Basic Safety standard (BSS) gives a yearly average concentration for radon level in the work place of 1000 Bq.m^{-3} (Sonntag & Frese, 2002).

This value is the midpoint of the range of 500–1500 Bq.m⁻³ recommended by the International Commission of Radiological Protection (Ann, 2000).

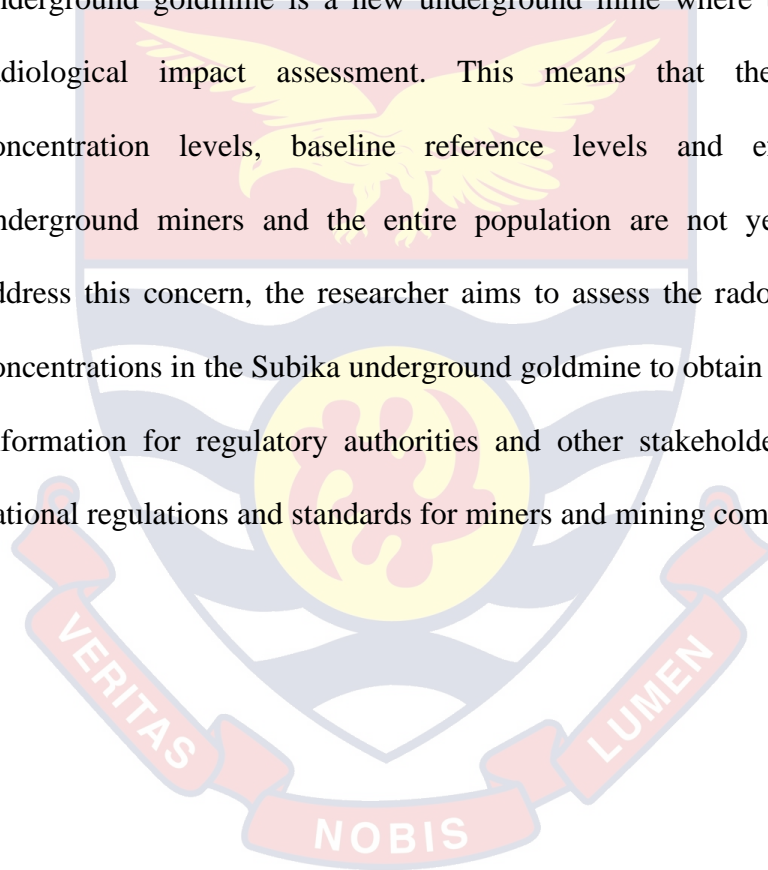
In the workplace employers are required under the ionizing radiation act of 1985 (United Kingdom) to remediate if the levels are above 1000 Bq.m⁻³ (Gillmore et al., 2000). Some other organization may wish to use a lower level than that specified in the BSS.

The above discussion shows that radon include in a risk to human life and that a lot of effort has been put into understanding radon and how it affects humans. Measurements of radon have been made all over the world and standards given to show radon danger levels. However, it is clear from the literature that enough information on radon concentration is not readily available in Ghana and therefore there is a need to fill this gap in any way possible. This study, which is aimed at assessing the radiological impact of an underground goldmine to determine the level of exposure to workers and members of the public is one of the contributions to reduce radon and other naturally occurring radioactive materials information gap in Ghana. This information is important for comparison purposes because similar underground gold mining exist in the western part of Ghana formerly called Gold Coast.

Chapter Summary

Epidemiological studies have revealed a strong correlation between lung cancer and exposure to radon and it was also identified as a human lung carcinogen in 1986 by the World Health Organization. The inhaled radon passes from lungs into the blood and body tissues and may irradiate different soft tissues causing cancers such as lung cancer, kidney cancer and prostatic cancer.

High concentration of radon is found in poorly ventilated structures, mines, caves, ancient tombs etc. Ghana has not yet carried out any systematic studies on radon levels on a national scale even though studies on radon have been carried out over the past two decades by some researchers in the country. These studies have been independent and uncoordinated and have focused only on a few areas of interest. However, studies on the concentration levels of radon and its progeny in underground goldmines in Ghana are limited. The Subika underground goldmine is a new underground mine where there has been no radiological impact assessment. This means that the average radon concentration levels, baseline reference levels and effective dose to underground miners and the entire population are not yet established. To address this concern, the researcher aims to assess the radon and its progeny concentrations in the Subika underground goldmine to obtain reference data and information for regulatory authorities and other stakeholders to prepare the national regulations and standards for miners and mining companies.



CHAPTER THREE

METHODOLOGY

Introduction

In this section, a description of the study area, population, sampling technique, sample preparation and measurement procedures are presented.

Description of Study Area

Location, Geology and Sampling Points of the Underground Mine

The Subika Underground Goldmine (SUG) area is located approximately 300 km northwest of the capital city, Accra, 107 km northwest of Kumasi, and 40 km south of the regional capital of Sunyani. The SUG is being developed at the southern end of a mineralized zone that extends approximately 70 kilometres (km) in the central portion of Ghana. The SUG is an underground pit operation located at Kenyasi in the Asutifi North District of the Brong Ahafo Region. The nearest industrial site or Mine is Mensin Gold Bibiani Limited at Bibiani about 70 km southwest of Ahafo (Plant Site coordinates: 7°02'00" N, 2°23'00" W).

The current economic evaluation of the Mine indicates that Subika Underground mine contains an inventory of approximately four million ounces of gold with an average grade of 4.5 g/t Au. The SUG has the potential to provide between 200 koz and 300 koz of gold annually at peak production, over a 15 to 18-year mine life.

The SUG is proposed to be ultimately an underground long-hole open stopping mine producing approximately two million tons of ore per annum. The Mine operations use trucking and ramp haulage to bring ore to the

surface. The decline (twin portal) constructed during the exploration phase serves as the main access portals for the Underground Mine and they will be advanced as two separate declines from the main decline as mining progresses to access the ore deeper underground.

The Subika deposit is considered to be a typical example of an orogenic-style gold deposit.

Orogenic gold deposits occur in variably deformed metamorphic terranes formed during Middle Achaean to younger Precambrian, and continuously throughout the Phanerozoic. The host geological environments are typically volcano-plutonic or clastic sedimentary terranes, but gold deposits can be hosted by any rock type. There is a consistent spatial and temporal association with granitoids of a variety of compositions. Host rocks are metamorphosed to greenschist facies, but locally can achieve amphibolite or granulite facies conditions. Global examples of these deposits include Muruntau (Uzbekistan), Golden Mile (Australia), Hollinger-McIntyre-Moneta (Canada), Jamestown (USA), and Obuasi (Ghana).

The underground mine was constructed 1000 meters below the reference level and the sampling areas were within ten (10) different levels below the reference level. All levels indicate the depth of the underground goldmine from the reference level.

Geographical Positions of Sampling Areas.

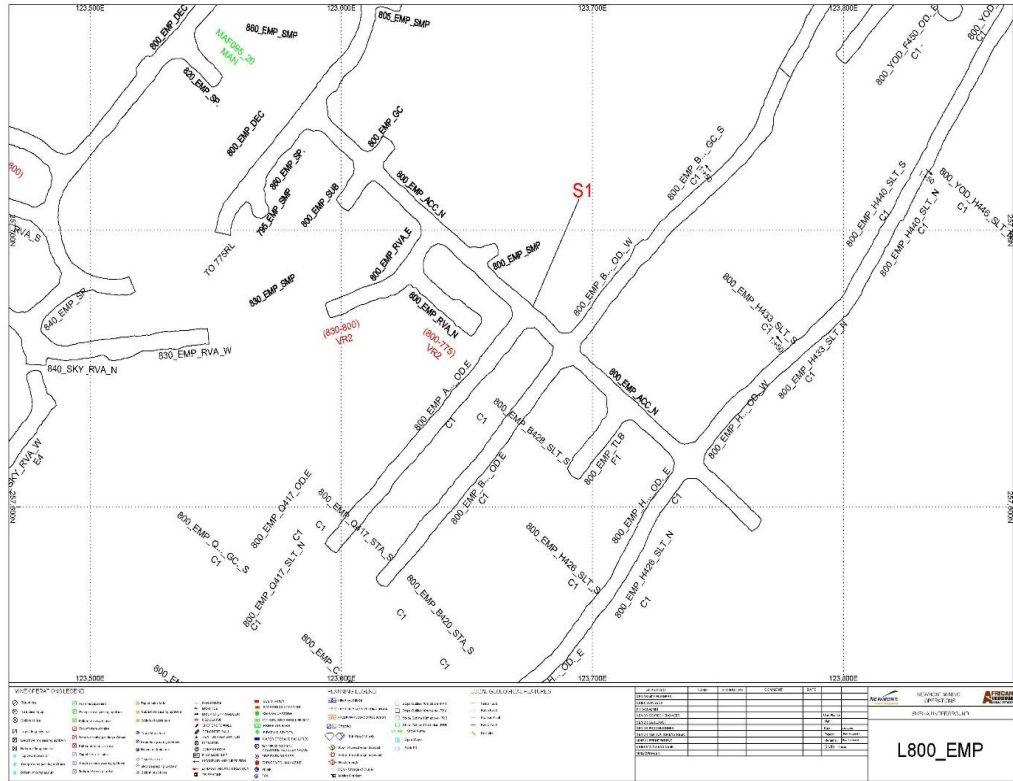


Figure 11: Sampling Area 1 (S1): Level 800 EMP

Source: Newmont Ghana Gold Limited

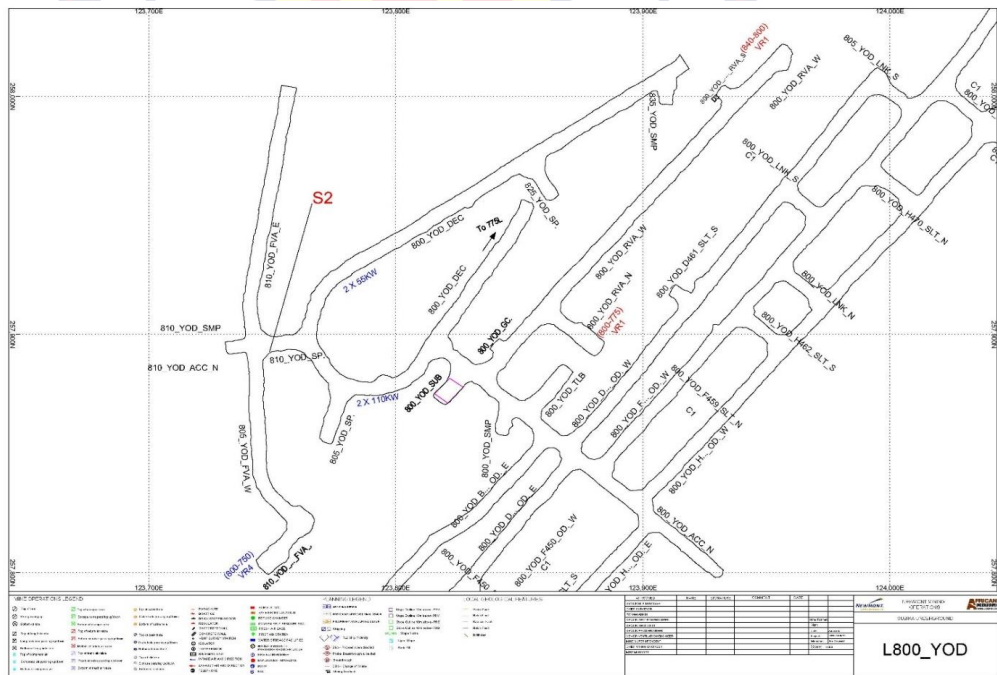


Figure 12: Sampling Area 2 (S2): Level 810 YOD

Source: Newmont Ghana Gold Limited

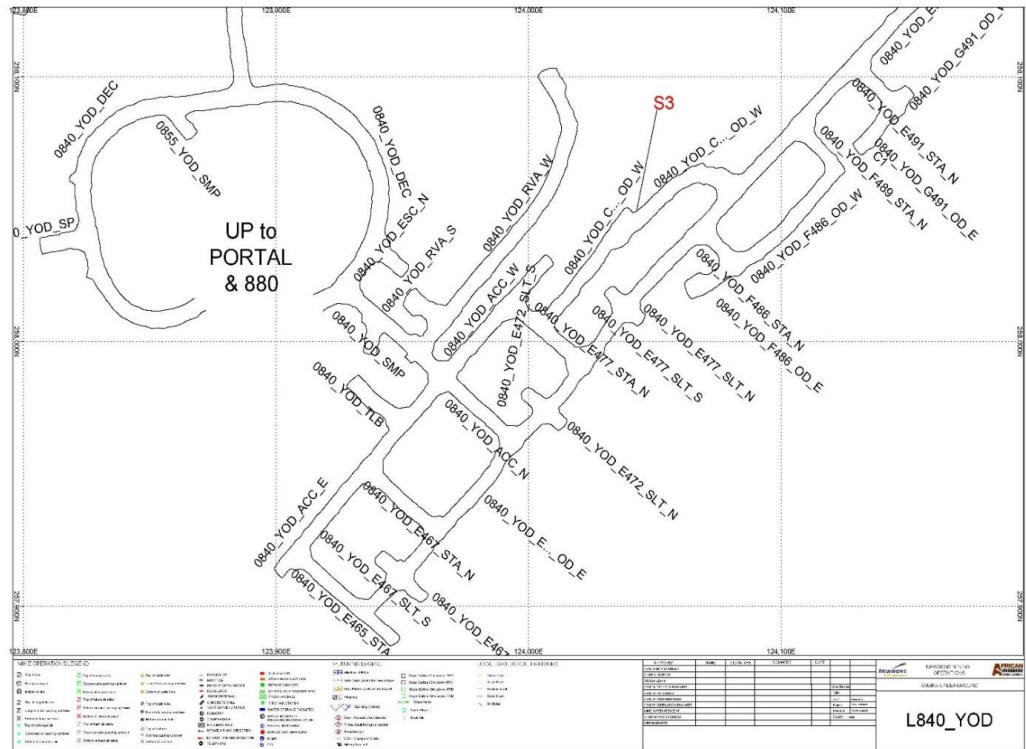


Figure 13: Sampling Area 3 (S3): Level 840 YOD

Source: Newmont Ghana Gold Limited



Figure 14: Sampling Area 4 (S4): Level 880 YOD

Source: Newmont Ghana Gold Limited

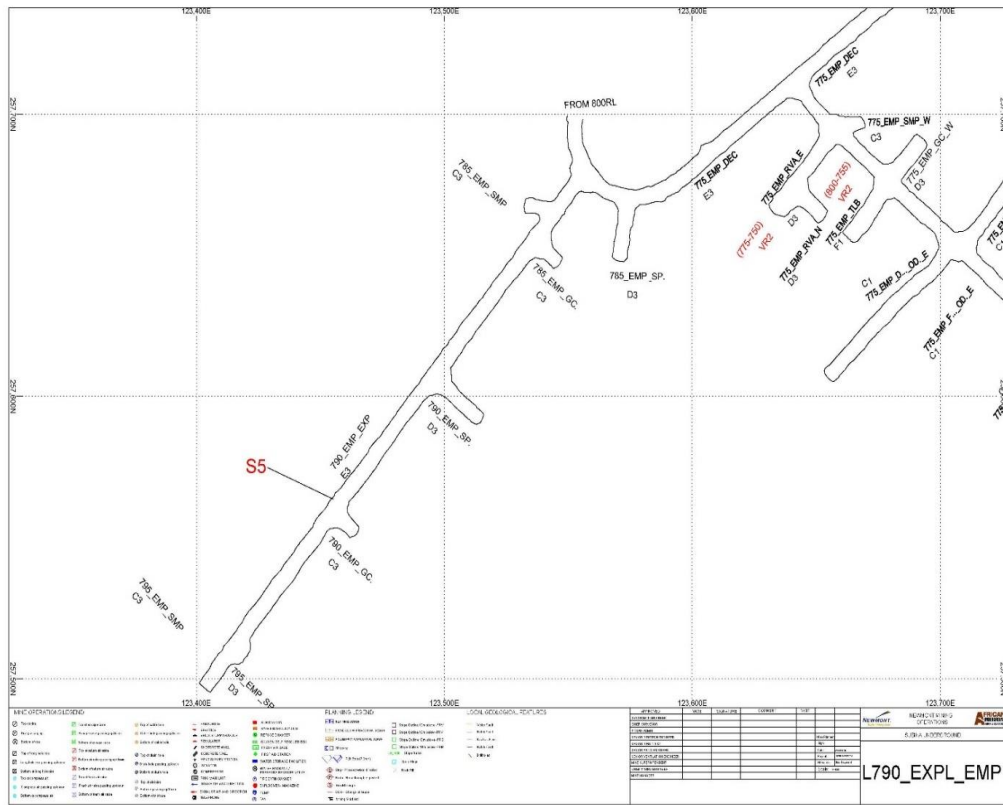


Figure 15: Sampling Area 5 (S5): Level 790 EXPL

Source: Newmont Ghana Gold Limited

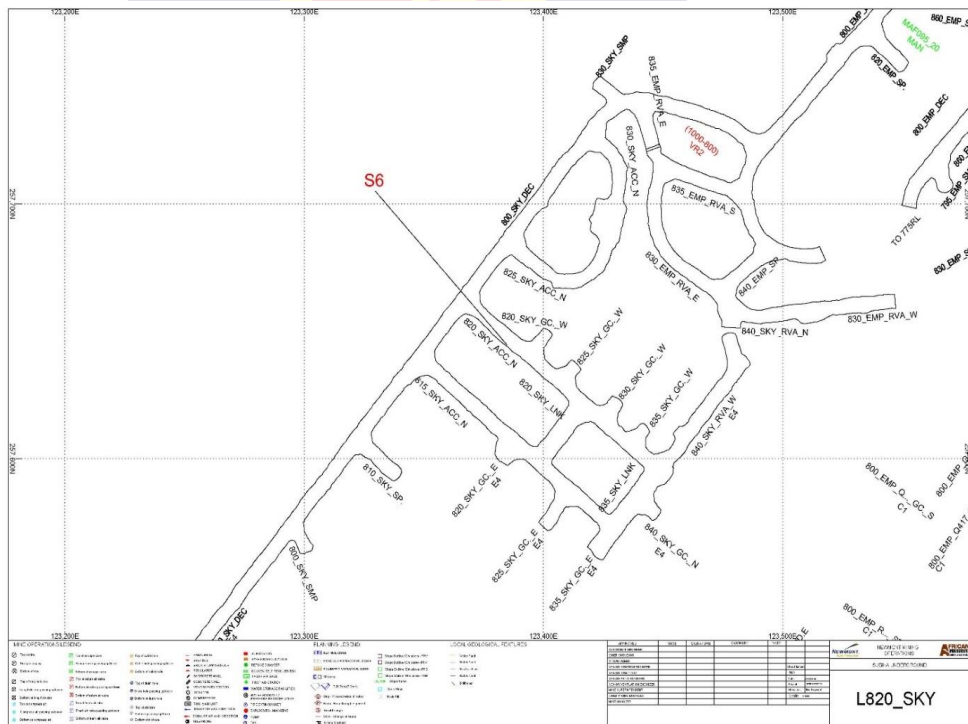


Figure 16: Sampling Area 6 (S6): Level 820 SKY ACCN

Source: Newmont Ghana Gold Limited

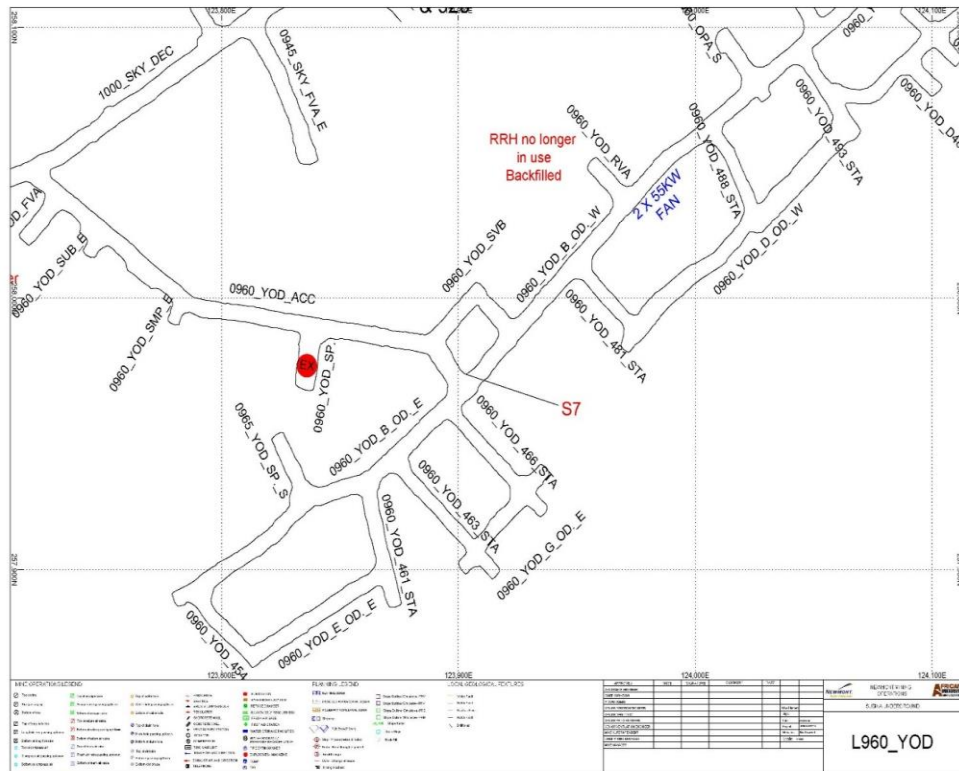


Figure 17: Sampling Area 7 (S7): Level 960 YOD

Source: Newmont Ghana Gold Limited

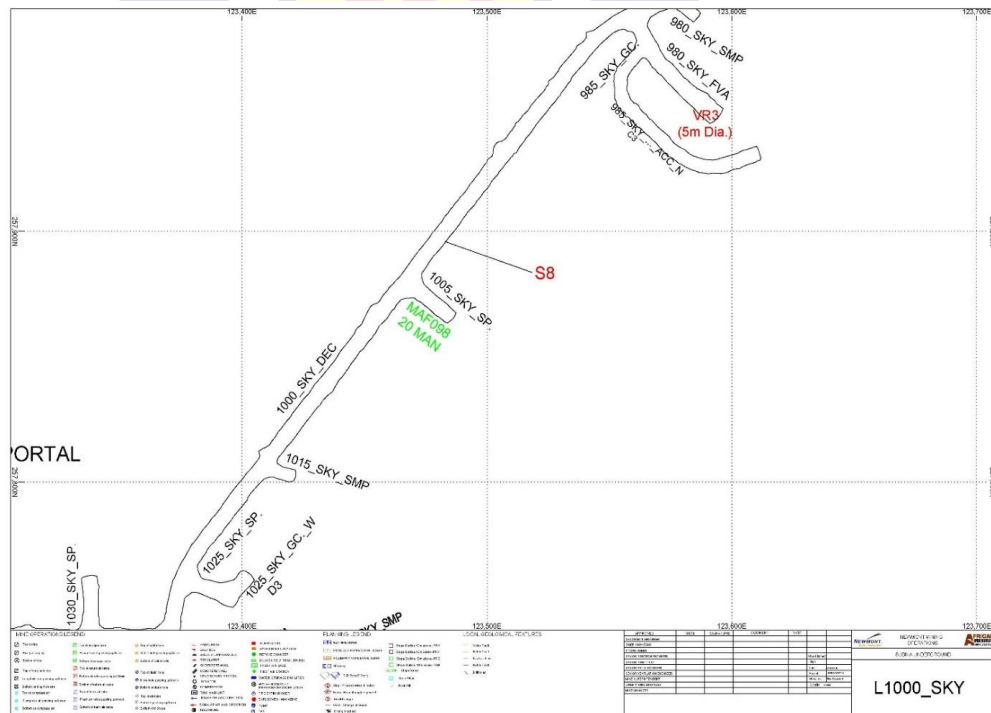


Figure 18: Sampling Area 8 (S8): Level 1000 SKY DEC

Source: Newmont Ghana Gold Limited

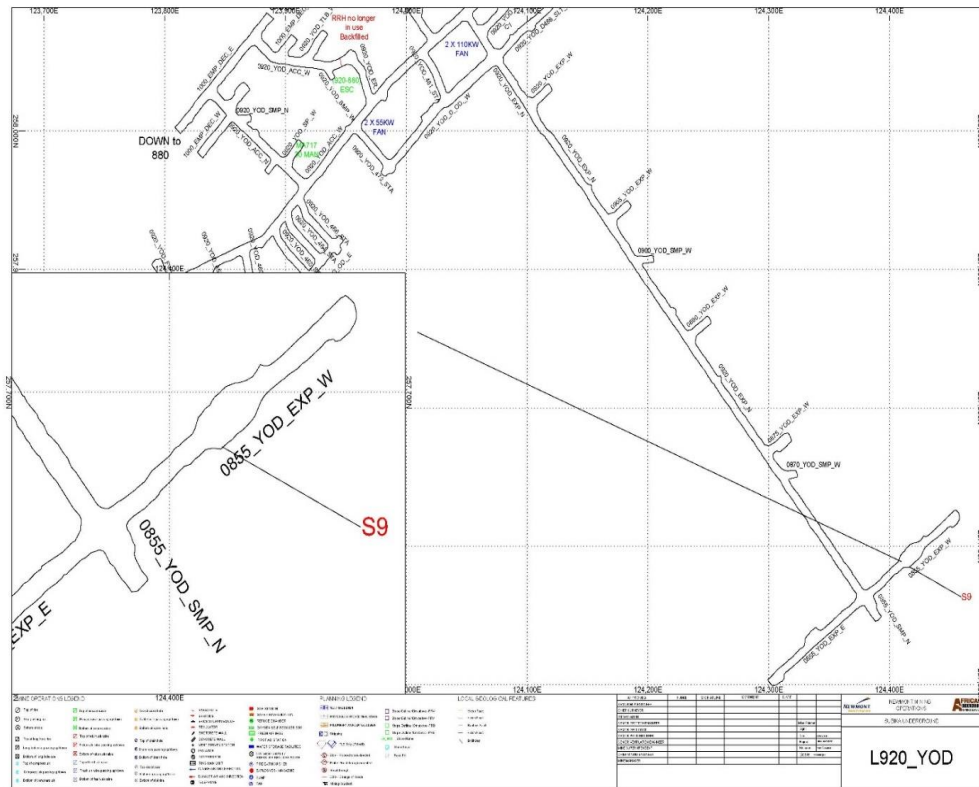


Figure 19: Sampling Area 9 (S9): Level 920 YOD

Source: Newmont Ghana Gold Limited

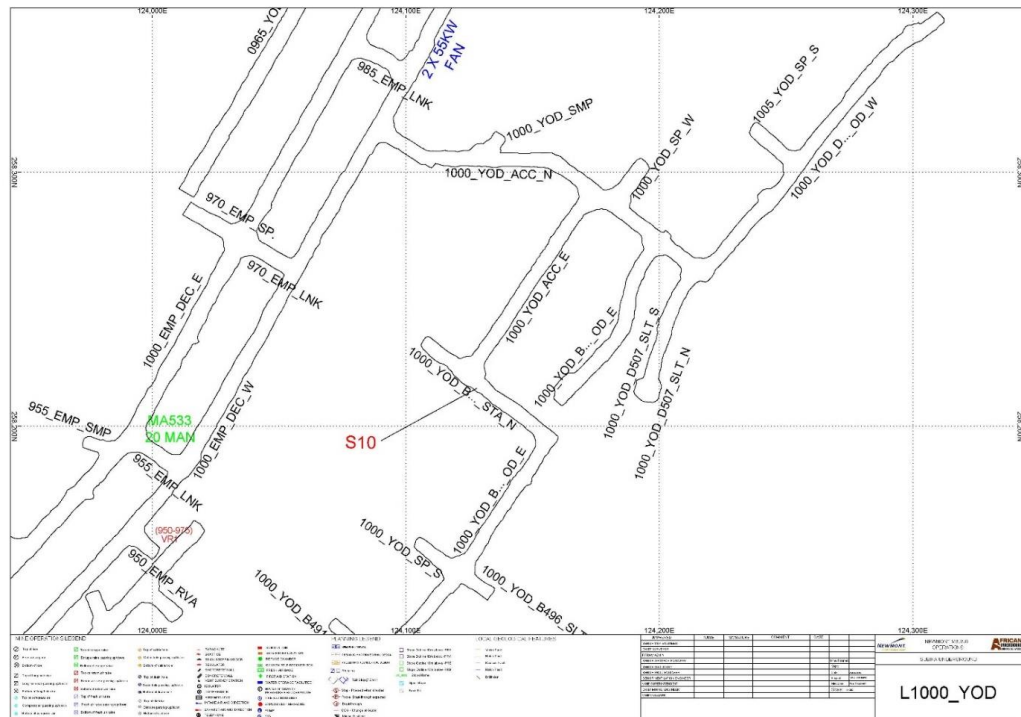


Figure 20: Sampling Area 10 (S10): Level 1000 YOD

Source: Newmont Ghana Gold Limited

Deployment of Detectors at the Sampling Points

The radon gas measurement was done using radon detectors made up of LR-115 (type II strippable) cellulose nitrate detectors manufactured by Kodak Pathé in France. The detectors of area $2\text{cm} \times 2\text{cm}$ were attached to a plastic dish with its sensitive side facing upwards and covered with a perforated plastic dish. The plastic dish with the radon detectors were installed at ten different location of the Subika underground mine

The detectors were planted in batches within the four quarters. The first quarter was between June to August 2018, the second quarter was between September to November 2018, the third quarter was between December 2018 to February 2019 and the fourth quarter was between March to May 2019. Each batch within the quarters was left at the sampling points for approximately four (4) weeks.

Forty (40) sampling points within the ten randomly selected points were chosen within the project site using a non- probability quota sampling. A total number of 40 dishes containing 80 detectors were deployed at the points for each batch (month) as shown in figure 21. In all a total number 320 detectors were deployed at the sampling points of which 20 of them were crushed by the heavy-duty vehicles underground leaving a total of 300 detectors to be analysed at the Nuclear Track detection Laboratory of Ghana Atomic Energy Commission.



Figure 21: Installation of Radon Detectors

Source: Field data 2019

Track Revelation

After exposure for one (1) month, the detectors were removed from the detector dish. 200 grams of sodium hydroxide pellet was weighed in a beaker with an electronic balance and the solution prepared in a 2L volumetric flask at the Nuclear Track Detection Laboratory of the Ghana Atomic Energy Commission. The detectors were then subjected to chemical etching in a 2.5 M concentration of sodium hydroxide solution at 60 °C, for two hours in a constant temperature water bath to enlarge the latent tracks produced by alpha particles from the decay of radon. After the etching, the detectors were washed with running cold water for 20 minutes to stop the etching process, then washed in distilled water for 15minutes. The detectors were then peeled whilst in the

distilled water and air dried on a cardboard as shown in figure 22. After a few minutes of drying in air, the detectors were ready for track counting.

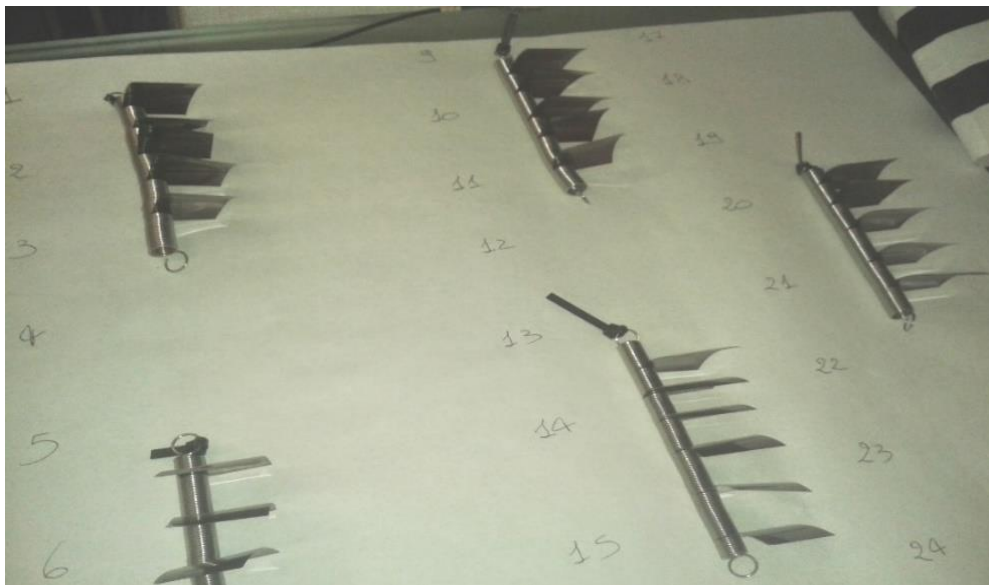


Figure 22: Air Dried Detectors

Source: Field data 2019

Image Acquisition and Counting of Tracks

The counting of tracks and the image acquisition was performed using a commercial scanner (Epson Perfection V600 Photo) manufactured in France, having 4800^x9600-dpi resolution and 48-bit for colour and 16-bit for grey maximum depth coupled to a laptop as shown in figure 23a. An important characteristic of the scanner is its double-lighting system. The films were inserted between two rigid transparent sheets on the scanner surface as shown in figure 23b. This arrangement provides a reasonably uniform illumination of the films, reducing the formation of folds and/or bubbles. The negative acquisition of the film image was carried out using 24-bit colour depth and 4800-dpi resolution. This choice produces an image that allows discerning appropriately tracks without requiring too much memory. A square area (1x1) cm² inside the exposed surface of the film was acquired as shown in Fig 24a.



a

b

Figure 23: Detectors Scanner Coupled to a Laptop

Determination of the Annual Effective Dose and Lung Cancer Risk

Radiation Dose Estimation

The exposure to radon daughters in the underground goldmine can be calculated on the basis of the measured radon concentration using the following equation and US EPA methodology (Pawel & Puskin, 2003; UNSCEAR, 2006).

$$ER = CR \times F \times n(2.7 \times 10^{-4}) \times 8760 / 170 \quad (14)$$

where, ER is exposure to radon daughters in WLM /y, CR is the radon concentration in $Bq\ m^{-3}$, 2.7×10^{-4} is the factor for the conversion of radon concentration to the WL per $Bq\ m^{-3}$, F is the equilibrium factor (0.4 for indoor), n is the occupancy factor, 8760 indicates total hours in the year, and 170 indicates the total working hours per month.

The annual effective dose due to radon in the underground mining has been estimated using the following formula (Quarto et al., 2015):

$$DE = ER \times DCF \quad (15)$$

where, DE is the annual effective dose (mSv y^{-1}) due to radon daughters, ER is the exposure to radon daughter in WLM y^{-1} as per equation (1) and DCF is the dose conversion factor (mSv per WLM). For the determination of effective doses for underground miners, the dose conversion factor of (DCF) of 5 mSv per WLM recommended by ICRP 65 has been used.

The excess lifetime cancer risk ($ELCR$) due to radon exposure of the population in the underground mine was determined using the following equation based on the methodology described in EPA report (Shoeib & Thabayneh, 2014)

$$ELCR = ER \times T \times FR \quad (16)$$

where, E_R is the radon daughter exposure in WLM per year (calculated by Eq. 1), T is the average lifetime expectancy for Ghanaians (62.4) and world average (70) (WHO,2015), and F_R is the risk coefficient for exposure to ^{222}Rn gas in equilibrium with its progeny. Based on the recommendation of the ICRP (International Commission on Radiological Protection), F_R is 5×10^{-4} per WLM (Valentin, 2007).

Soil and Rock Samples

Forty (40) sampling points within the 10 levels were selected, using the non- probability quota sampling technique, for radon detectors, soil and rocks samples. The choice of sampling was considered since the underground mine has been sub-divided into sections and sampling points were chosen based on areas that human activities often take place.

The soil and rock samples were taken quarterly from the sampling points making a total of 40 soil and rock samples in a quarter and 160 soil and rock samples for the year monitored. A total number of Forty (40) composite soil

samples were made from the 160 samples collected from the 10 levels in a year for analysis

Sample Preparation

The samples collected were used as representative samples of the soil and rock at the 10 levels of the underground mine and were prepared and processed in the following steps for reproducible results.

Soil and Rock

Drying

Soil and rock Samples were spread on clean stainless-steel trays and air dried for 24hrs. Initial sieving of soil was made and the pebbles, grass and any residual roots, leaves and branches of plants removed. After the initial sieving the samples were dried in an electric oven at a temperature of 110 °C for 10 hours.

Grinding

If the chemical and radiometric analysis is to be performed, it is essential that all surfaces coming into contact with the soil be stainless steel, plastic or wooden, preferably of a material, which cannot contaminate the sample. The dried samples were further crushed into fine powder at the Food and Environmental Laboratory of the Radiation Protection Institute, Ghana Atomic Energy Commission, until they could pass through a sieve of mesh size 20 μ m so that clay and material particles may be homogenized into fine powder size of reference material (Ahmed, 2005; Tufail et al., 1992). (The IAEA reference materials IAEA-RGU-1(U-ore), IAEA-RGTh-1 (Th-ore) and IAEA-RGK-1 (K-ore) with densities (1.33 ± 0.03)). Similarly, soil samples to be measured were prepared into the similar cylindrical containers that was used for

quality control and validation of analytical technique. The proper homogenization of the soil sample is essential for gamma spectroscopy system. The homogenised samples were transferred to Marinelli Beakers, which were completely sealed and stored for 1 month to allow the short-lived daughters of ^{238}U and ^{232}Th decay series (^{214}Pb , ^{214}Bi , ^{214}Po) to attain equilibrium with their long-lived parent radionuclides (^{226}Ra , ^{220}Ra) (ASTM, 1983; 1986). The sealed samples were weighed and each counted using a high purity germanium detector.

Direct gamma spectrometric analysis without pre-treatment (non-destructive) was used for the measurement of gamma rays for the soil samples using a High Purity Germanium detector (HPGE). The gamma spectrometry system consists of HPGE detector coupled to a computer based multi-channel analyser (MCA). The relative efficiency of the detector is 40 % with energy resolution of 2.0 keV at gamma ray energy of 1332 keV of ^{60}Co . The identification of individual radionuclides was performed using their characteristic gamma-ray energies and the quantitative analysis of radionuclides was performed using the Genie 2000 gamma acquisition and analysis software. The detector is housed in a 100 mm passive shielding of lead lined with copper, cadmium and plexiglass (3mm each) to reduce the background radiation. The detector is cooled in liquid nitrogen at a temperature of $-196\text{ }^{\circ}\text{C}$ (77 k). In order to determine the background distribution in the environment around the detector (quality control), ten (10) empty Marinelli beakers were thoroughly cleaned using nitric acid and counted for 36000 s in the same geometry as the samples. The background spectra were used to correct the net peak area of gamma rays of measured isotopes. The background spectra were also used to determine the

minimum detectable activities of radionuclides at each photo peak for the detector.

The activity concentration of ^{226}Ra was determined using the γ -ray emissions as shown in figure 36 and the respective γ -yield of ^{214}Pb at 351.9 keV (35.8%) and ^{214}Bi at 609.3 keV (44.8%). The ^{228}Ra activity concentration was determined through the γ -ray emissions of ^{228}Ac at 911 keV (26.6%), and the ^{228}Th activity concentrations were determined through the γ -ray emissions of ^{212}Pb at 238.6 keV (43.3%) and ^{208}Tl at 583 keV (30.1%) and 2614.7 keV (35.3%) taking into consideration a branching ratio of 33.7% from ^{212}Bi towards ^{208}Tl . The ^{40}K activity concentration was determined directly from its emission line at 1460.8 keV (10.7%) while the ^{137}Cs and ^{210}Pb activity concentrations were determined directly from the γ -ray emissions lines at 661.67 keV (85.1%) and 46.5 keV (4.3%) respectively. Finally, the ^{238}U activity concentration was determined through the γ -ray emissions of its daughter ^{234}Th (4.8%) (Darko, E, & Faanu, A., 2017).

Calibration of Gamma Spectrometry System

Prior to the measurements, the detector and measuring assembly were calibrated for energy and efficiency to enable both qualitative and quantitative analysis of the samples to be performed. A multi – element standard with source number AJ-9177 (supplied by the Eckert and Ziegler-calibration, Berlin, Germany) containing radionuclides with known energies (^{241}Am (59.54 keV), ^{109}Cd (88.03 keV), ^{57}Co (122.06 keV), ^{139}Ce (165.86 keV), ^{203}Hg (279.20 keV), ^{113}Sn (391.69 keV), ^{85}Sr (514.01 keV), ^{137}Cs (661.66 keV), ^{60}Co (1173.2 keV and 1332.5 keV) and ^{88}Y (898.04 keV and 1836.1 keV) and activities in a 1L Marinelli beaker was used.

Energy Calibration

The energy calibration was performed by matching the principal gamma ray peaks observed in the spectrum of the standard to the channel numbers. The formulae relating the energy and the channel number was expressed as (Darko et al., 2005)

$$E = A_0 + A_1CN \quad (17)$$

where, E is the energy, CN is the channel number for a given radionuclide, and A_0 and A_1 are calibration constants for a given geometry. A graph of energy against channel number was plotted as shown in figure 24.

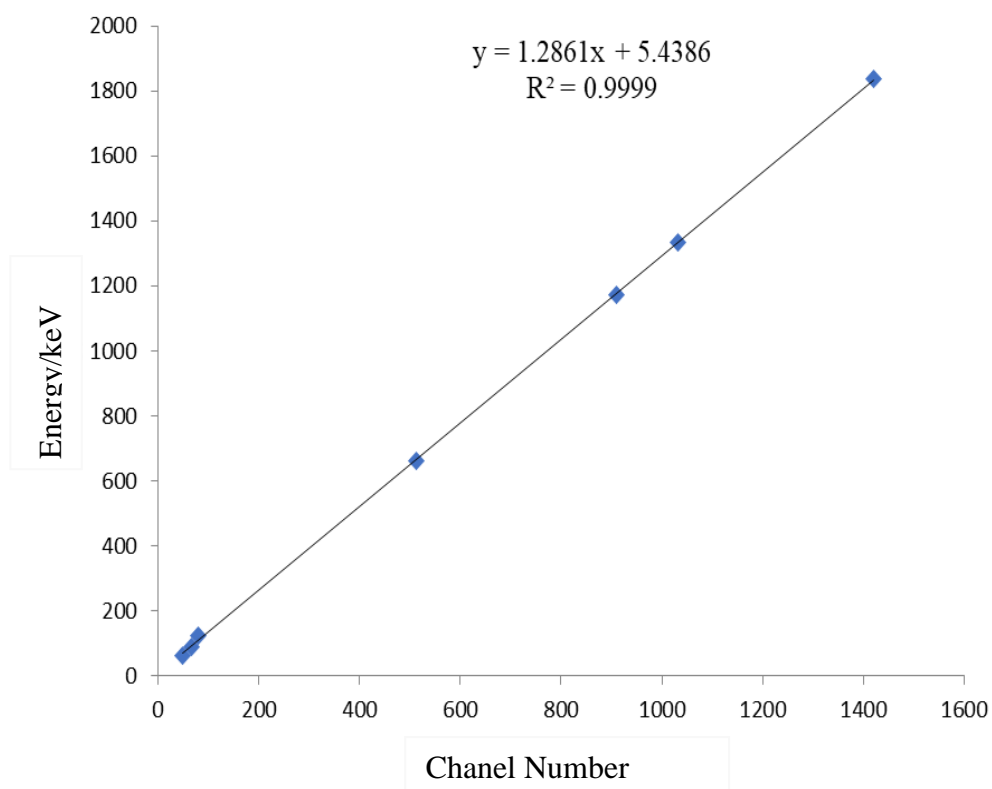


Figure 24: Energy Calibration Curve for 1000 ml Marinelli Geometry

Source: Eckert and Ziegler-Calibration

Efficiency Calibration

Efficiency calibration was performed by acquiring a spectrum of the standard until the count rate of total absorption could be calculated with a statistical uncertainty of $< 1\%$ at a confidence level of 95%.

The net count rate was determined at the photo peaks for all the energies to be used for the calculation of the efficiency. The efficiency was then related to the count rate and the activity of the standard by

$$\eta(E) = \frac{N_T - N_B}{P_E A_{STD} T_{STD}} \quad (18)$$

where, P_E is the gamma ray emission probability for the energy E , $\eta(E)$ is the efficiency of the detector, N_T is the total count under a photo peak in a peak range, N_B is the background counts, A_{STD} is the activity of the calibration standard for a given radionuclide in Bq at the time of measurement and T_{STD} is the counting time (Gazineu & Hazin, 2008).

The efficiency is related to the energy by the expression (Adjirackor et al., 2014).

$$\ln(E) = B_0 + B_1 \ln E + B_2 (\ln E^2) \quad (19)$$

where, B_0 , B_1 , B_2 are calibration constants for a given geometry and the other symbols have the usual meaning given earlier in the passage. The efficiency calibration curve is shown in figure 25.

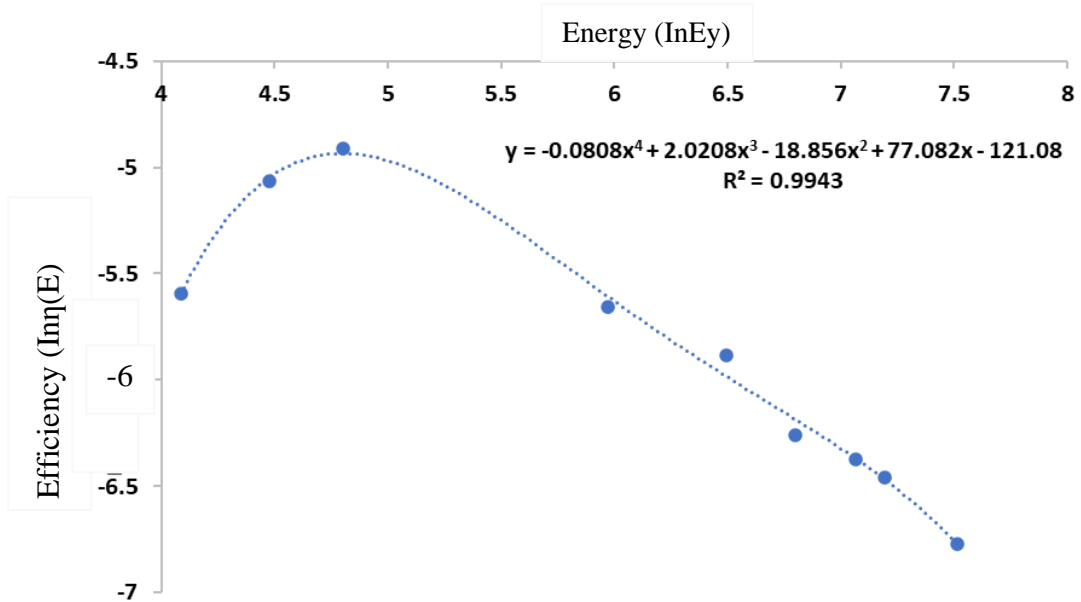


Figure 25: Efficiency Calibration Curve for 1L Marinelli Beaker Geometry

Source: Eckert and Ziegler-Calibration

From the efficiency calibration curve, the following expression was obtained:

$$y = -0.0808x^4 + 2.0208x^3 - 18.856x^2 + 77.082x - 121.08 \quad (20)$$

for $E_\gamma > 100\text{keV}$ where $y = \ln\eta(E_\gamma)$ and $x = \ln(E_\gamma)$

Specific activity concentration

The specific activities of samples were calculated from the expression

$$A_{SP} = \frac{N_{sam} e^{(\lambda T_d)}}{P_E \eta(E) T_C M_{sam}} \quad (21)$$

where M_{sam} is the mass of sample (kg), N_{sam} is the net counts for the sample in the peak range, P_E is the gamma emission probability, T_C is the counting time, $\eta(E)$ is the photopeak efficiency and T_d is the delay time between sampling and counting. The factor $\exp(\lambda T_d)$ is the correction for decay between sampling and counting. The world accepted criteria for ^{226}Ra , ^{232}Th and ^{40}K are 35, 40 and 400 Bq kg^{-1} respectively (UNSCEAR, 2000).

Minimum Detectable Activity

The minimum detectable activity (MDA) of the γ -ray measurements were calculated according to the formula:

$$MDA = \frac{\sigma\sqrt{B}}{\varepsilon PTW} (\text{Bqkg}^{-1}) \quad (22)$$

where, σ is the statistical coverage factor equal to 1.645 confidence level 95%, B is the background counts for the region of interest of a certain radionuclide, T is the counting time in seconds, P is the gamma yield for any particular element, W is the weight of the empty Marinelli beaker and ε is the efficiency of the detector. The minimum detectable activity (MDA) derived from background measurements was approximately 0.12 Bq kg^{-1} for ^{226}Ra , 0.11 Bq kg^{-1} for ^{232}Th and 0.15 Bq kg^{-1} for ^{40}K . Concentration values below these detection limits have been taken in this work to be below the minimum detection limit (MDL).

Radiological Impact Assessment of Soil and Rock Samples

Estimation of Hazard Indices

Radium Equivalent Activity (Ra_{eq})

The exposure due to γ -radiation is usually defined in terms of radium equivalent activity Ra_{eq} is given by Eq. (24) (Murugesan, et al., 2011)

$$Ra_{eq} = A_{Ra} + 1.43A_{Th} + 0.077A_K \quad (23)$$

The above equation is based on the assumption that 370 Bq kg^{-1} of ^{226}Ra , 259 Bq kg^{-1} of ^{232}Th , and 4810 Bq kg^{-1} of ^{40}K produce the same γ -dose rate. The radium equivalent is related to both the external γ -dose and the internal γ -dose from radon and its progeny. The permissible maximum value of

the radium equivalent activity is 370 Bq kg^{-1} , which corresponds to an effective dose of 1 mSvy^{-1} for to the inhabitants of dwellings (Esirole, et al., 2019).

External Hazard Index (H_{EX})

Some authors proposed a model for a room in the house where the inhabitants live with infinitely thick walls without windows and doors and calculated Hex using the following relation (Model I) (Esirole et al., 2019):

$$H_{EX} = \frac{A_{Ra}}{370} + \frac{A_{Th}}{259} + \frac{A_K}{4810} \leq 1 \quad (24)$$

Other authors modified such model to a room with windows and doors and calculated Hex using the following equation (Model II) (Baykara et al., 2011):

$$H_{EX} = \frac{A_{Ra}}{740} + \frac{A_{Th}}{518} + \frac{A_K}{9620} \leq 1 \quad (25)$$

where, the three factors of Eq. (25) are decreased to half their values in Eq. (24). In model II the presence of doors and windows will cause some kind of ventilation in the room which will decrease the exposure of inhabitants to radiation and decrease all kinds of doses (Mattsson et al., 2008). The value of this index must be less than unity in order to keep the radiation hazard insignificant. The prime objective of this index is to limit the radiation dose to the accepted dose limit of 1 mSvy^{-1} (Hewamanna et al., 2001).

Internal Hazard Index (H_{IN})

Inhalation of alpha particles emitted from the short-lived radionuclides (radon ^{222}Rn , the daughter product of ^{226}Ra) and thoron (^{220}Rn , the daughter product of ^{224}Ra) is also hazardous to the respiratory organs. This hazard can be

controlled by the internal hazard index (H_{IN}), (Righi & Bruzzi, 2006) which is given by the following Eq. 26.

$$H_{IN} = \frac{A_{Ra}}{185} + \frac{A_{Th}}{259} + \frac{A_K}{4810} \leq 1 \quad (26)$$

For the safe use of a certain building material in the construction of dwellings, the index (H_{IN}) should be less than unity.

External γ -Radioactivity Level Index (I_γ)

The external gamma index is also known as the representative level index and was calculated from the following relation in Eq. 27 (El-Gamal et al., 2007; NEA-OECD, 1979): It's the external radiation exposure due to gamma radiations.

$$I_\gamma = \frac{A_{Ra}}{300} + \frac{A_{Th}}{200} + \frac{A_K}{3000} \quad (27)$$

The OECD group of experts suggested some criteria for a definition of different levels to be (representative, first enhanced, second enhanced) (NEA-OECD, 1979).

$I_\gamma = 1$ as an upper limit

$I_\gamma \leq 1$ corresponds to 0.3 mSvy^{-1}

$I_\gamma \leq 3$ corresponds to 1 mSvy^{-1}

Concerning different building materials, the ranges are

Materials used in bulk amounts like bricks $I_\gamma < 1$

Superficial and other materials like tiles $I_\gamma < 6$

Internal (α -Radioactivity) Level Index (I_α)

The excess alpha radiation due to radon inhalation originating from building materials is estimated using Eq. 28 (El Galy et al., 2008):

$$I_{\alpha} = \frac{A_{Ra}}{200} \leq 1 \quad (28)$$

I_{α} should be lower than the maximum permissible value of $I_{\alpha} = 1$ which corresponds to 200 Bq kg⁻¹. For alpha radiation and taking into consideration that a building material with Ra concentration lower than 200 Bq kg⁻¹ could not cause indoor radon concentration higher than 200 Bq m⁻³.

Exposure Rate and Annual Effective Dose Equivalent at 1m from a

Radioactive Source

Exposure Rate (ER)

The exposure rate was calculated using the relation in Eq. 29 (Akhtar et al., 2005):

$$ER(\mu R h^{-1}) = 1.90A_{Ra} + 2.82A_{Th} + 0.0179A_K \quad (29)$$

Dose rate (DR) and its Relation with Exposure (ER)

The dose rate was calculated using the relations in Eq. 30 (O'Brien & Sanna, 1976)

$$ER(mSv y^{-1}) = 0.0833(\mu Sv h^{-1}) \quad (30)$$

Estimation of Annual Dose Rate

Air absorbed Gamma Dose Rate (D_{air})

The absorbed gamma dose rate in air 1 m above the ground surface for the uniform distribution of radionuclides (²²⁶Ra, ²³²Th, and ⁴⁰K) was computed on the basis of provided guidelines (Baykara et al., 2011; Hewamanna et al., 2001). The conversion factors used to compute absorbed gamma dose rate in air (D_{air}) per unit activity concentration in (1 Bq kg⁻¹) are 0.462 for ²²⁶Ra, 0.621 for ²³²Th, and 0.0417 for ⁴⁰K. Such dose parameter was calculated applying the following relation in Eq. 31 (Kurnaz et al., 2007):

$$D_{air} (nGyh^{-1}) = 0.462A_{Ra} + 0.621A_{Th} + 0.0417A_K \quad (31)$$

The population-weighted values give an absorbed dose rate in air outdoor from terrestrial gamma radiation a value of 57 nGy h⁻¹.

Annual Effective Dose Equivalent (AEDE)

To estimate the AEDE the conversion factor (0.7 Sv Gy⁻¹) from absorbed dose rate in air in nGy h⁻¹ to effective dose rate in mSv yr⁻¹ is used with outdoor occupancy factor of 0.2 and indoor occupancy factor of 0.8. The AEDE was calculated using the following formulae in Eq. 32&33 (Esirole et al., 2019):

$$AEDE(Indoor) = D_{air} (nGyh^{-1}) \times 8766 \times 0.8 \times 0.7 SvGy^{-1} \times 10^{-6} \quad (32)$$

$$AEDE(Outdoor) = D_{air} (nGyh^{-1}) \times 8766 \times 0.2 \times 0.7 SvGy^{-1} \times 10^{-6} \quad (33)$$

These indices measure the risk of stochastic and deterministic effects in the irradiated individuals. The recommended value of the annual effective dose equivalent is 0.48 mSv yr⁻¹ and the criterion of the total annual effective dose equivalent (indoors + outdoors) should be less than 1 mSv yr⁻¹ (Esirole et al., 2019).

The Annual Gonadal Dose Equivalent (AGDE)

The gonads, the active bone marrow and the bone surface cells are considered to be the organs of importance. An increase in AGDE has been known to affect the bone marrow, causing destruction of the red blood cells that are then replaced by white blood cells. The annual gonadal dose equivalent (AGDE) due to the specific activities of ²²⁶Ra, ²³²Th and ⁴⁰K was calculated using the following relation (Kurnaz et al., 2007).

$$AGDE(\mu Svy^{-1}) = 3.09A_{Ra} + 4.18A_{Th} + 0.0314A_K \quad (34)$$

The world averages of AGDE of a house containing activity concentrations of ^{226}Ra , ^{232}Th and ^{40}K are 35, 35 and 370 mSv yr⁻¹, respectively. The reference value of AGDE from UNSCEAR is 300 mSv yr⁻¹.

Excess Lifetime Cancer Risk (ELCR)

This gives the probability of developing cancer over a lifetime at a given exposure level. The ELCR has been calculated using the following equation (Kurnaz et al., 2007):

$$ELCR(\text{mSvy}^{-1}) = AEDE \times DL \times RF \quad (35)$$

where DL is the duration of life (70 years average) and RF is the risk factor (Sv) i.e. fatal cancer risk per Sievert. For stochastic effects, the ICRP 106 used a value of $RF = 0.05$ for the public.

Effect of Environmental Factors on Radon Concentration in the Underground Goldmine

The Multiple linear regression model assumes a linear relationship between the Indoor radon concentration as dependent variable and the environmental factors as predictor variables

General model

$$y(t) = \beta_0 + \beta_1 x_1(t) + \dots + \beta_n x_n(t) + \varepsilon \quad (36)$$

where

$y(t)$ the value of the dependent variable
 $x_1(t), x_2(t), \dots, x_n(t)$ the current variable, value of the dependent variable at a time t given by the values of the independent variables.

β_0 constant regression

β_n predictor coefficient $X_n(t)$

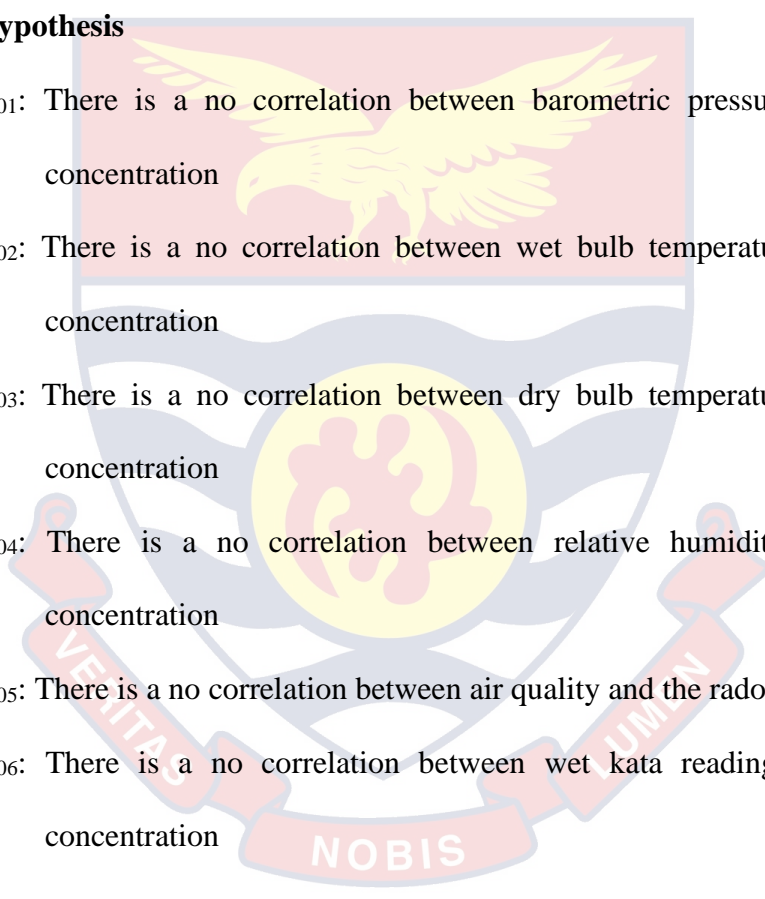
ε time error

Specific Model

$$RC = \alpha + \beta_1 BP + \beta_2 WBT + \beta_3 DBT + \beta_4 RH + \beta_5 AQ + \beta_6 WKT + \varepsilon \quad (37)$$

where RC = Radon Concentration (dependent variable) $\beta_1 BP$ = Barometric Pressure (I.V) $\beta_2 WBT$ = Wet Bulb Temperature (I.V), $\beta_3 DBT$ = Dry Bulb Temperature (I.V) $\beta_4 RH$ = Relative Humidity (I.V), $\beta_5 AQ$ = Air Quantity (I.V), $\beta_6 WKT$ β_6 WKT = Wet Kata Temperature (I.V).

Hypothesis

- 
- H₀₁: There is a no correlation between barometric pressure and the radon concentration
- H₀₂: There is a no correlation between wet bulb temperature and the radon concentration
- H₀₃: There is a no correlation between dry bulb temperature and the radon concentration
- H₀₄: There is a no correlation between relative humidity and the radon concentration
- H₀₅: There is a no correlation between air quality and the radon concentration
- H₀₆: There is a no correlation between wet kata readings and the radon concentration

Statistical Modelling

The time series analysis using moving averages was used to forecast and predict radon concentrations underground at a particular depth. The time series analysis reduces the error or assumes more perfect linear equations. A time series is a collection of data for some variables. The purpose of time-series analysis is to predict or forecast future values of the variable from past observations.

The least square method is used to describe the equation for the trend of radon concentration at different depths.

The trend equation is given by

$$y = a + bt \quad (38)$$

where

y = The protected value of the y variable for a selected value of t .

a = The Y – intercept and it's the estimated value of y when $t = 0$

b = the gradient or the slope of the line or the average change in y for each change of one unit in t .

t = any value of time that is selected.

Assumptions for the Model

1. The line of best fit is based on the assumption that there exists a linear relationship between the dependent variable (Radon Concentration) and independent variables (Barometric Pressure, Relative Humidity, Wet bulb temperature, Dry bulb temperature, Wet kata temperature).

This model assumes that the line of best fit is derived by minimizing the deviations of the points of the pair data from the line of regression. In the case of this research the trend equation will be modified as

$$y = a + bx \quad (39)$$

$$a = \frac{\sum y - b \sum x}{n} \quad b = \frac{n \sum xy - \sum x \sum y}{n \sum x^2 - (\sum x)^2} \quad (40)$$

where y = Radon Concentration b = regression coefficient x = depth from reference level

These values are substituted into equation 41 to obtain the trend equation using SPSS. Results from regression analysis may be used for forecasting and predictions of the radon concentration at different depths.

2. The model also assumes that all conditions at various depths of the underground mine have insignificant change, thus if all ventilation measures are considered at different depths as compared to the already existed depths underground.
3. In order to ascertain the reliability of the trend equation for making predictions interpolation (Prediction within the observed values of the dependent variables) and extrapolation (Prediction outside the observed values of the dependent variables) will be used, in this case the reliability of the model can be guaranteed. Extrapolation predictions cannot be guaranteed hence must be treated with caution.
4. The coefficient of determination will be used to determine the proportion or the percentage of the error or variation in the dependent variable 'explained' by the variation in the independent variable) using the Pearson's correlation coefficient.

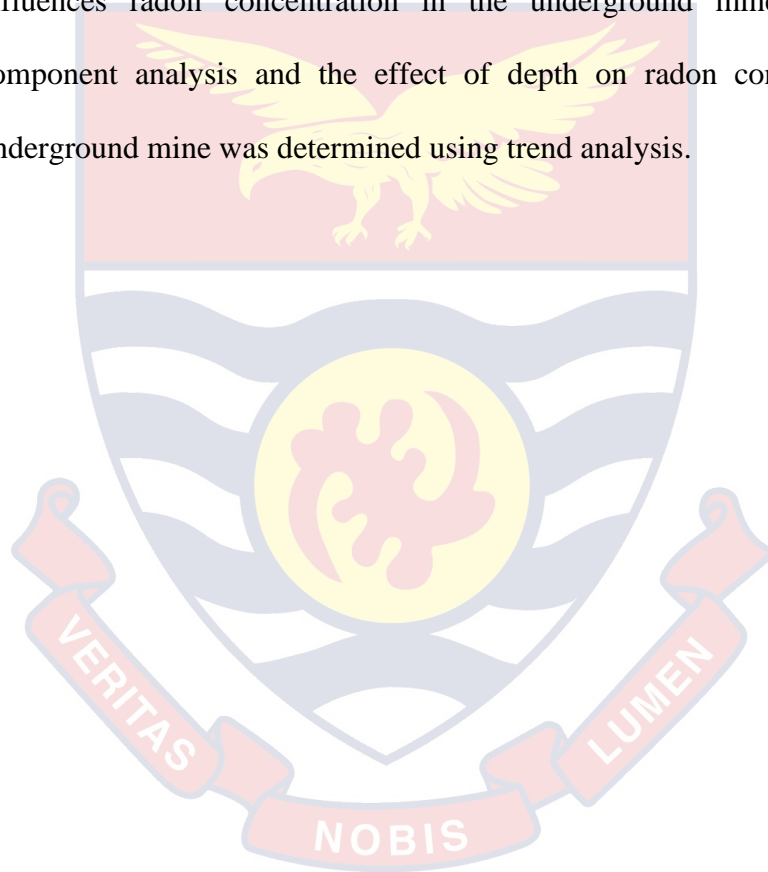
Chapter Summary

The radon gas measurement was done using radon detectors made up of LR-115 (type II strippable) cellulose nitrate detectors manufactured by Kodak Pathé in France to determine the annual effective dose and average lifetime cancer risk to the occupationally exposed workers.

Direct gamma spectrometric analysis without pre-treatment (non-destructive) was used for the measurement of gamma rays for the soil and rock samples collected from the ten levels in the underground mine using a High

Purity Germanium detector (HPGE). The gamma spectrometry system consists of HPGE detector coupled to a computer based multi-channel analyser (MCA) to determine the activity concentrations of terrestrial radionuclides to enable the assessment of radiological impact of occupationally exposed workers and the members of the public who may use the rock and soil samples for construction of buildings and building materials.

Statistical analyses were employed to determine the factors that influences radon concentration in the underground mine using principal component analysis and the effect of depth on radon concentration in the underground mine was determined using trend analysis.



CHAPTER FOUR

RESULTS AND DISCUSSION

Introduction

This chapter is concerned with the analysis, discussion and representation of results.

Radon Concentration in the Underground Goldmine

Table 6: Radon Concentrations at Locations for First Quarter

Location	Level	Radon Concentration Min-Max (Bqm ⁻³)	Radon Concentration Mean (Bqm ⁻³)	Skewness	Kurtosis
S1	800	4.25-47.73	28.97±16.22	-0.461	1.467
S2	810	4.45-22.34	9.48±5.90	1.769	3.224
S3	840	2.10-40.50	14.71±15.42	1.321	-0.106
S4	880	5.58-49.25	36.75±15.67	-2.163	5.033
S5	790	4.49-37.76	21.27±13.62	0.064	-2.265
S6	820	2.71-14.37	6.90±4.12	1.074	0.075
S7	960	2.59-12.38	8.39±3.63	-0.663	-0.368
S8	1000	2.14-43.38	14.37±14.45	1.521	1.427
	SKYDEC				
S9	920	3.80-43.87	23.08±13.37	-0.005	-0.940
S10	1000	3.32-50.42	22.69±19.15	0.419	-1.673
	YOD				
Average		2.10-50.42	19.08±15.49	0.640	-1.171

Source: Field Data 2018

The measured minimum and maximum radon gas concentration for the first quarter ranged from (2.10- 50.42) Bq/m³, with a mean and standard deviation of (19.08±15.49) Bq/m³. Level 880 with radon concentration of 36.75 Bqm⁻³ recorded the highest value of radon concentration for the first quarter as

shown in table 6. With respect to the distribution of radon concentration within the quarters using skewness and kurtosis. The pattern of radon concentration distribution in the first quarter shows a positive skewness in level 810, 840, 790, 820, 1000 SKY DEC, 920 and 1000 YOD and a negative skewness in level 800,880 and 960.

The pattern of radon concentration distribution in the first quarter shows a platykurtic distribution in level 800, 810, 820 and 1000 SKY DEC and a leptokurtic distribution in level 840,790, 960, 920 and 1000 YOD. However, a positive skewness and leptokurtic distribution was observed in the first quarter which was between the month of June to August. The insignificant values of both the values of skewness and kurtosis suggest a slightly symmetric or mesokurtic distribution in the first quarter.

Table 7: Radon Concentrations at Locations for Second Quarter

Location	Level	Radon Concentration Min-Max (Bqm ⁻³)	Radon Concentration Mean (Bqm ⁻³)	Skewness	Kurtosis
S1	800	39.92-176.37	112.09±54.23	-0.381	-1.614
S2	810	45.77-232.27	137.09±73.50	0.153	-1.540
S3	840	24.46-143.56	101.65±41.49	-0.985	0.217
S4	880	66.45-267.91	141.05±75.25	1.569	3.318
S5	790	32.68-151.84	94.46±51.08	0.131	-2.234
S6	820	175.72-182.49	177.68±3.25	1.867	3.495
S7	960	55.04-173.28	97.05±45.10	1.092	-0.304
S8	1000	55.04-147.24	93.58±38.57	0.651	-1.281
SKYDEC					
S9	920	94.63-193.87	130.74±43.01	1.025	-1.033
S10	1000	112.84-238.67	167.86±57.74	1.136	1.385
YOD					
Average		24.46-283.76	123.64±55.78	0.557	0.256

Source: Field Data 2018

The measured minimum and maximum radon gas concentration for the second quarter ranged from (24.46- 283.76) Bq/m³, with a mean and standard deviation of (123.64±55.78) Bq/m³

Level 820, 1000 YOD, 880, 810 and 920 with Radon concentration of 177.68 Bqm⁻³, 167.86 Bqm⁻³, 141.05 Bqm⁻³, 137.09 Bqm⁻³ and 130.74 Bqm⁻³ respectively recorded the highest value of radon concentration for the second quarter as shown in table 7.

The pattern of radon concentration distribution in the second quarter shows a positive skewness in level 810, 880, 790, 820, 1000 SKY DEC, 920 and 1000 YOD and a negative skewness in level 800 and 840. The pattern of radon concentration distribution in the second quarter shows a platykurtic distribution in level 840, 880, 820 and 1000 YOD and a leptokurtic distribution in level 800,840, 790, 960, 1000 SKY DEC and 920. However, a positive skewness and leptokurtic distribution was observed in the first quarter which was between the month of September to November. The insignificant values of both the values of skewness and kurtosis suggest a slightly symmetric (normal) or mesokurtic distribution in the second quarter apart from level 880 and 820 that showed a high platykurtic distribution of 3.318 and 3.495 respectively. A high leptokurtic distribution of -2.234 was observed in level 790.

Table 8: Radon Concentrations at Locations for Third Quarter

Location	Level	Radon Concentration Min-Max (Bqm ⁻³)	Radon Concentration Mean (Bqm ⁻³)	Skewness	Kurtosis
S1	800	36.00-111.00	61.61±42.71	1.729	-1.523
S2	810	31.00-141.00	89.84±41.12	-0.323	-1.110
S3	840	68.00-195.00	115.89±50.55	0.665	-0.940
S4	880	56.00-186.00	105.22±54.62	0.834	-1.355
S5	790	63.00-96.00	74.57±13.90	1.045	-0.869
S6	820	40.00-151.00	97.45±62.06	-0.010	-5.940
S7	960	41.00-127.00	71.74±41.42	0.950	-1.844
S8	1000 SKY DEC	34.00-185.00	95.17±59.66	0.631	-1.010
S9	920	33.00-72.00	53.92±15.91	-0.446	-1.612
S10	1000 YOD	40.00-166.00	91.13±56.75	0.717	-1.934
Average		31.00-195.00	86.60±46.03	0.782	-0.522

Source: Field data 2019

The measured minimum and maximum radon gas concentration for the third quarter ranged from (31.00- 195.00) Bq/m³, with a mean and standard deviation of (86.60±46.03) Bq/m³. Level 840 YOD and 880 YOD with Radon concentration of 115.89 Bqm⁻³ and 105.22 Bqm⁻³ respectively recorded the highest value of radon concentration for the third quarter as shown in table 8.

The pattern of radon concentration distribution in the third quarter shows a positive skewness in level 800, 840, 880, 790, 960,1000 SKY DEC and 1000 YOD and a negative skewness in level 810, 820 and 920. The pattern of radon concentration distribution in the second quarter shows a leptokurtic distribution in all the ten levels. However, a positive skewness and leptokurtic distribution

was observed in the first quarter which was between the month of December to February. The insignificant values of both the values of skewness and kurtosis suggest a slightly symmetric or mesokurtic distribution in the second quarter apart from level 820 that showed a high leptokurtic distribution of 5.940.

Table 9: Radon Concentrations at Locations for Fourth Quarter

Location	Level	Radon Concentration Min-Max (Bqm ⁻³)	Radon Concentration Mean (Bqm ⁻³)	Skewness	Kurtosis
S1	800	25.00-44.00	32.99±6.30	0.187	-1.202
S2	810	18.00-30.00	22.57±4.60	0.599	-1.329
S3	840	16.00-27.00	22.79±4.59	-0.777	-1.245
S4	880	21.00-38.00	28.97±6.10	0.123	-1.399
S5	790	26.00-46.00	34.13±7.68	0.754	-0.934
S6	820	18.00-30.00	26.30±3.78	-1.509	1.797
S7	960	25.00-36.00	28.99±3.66	0.863	0.345
S8	1000	18.00-29.10	24.58±3.63	-0.498	-1.182
	SKY DEC				
S9	920	30.00-31.00	29.95±0.40	0.599	-1.329
S10	1000	24.00-31.00	28.04±2.39	-0.850	0.234
	YOD				
Average		16.00-46.00	27.78±5.86	0.692	1.219

Source: Field data 2019

Finally, the measured minimum and maximum radon gas concentration for the fourth quarter ranged from (16.00- 46.00) Bq/m³, with a mean and standard deviation of (27.78±5.86) Bq/m³. Level 800 and 790 with Radon concentration of 32.99 Bqm⁻³ and 34.13 Bqm⁻³ respectively recorded the highest value of radon concentration for the fourth quarter as shown in table 9.

The pattern of radon concentration distribution in the fourth quarter shows a positive skewness in level 800, 840, 880, 790, 960, and 920 and a negative skewness in level 840, 820, 1000 SKY DEC and 1000 YOD. The pattern of radon concentration distribution in the second quarter shows a platykurtic distribution in level 820, 960 and 1000 YOD and a leptokurtic distribution in level 800,810,840,880,790, 1000 SKY DEC and 920. However, a positive skewness and platykurtic distribution was observed in the first quarter which was between the month of March to May. The insignificant values of both the values of skewness and kurtosis suggest a slightly symmetric (normal) or mesokurtic distribution in the second quarter.

A positive value indicates a positive skew and a positive skew distribution indicates that majority of the distributed radon concentrations are clustered around the left tail of the distribution while the right tail of the distribution is longer or the activity concentration distribution of radon contains lower activity concentrations as compared to higher activity concentrations. This distribution will tend to have a mean activity concentration of radon being greater than the mode. Also, a negative value indicates that the distributed radon concentrations are clustered around the right tail of the distribution while the left tail of the distribution is longer or the activity concentration distribution contains higher activity concentrations of radon as compared to lower activity concentrations. This distribution will tend to have a mean activity concentration of radon being less than the mode.

Kurtosis describes the shape or peakedness of a distribution and how data set are clustered or spread around the mean. A positive value indicates a leptokurtic distribution and a leptokurtic distribution indicates that the

distributed radon concentrations are clustered around the mean radon concentration and only few are distant from the mean, as well as the possibility of extreme values or outliers which explains the fat tails of a leptokurtic distribution. A negative value indicates a platykurtic distribution and a platykurtic distribution indicates that the distributed radon concentrations are scattered around the mean radon concentration with few extreme values or outliers.

The highest radon concentration was observed in the second quarter (September-November) where the season was warm and the lowest radon concentration was observed in the first quarter (June-August) where the season was colder.

This means that in the cold season warmer air flows naturally (advection or the transfer of heat or matter by the flow of a fluid, especially horizontally in the atmosphere) out of the underground mine, carrying radon into the atmosphere. This results in a significant decrease in the activity concentration of radon inside the underground mine, compared to the warm season, when radon-rich air, cooler than the atmospheric air, stagnates inside the mine causing an increase in radon concentration. The increase in radon concentration could also be due to the increase in moisture content in the underground mine during the warm season since exhalation rate of radon gas from porous rocks increases with increase in moisture content (IAEA, 1992a; Sahu et al., 2014, Munazza Faheem, 2008).

Increasing ventilation rate would increase air change rate that could possibly reduce indoor radon concentration. When ventilation rate increases, convection mechanism resulting from pressure gradient would cause the deple-

tion of radon from indoor environment (Fijałkowska-Lichwa & Przylibski, 2011).

The highest recorded values for all the four quarters are below the reference levels for both mines and workplaces. Generally, the radon soil concentrations at all the 10 locations in the underground goldmine fall below the reference levels from the international commission for radiological protection (ICRP) as shown in table 10.

Table 10: ICRP 115 and Task Group Reference Levels

Location	Reference levels (Bqm ⁻³)
Homes	300
Workplaces	1000
Mines	1000
Building Work	300

Source: (Tirmarche et al., 2010)

Radiological Impact Assessment of Indoor Radon

The European Union (EU) has adopted the International Commission for Radiological Protection (ICRP) recommendations into its protection standards. Member states are required to develop national action plans for addressing the long-term health risks of radon exposure in workplaces (Daniels et al., 2017). The EU recommends 300 Bq·m⁻³ for ²²²Rn concentrations as a suitable radon Derived Reference Level (DRL) as shown in table 19, although provisions for selecting a different level have been offered. Ireland was first to respond by publishing the National Radon Control Strategy in 2014 (Dowdall et al., 2016). The plan established a workplace DRL of 400 Bq·m⁻³ for ²²²Rn, measured over three consecutive months. Exceeding the DRL triggers immediate federal notification and evaluation by the employer to determine if remediation is

justified. Remediation is mandatory if the average ^{222}Rn level exceeds 800 $\text{Bq}\cdot\text{m}^{-3}$.

Table 11: Annual Radon Concentration (Bqm^{-3})

Level	Block	Annual Radon Concentration (Bqm^{-3})
800	EMP	49.51
810	YOD	58.89
840	YOD	62.96
880	YOD	71.56
790	EMP	50.48
820	SKY ACCN	54.57
960	YOD	50.00
1000	SKY DEC	48.15
920	YOD	61.18
1000	YOD	73.49
Annual Average		58.51

Source: Field data 2019

According to the results in table 11 the mean radon concentration of 58.51 Bqm^{-3} is lower than the radon concentration monitored in of the oldest mines in Ghana called the Obuasi mines, The dose reference level (DRL) set by the European union, a remedial action level of 1000 Bqm^{-3} set by the International Commission for Radiological Commission (ICRP), Radon concentration in caves in Czech Republic as well as an underground goldmine in Kosovo as shown in table 19. The difference in the radon concentration may be due to the different geology of each study area as well as the rate of ventilation since Kosovo mine reported a poor ventilation system at the mine (Hodolli et al 2015). However, radon emanation levels depend on the radon concentration in the soil and the underlying rocks structure in addition to other

factors like grain size, mineralogy, porosity, permeability, moisture content as well as the age of the underground mine.

Table 12: Comparison of Radon Concentrations to International Standards and Published Work

Country	Radon Concentration (Bqm ⁻³)	Location	Reference
Ghana	436.80	Obuasi Mines	Darko et al 2005
Kosovo	527.2	Underground gold mine	Hodolli et al 2015
Czech Republic	1000-7000	Caves	Hodolli et al 2015
ICRP	1000	Mines/Workplaces	ICRP 115
European Union (DRL)	300	Workplaces	Daniels & Schubauer-Berigan, 2017
This study	58.51	Subika Underground Mine (Newmont Ahafo)	Phd Thesis

In its most recent recommendations on radon exposure, the International Commission on Radiological Protection (ICRP) encouraged national authorities to set a radon reference level (RL) based on an annual effective dose within the range of 1 to 20 mSv for members of the public and workers alike (Lecomte et al., 2014). The ICRP suggested a benchmark of 10 mSv effective dose equivalent per year as a practical starting point for considerations by nations developing radon management strategies and also recognized an effective dose conversion factor (DCF) for Radon and its short-lived decay product (RnDP) exposures of approximately 10 mSv per Working Level Month (WLM), where 1 WLM = 3.54 mJ·h·m⁻³. Thus, the derived reference level (DRL) is 1

WLM·y⁻¹, or average annual ²²²Rn concentration of about 200 and 800 Bq·m⁻³ at home and in the workplace, respectively.

The average values of exposure rate to radon daughters in this study as shown in table 12 is lower than the derived reference level (DRL) of 1 WLM·y⁻¹ by the international Commission for radiological protection (ICRP) and the National Institute for occupational Safety and Health (NIOSH) as well as 4 WLM·y⁻¹ by the US Mine Safety and Health Administration regulation as shown in table 12.

Table 13: Annual Radon Exposure (WLM y⁻¹), Annual Effective Dose (mSv y⁻¹) and Excess Lifetime Cancer Risk (%)

Level	Block	Annual Radon daughter exposure (WLMy ⁻¹)	Annual Effective dose (mSvy ⁻¹)	Excess Life Cancer Risk ELCR (%) (Ghanaians)	Excess Life Cancer Risk ELCR (%) (Worldwide)
800	EMP	0.22	2.20	0.70	0.80
810	YOD	0.26	2.62	0.80	0.90
840	YOD	0.28	2.80	0.90	0.01
880	YOD	0.32	3.19	1.00	1.10
790	EMP	0.22	2.25	0.70	0.90
820	SKY ACCN	0.24	2.43	0.80	0.90
960	YOD	0.22	2.23	0.70	0.80
1000	SKY DEC	0.21	2.14	0.70	0.80
920	YOD	0.27	2.72	0.80	1.00
1000	YOD	0.33	3.27	1.00	1.10
Annual Average		0.26	2.61	0.80	0.90

Source: Field Data 2019

Table 14: Comparison of Annual Radon Daughter Exposure (WLM y^{-1}) to Protection Standards and Guidance for Occupational Exposure to Radon Progeny

Agency	Covered Population	Annual Level (WLM $\cdot y^{-1}$)	Reference
ICRP (Guidance)	Workers/Public	1	Publication No. 126
NIOSH (Guidance)	Underground miners	1	Publication No. 88-101
MSHA (Regulation)	Underground miners	4	10 CFR Part 57

ICRP, International Commission for Radiological Protection
 NIOSH, National Institute for Occupational Safety and Health
 MSHA, Mine Safety and Health Administration
 CFR, Code of Federal Regulations

The ICRP also recognized that planned occupational exposures above the reference level (RL) may be unavoidable. In those cases, the exposure should be treated as occupational and managed using a set of radiation protection requirements for radiation workers. However, a worker's annual effective dose from radon should be kept below 20 mSv after accounting for the exposure situation (e.g., equilibrium, occupancy, breathing rate, respiratory protection, etc.) as shown in table 14.

The values of annual effective doses calculated for radon inhalation by the underground workers in this study were found to vary in the range 2.20–3.27 mSv y^{-1} at the 10 different levels in the underground mine with a mean of 2.61mSv y^{-1} . The minimum value of the annual radon dose was in level 800 and the maximum value was in level 1000 YOD as shown in table 13.

According to UNSCEAR (2006), the worldwide average dose due to inhalation of radon and its decay product is 1.15 mSv y^{-1} . The ICRP suggested a

benchmark of 10 mSv effective dose equivalent per year as a practical starting point for considerations by nations developing radon management strategies.

Therefore, the dose received by the underground workers is above the worldwide average dose limit and lies below the suggested benchmark of ICRP for nations developing radon management strategies as well as the annual effective dose of occupationally exposed workers as shown in table 14.

The National Council on Radiation Protection and Measurements (NCRP) first published recommendations on radon exposure in 1984. The NCRP advised against exceeding an excess risk of death from lung cancer of 2% or greater over the lifetime of any individual exposed to enhanced levels of radon as shown in table 14. Using the underground miner epidemiologic data available at the time, the NCRP related this risk to Radon and its short-lived decay product (RnDP) exposures of $2 \text{ WLM}\cdot\text{y}^{-1}$.

The mean excess lung cancer risk estimated by this work in table 20 was found to range between 0.7% and 1% with an average value of 0.8% for Ghanaian workers and a range of 0.8% and 1.1% with an average value of 0.9% for other nationals. The average of Excess Lifetime Cancer Risk (ELCR) is less as compared to the National Council for Radiation Protection and Measurement (NCRP) over the lifetime of any individual exposed to enhanced levels of radon (Pawel & Puskin, 2003). It is also less than the estimated excess lifetime lung cancer risk for continuous exposure at the United States Environmental Protection Agency (US EPA) of 2.3% for the U.S. population, 4.1% for ever-smokers, but higher than 0.73% for never smokers and the worldwide value $0.29 \times 10^{-9} \%$ from UNSCEAR as shown in table 15.

Table 15: Comparison of Annual Effective Dose and Excess Life Time Cancer Risk to International Standards and Published.

Agency	Covered Population	Annual Effective dose (mSvy ⁻¹)	Excess Life Cancer Risk ELCR (%)	Reference
ICRP	Occupationally exposed workers	20	-	Publication No. 65
	Nations developing radon management strategies.	10	-	Publication No. 65
UNSCEAR (worldwide average value)	Individual exposed to enhanced radon	1.15	0.29×10^{-9}	UNSCEAR, 2006
NCRP	Individual exposed to enhanced radon	-	2.00	Report No. 77
US EPA	US population	-	2.30	Pawel & Puskin, 2003
	Ever Smokers	-	4.10	
	Never Smokers	-	0.73	

ICRP, International Commission for Radiological Protection
 UNSCEAR, United Nations Scientific Committee on Atomic Radiation
 NCRP, National Council for Radiation Protection and Measurement
 US EPA, United States Environmental Protection Agency

Effect of Environmental Factors on Radon Concentration

Table 16: Descriptive Statistics of Variables

Variables	Min-Max	Mean ±SD	Skewness	Kurtosis	Kolmogorov-Smirnov <i>P- values</i>
Radon Concentration	2.0-284.0	58.5±1.42	1.42	1.35	0.22
Barometric Pressure	99.5-102.5	101.1±0.9	-0.43	-1.02	0.24
Wet Bulb Temperature	24.6-32.0	28.4±1.6	-0.55	0.77	0.15
Dry Bulb Temperature	27.7-33.1	30.9±1.7	-0.79	-0.64	0.15
Relative Humidity	78.1-97.9	87.40±5.2	0.52	-0.67	0.14
Air Quantity	2.8-33.7	15.3±9.2	0.94	-0.25	0.23
Wet Kata Temperature	7.5-26.4	15.2±5.4	0.37	-0.66	0.12

Source: Field Data 2019

The annual Radon concentration in the underground mine ranges from a minimum of 2 Bqm⁻³ to a maximum of 284 Bqm⁻³ with a mean concentration of 58.51Bqm⁻³.The mean value of the measured Barometric pressure, Wet bulb temperature, Dry bulb temperature, Relative humidity, Air quality and Wet Kata temperature were 101.08 KPa, 28.36 °C, 30.89 °C, 87.40 %, 15.28 m³/s, 15.24 mcal/cm²s respectively as shown in table 16.

The distribution of Radon concentration, Relative Humidity, Air Quantity and Wet kata temperatures were slightly positively skewed; thus, the mean of the distributed results is greater than the mode and majority of the distributed results are clustered around the left tail of the distribution while the

right tail of the distribution is longer or distributed results contains lower values as compared to higher values. The distribution of Barometric pressure, wet bulb temperature and dry bulb temperature was slightly negatively skewed; thus, the mean of the distributed results is less than the mode and majority of the distributed results are clustered around the right tail of the distribution while the left tail of the distribution is longer or distributed results contains higher values as compared to lower values. Also, radon concentration and wet kata temperature values exhibited a slightly platykurtic distribution; thus, their values were scattered around the mean value with few outliers while barometric pressure, dry bulb temperature, relative humidity, air quality and wet kata values exhibited a slightly leptokurtic distribution; thus, their values are clustered around their mean values with a possibility of outliers. Also, since ($P > 0.5$) in the Kolmogorov-Smirnov test as shown in table 16 the variables are normally distributed; thus, the representative values give a true reflection of the effect of the environmental factors on the radon concentration in the underground mine.

Regression Analysis

This includes the model summary, ANOVA table and regression coefficients

Table 17: Model Summary

Model	R	R Square	Adjusted Square	R	Std. Error of the Estimate
1	0.503 ^a	0.253	0.117		44.836

a. Predictors: (Constant), Wet Kata Temperature, Relative Humidity, Barometric Pressure, Air Quantity, Wet Bulb Temperature, Dry Bulb Temperature

Source: Field Survey 2019

Regression coefficient $R = 0.503$ in table 17 explains there is a moderate positive relationship between the independent variables (Barometric Pressure, Relative Humidity, Wet bulb temperature, Dry Bulb temperature, Wet Kata temperature) and radon concentration. The adjusted $R^2 = 0.117$ in table 24 also shows that 11.7% variation in radon concentration is explained by barometric pressure, wet bulb temperature, dry bulb temperature, relative humidity, air quantity and wet kata temperature and 88.3% could be due to other influencing factors which that were not considered in the study.

Table 18: ANOVA^a

Model	Sum of Squares	df	Mean Square	F	Sig
Regression	22432.321	6	3738.720	1.860	0.118 ^b
Residual	66338.245	33	2010.250		
Total	88770.566	39			

a. Dependent Variable: Radon Concentration

b. Predictors: (Constant), Wet Kata Temperature, Relative Humidity, Barometric Pressure, Air Quantity, Wet Bulb Temperature, Dry Bulb Temperature

Data Source: Field Survey 2019

The P-value in analysis of variance (ANOVA) in table 18 shows the influence of the independent variables on radon concentration in the underground gold mine are not statistically significant at the 5% level of significance ($P > 0.05$), thus there is not enough statistical evidence to conclude that the independent variables have a significant relationship with radon concentration.

Table 19: Coefficients^a

Model	Unstandardized Coefficients		Standardized Coefficients Beta	t	Sig.
	B	Std. Error			
(Constant)	1097.466	915.779		1.198	0.239
Barometric Pressure	-9.579	9.177	-0.170	-1.044	0.304
Wet Bulb Temperature	-18.250	10.172	-0.619	-1.794	0.082
Dry Bulb Temperature	8.647	11.015	0.307	0.785	0.438
Relative Humidity	2.307	2.025	0.255	1.139	0.263
Air Quantity	-1.044	0.812	-0.202	-1.285	0.208
Wet Kata Temperature	-0.006	1.591	-0.001	-0.004	0.997

Source: Field Data 2019

This table generated the specific regression equation as shown in equation 42

$$RC = 1098 - 0.170BP - 0.619WBT + 0.307DBT + 0.255RH - 0.202AQ - 0.001WKT \quad (42)$$

where *RC* - Radon Concentration, *BP* -Barometric Pressure, *WBT* -Wet Bulb Temperature, *DBT* -Dry Bulb Temperature, *RH* -Relative Humidity, *WKT* -Wet Kata Temperature

The regression coefficient for barometric pressure (B_1) = -0.170 depicts a negative correlation between barometric pressure and radon concentration and it implies that 1% increase in barometric pressure will decrease radon concentration by 17% holding *WBT*, *DBT*, *RH*, *AQ* and *WKT* constant as shown in table 19 and equation 42 but was statistically insignificant at the 5% level of significance ($P > 0.05$) hence, the null hypothesis is accepted. Increase in barometric pressure will cause a decrease in radon exhalation from porous rock in the underground mine environment, leading to a reduction of radon concentration (IAEA, 1992a; Sahu et al., 2016).

The regression coefficient for wet bulb temperature (B_2) = -0.619 depicts a negative correlation between wet bulb temperature and radon concentration and it implies that 1% increase in wet bulb temperature will decrease radon concentration by 61.9% holding BP, DBT, RH, AQ and WKT constant as shown in table 19 and equation 42 but was statistically insignificant at the 5% level of significance ($P > 0.05$) hence the null hypothesis is accepted.

A wet bulb thermometer measures the extent of cooling as moisture dries from a surface (evaporative cooling). At this point the underground mine experiences some coolness due to ventilation and warmer air which causes significant increase in the wet bulb temperature flows naturally out of the underground mine, carrying radon into the atmosphere. This results in a significant decrease in the activity concentration of radon inside the underground mine (Fijałkowska-Lichwa & Przylibski, 2011).

The regression coefficient for Dry bulb temperature (B_3) = 0.307 depicts a positive correlation between Dry bulb temperature and radon concentration and it implies that 1% increase in wet bulb temperature will increase radon concentration by 30.7% holding BP, WBT, RH, AQ and WKT constant as shown in table 19 and equation 42 but was statistically insignificant at the 5% level of significance ($P > 0.05$) hence the null hypothesis is accepted.

The dry-bulb temperature is an indicator of heat content. The underground mine is a warm environment and the moisture content in the underground mine increases at high temperatures. The increase in radon concentration could be due to the increase in moisture content when temperatures are high since exhalation rate of porous rocks increases with increase in moisture content (IAEA, 1992a; Sahu et al., 2016)

The regression coefficient of Relative Humidity (B_4) = 0.255 depicts a positive correlation between Relative Humidity and Radon Concentration and it implies that 1% increase in Relative Humidity will increase radon concentration by 25.5% holding BP, DBT, WBT, AQ and WKT constant as shown in table 19 and equation 42 but was statistically insignificant at the 5% level of significance ($P > 0.05$) hence the null hypothesis is accepted. Humidity also refers to the degree of moisture or water vapour found in the atmosphere, when air contains moisture, it is said to be humid. Conditions such depth of workings, machinery and work-related activities also contribute to high temperatures in the underground mine and hot places like the underground mine tend to be more humid than cool places because heat causes water to evaporate faster. The increase in radon concentration could be due to the increase in amount of water present in the pore space (moisture content) since exhalation rate of porous rocks increases with increase in moisture content (IAEA, 1992a; Sahu et al., 2016)

The regression coefficient for Air Quantity (B_5) = -0.202 depicts a negative correlation between Air Quantity and Radon Concentration and it implies that 1% increase in Air Quantity will decrease radon concentration by 20.2% holding BP, DBT, RH, WBT and WKT constant as shown in table 19 and equation 42 but was statistically insignificant at the 5% level of significance ($P > 0.05$) hence the null hypothesis is accepted.

Air Quantity is the product of air velocity within a particular area of interest. An increase in air velocity tends to increase the ventilation rate thereby cooling the underground mine allowing warm air to move out which reduces the radon concentration in the underground mine. Air velocity alone is not so much

significant, but, its combination with wet-bulb temperature produce reliable results in hot and humid mine environment. (Neingo & Tholana, 2016).

The regression coefficient for wet kata temperature (B_2) = -0.001 depicts a negative correlation between Wet Kata temperature and Radon Concentration and it implies that 1% increase in wet kata temperature will decrease radon concentration by 0.1% holding BP, DBT, RH, AQ and WBT constant as shown in table 19 and equation 42 but was statistically insignificant at the 5% level of significance ($P > 0.05$) hence the null hypothesis is accepted.

Wet kata readings are used to measure the cooling power of the environment for acclimated men. The cooling power of the environment is the rate of cooling experienced by a person. Hence an increase in the rate of ventilation cools the mine thereby reducing the radon concentration.

Table 20: Multicollinearity of Independent Variables

Collinearity Statistics	
Tolerance	VIF
0.854	1.171
0.190	5.255
0.148	6.746
0.452	2.210
0.919	1.088
0.693	1.444

a. Dependent Variable: Radon Concentration

Source: Field Data 2019

Table 21: Collinearity Diagnostics of variables

Model Dimension	Eigenvalue	Condition Index	Variance Proportions						
			(Constant)	Barometric Pressure	Wet Bulb Temperature	Dry Bulb Temperature	Relative Humidity	Air Quantity	Wet Kata Temperature
1	6.671	1.000	0.00	0.00	0.00	0.00	0.00	0.00	0.00
2	0.230	5.381	0.00	0.00	0.00	0.00	0.00	0.88	0.00
3	0.093	8.477	0.00	0.00	0.00	0.00	0.00	0.09	0.70
4	0.005	38.255	0.00	0.00	0.01	0.03	0.22	0.01	0.09
5	0.001	67.113	0.01	0.01	0.16	0.00	0.10	0.01	0.10
6	0.000	173.363	0.01	0.02	0.81	0.97	0.65	0.00	0.07
7	3.030E-005	469.229	0.98	0.97	0.02	0.00	0.03	0.00	0.04

a. Dependent Variable: Radon Concentration

Source: Field Data 2019

The tolerance value of less than 0.10 indicates a multicollinearity problem (O'Brien & Robert, 2007). In the above table the tolerance values of all independent variables are 0.854, 0.190, 0.148, 0.452, 0.919 and 0.693 as shown in table 20 are less the 0.10 which shows all the independent variables have multicollinearity problem.

The reciprocal of the tolerance is known as the Variance Inflation Factor (VIF). The VIF of 5 and above indicates a multicollinearity problem (O'Brien & Robert, 2007). In table 20 the VIF values of independent variables are 1.171, 5.255, 6.746, 2.210, 1.088 and 1.444 indicates three of out of the six the independent variables have issues of multicollinearity.

Eigen values close to 0 indicate dimensions which explain little variance (Agarwal, S., & Adjirackor, T. 2016). In table 21 eigen values of

0.230, 0.093, 0.005, 0.001, 0.00 and 0.000003 are close to zero which shows little variance among the independent variables which indicates a possibility of high correlations among the independent variables which is also an issue of multicollinearity.

The condition index summarizes findings thus, a condition index over 15 indicate a possible multicollinearity problem and a condition index over 30 suggests a serious multicollinearity problem (Agarwal, S., & Adjirackor, T. 2016). In table 21 four out of the six independent variables have a multicollinearity problem. The statistical insignificance of the independent variables on the radon concentration in underground mine could be due to the issue of multicollinearity among some of the independent variables.

Multicollinearity independent variables are highly correlated to each other which reduces affects the significance of the effect on the dependent variable. Hence the need of a principal component analysis and factor analysis to deduce the actual variables influencing radon concentration in the underground mine.

Cluster, Factor and Principal Component Analysis

Cluster Analysis was used to determine components (variables) that are significant at a particular level (cluster) in the underground mine. Principal Component Analysis (PCA) and Factor Analysis were used to determine the factors/Components that will significantly have an effect on the radon concentration.

Table 22: Cluster Analysis

Level	Cluster	RC (Bq/m ³)	BP X1 (kPa)	WBT X2 (°C)	DBT X3 (°C)	RH X4 (%)	AQ X5 (m ³ /s)	WKT X6 (mcal/cm ² s)
800	1	39.14	101.70	29.88	32.00	86.95	23.78	19.35
810	2	64.75	101.60	26.23	29.03	84.80	19.13	22.58
840	3	63.76	101.20	28.18	31.83	84.10	12.50	12.73
880	4	78.00	100.70	29.33	32.38	84.28	8.98	13.43
790	5	56.11	101.68	29.50	31.15	89.98	10.98	15.83
820	6	77.08	101.50	28.30	30.83	85.35	12.10	14.10
960	7	51.54	100.33	27.90	29.23	94.53	10.98	19.56
1000 YOD	8	77.13	100.50	27.78	31.38	88.13	8.98	11.65
920	9	59.42	100.40	29.10	31.38	87.05	16.38	10.63
1000 SKY DEC	10	77.43	100.63	27.05	29.93	89.03	32.33	15.48

Source: Field Data 2019

The following variables were observed at each level in the underground goldmine: Wet bulb temperature (°C), Dry bulb temperature (°C), Relative humidity (%), Barometric pressure (kPa), Air quantity (m³/s), Wet Kata temperature (mcal/cm²s) and Radon concentration (Bqm⁻³). Additionally, a multivariate statistical analysis was performed. A cluster analysis (CA) was applied by using the 10 different levels in the underground goldmine forming 10 groups. The aforementioned groups differ in their variables as shown in Table 22, and one can observe the centroids of each variable in each group. This analysis indicates group 4 recorded the highest radon concentration, Dry bulb temperature which explains the positive relationship between the variables. Group 1 recorded the highest barometric pressure and wet bulb temperature and these two variables have a negative relationship with radon concentration.

Group 2 recorded the highest wet kata temperature which represented the level that acclimatized workers experienced the highest rate of cooling. Group 7 recorded the highest relative humidity and Group 10 recorded the highest Air quantity since it's the first level after the reference level which makes it closer to the entrance of the underground mine as compared to the other levels.

Table 23: Principal Component Analysis

Component Number	Eigen Value	% of variance	Cumulative %
1	2.09	34.90	34.90
2	1.37	22.75	57.65
3	1.05	17.51	75.16
4	0.82	13.66	88.81
5	0.55	9.16	97.97
6	0.12	2.03	100

Source: Field Data 2019

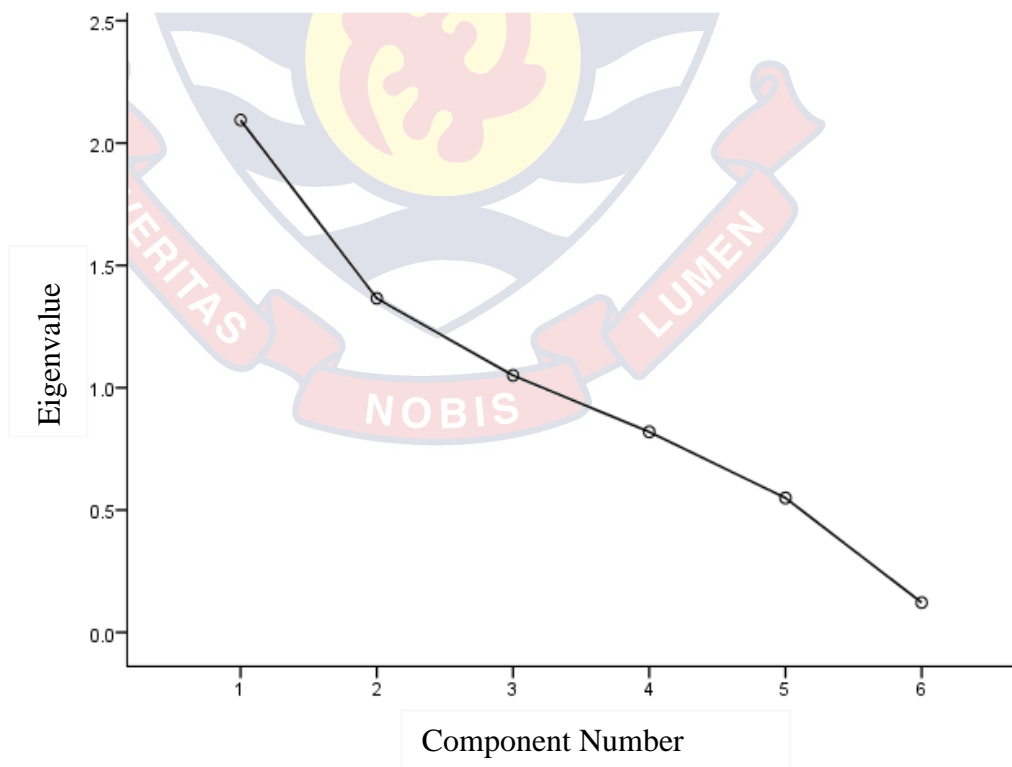


Figure 26: Principal Component Analysis Scree Plot

Source: Field data 2019

A principal component analysis and factor analysis was performed to determine the associations between the analysed variables and estimate the possible origins of the radon concentrations in the indoor environments of the underground goldmine. The first three components of this principal component analysis obtained an eigenvalue above 1 were extracted and represent 75.16% of the variability in the observed data (Table 23) and the scree plot in (Figure 26) which is assumed sufficient for the analysis performed.

Table 24: Weight of Each Component

Variables	Components		
	1	2	3
WBT	0.889		
DBT	0.877		
BP		0.861	
WKT	-0.542	0.620	
RH			0.890
AQ			-0.507

Source: Field data 2019

Table 24 presents the weights for each component variable. In it, one can observe that for component 1, wet bulb temperature and dry bulb temperature have the highest weights, 0.889 and 0.887, respectively; the greatest weights for component 2 correspond to barometric pressure and wet kata temperature with values of 0.861 and 0.620, respectively; while the greatest weight for component 3 corresponds to relative humidity. The negative values are considered to carry negligible weights.

Table 25: Factor Analysis

Variables	Components		
	1	2	3
BP	0.170	0.720	0.050
WBT	0.469	0.210	0.237
DBT	0.410	-0.015	-0.248
RH	-0.030	0.110	0.737
AQ	-0.175	0.173	0.418
WKT	-0.227	0.468	0.001

Source: Field data 2019

The purpose of the Factor Analysis (FA) was to strengthen the Principal Component Analysis (PCA) results and obtain a number of factors to explain most of the variability in the environmental factors (Wet bulb temperature ($^{\circ}\text{C}$), Dry bulb temperature ($^{\circ}\text{C}$), Relative humidity (%), Barometric pressure (kPa), Air quantity (m^3/s), Wet Kata temperature ($\text{mcal}/\text{cm}^2\text{s}$)).

As shown in table 23 three environmental factors were found to represent 75.16% of the variability in the original data. The FA explains the greater factors the influences the radon concentration in the underground mine. It was observed that the wet bulb temperature has the greatest weight in factor 1 with values of 0.469, the greatest weight for factor 2 correspond to Barometric pressure with a value of 0.720 while the greatest weight for factor 3 with a value of 0.737 correspond to Relative humidity as shown in table 25. These findings allow us to infer that component 1, or factor 1, is influenced by environmental conditions relating to wet bulb temperature. In contrast, component 2, or factor 2, favors barometric pressure. On the other hand, component 3 or factor 3 favors relative humidity. These results also explain that wet bulb temperature,

barometric pressure and relative humidity are the main environmental factors that influences radon concentration in the underground goldmine.

Table 26: PCA Regression Coefficients

Model	Unstandardized		Standardized	t	P-
	Coefficients				
	B	Std Error	Beta		
Constant	64.425	7.169		8.987	0.000
Wet Bulb Temps	-14.479	7.260	-0.303	-1.1994	0.045
Barometric pressure	-10.229	7.260	-0.214	-1.409	0.167
Relative Humidity	8.193	7.260	0.172	1.129	0.267

a. Dependent Variable: RC
Source: Field data 2019

The principal component regression was modelled to ascertain the significance of the main factors that has influence on the radon concentration in the underground goldmine. Table 26 shows a significant negative relationship between wet bulb temperatures and radon concentration at the 5% level of significance ($P < 0.5$). Thus, a unit increase in the wet bulb temperature will cause a decrease of 30.3% in the radon concentration underground.

The statistical significance between temperature and radon concentration due to a good ventilation system and it also signals that, it is a variable that must be of interest to the environmental health and safety department of the mine. It has to be closely monitored to inform if ventilation rate has to be increased to reduce radon concentration in the underground mine.

Relative humidity exhibited a positive correlation with radon concentration but was statistically insignificant at the 5% level of significance

($P > 0.05$). Thus, a unit increase in Relative Humidity will cause an increase of 17.2% in the radon concentration and vice versa in the underground mine.

The statistical insignificance of the Relative Humidity on radon concentration might be due to the fact that the rocks type in the underground mine has low exhalation rate since rock types have different exhalation rate. or it could also be due to a good ventilation system in the underground mine since indoor humidity is influenced by ventilation rates. Ventilation usually reduces indoor moisture levels (Flannigan and Morey, 2009) thereby cooling down the warm environment and decreasing radon concentration as warm air rises and escapes to the atmosphere through the ventilation system.

Barometric pressure also exhibited a negative correlation with radon concentration but was statistically insignificant at the 5% level of significance ($P > 0.05$). Thus, a unit increase in Barometric pressure will cause a decrease of 21.1% in the radon concentration underground.

The statistical insignificance of barometric pressure and relative humidity could also be due to the low emanation of radium from solid like rocks and low diffusing rate of radon gas in solid grains in the underground mine or a good ventilation system. When ventilation rate increases, convection mechanism resulting from pressure gradient would cause the depletion of radon from indoor environment (Flannigan and Morey, 2009).

The result of the positive correlation between indoor radon concentration and indoor humidity agrees with the results of some researchers, Kearfott et al. (1992), Blaauboer and Smetsers (1997) and (Alonso et al., 2013). However, the results were contrary to the results described by Yu et al. (1999)

who found the decline in radon gas concentrations could be associated with a rise in relative humidity.

The results for temperature and barometric pressure was different from Xie, Liao, Wang, and Kearfott (2017) who detected that that indoor barometric pressure and temperature are generally constant with the average values of 97,000Pa and 23⁰C, respectively. Indoor radon concentrations have no apparent correlation with indoor barometric pressure and indoor temperature. This difference could be due to the factors associated with different indoor environment thus, homes and underground mines.

Time Series Model

Radon concentrations and depth form the reference level are used to generate a linear regression model for forecasting and prediction of radon concentration at deeper levels or depths in the underground mine using the moving average trend analysis in time series as shown in table 34.

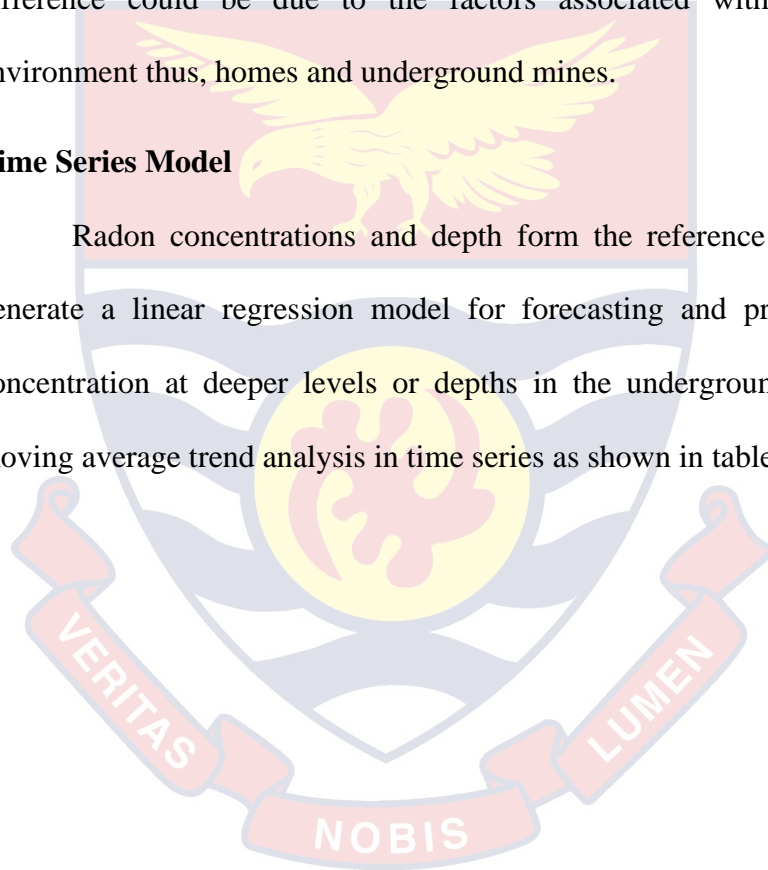


Table 27: Time Series Moving Averages

Quarter	Distance below Reference level	Radon Concentration (Bq/m ³)	Four quarter Moving Total	Four Quarter Moving Average	Centred Moving Average	Ratio-to-Moving Average
Level	[1000-levels(m)]	I	II	III=II/4	A=III1+III2/2	IV=I/A
I	YOD 0	22.69				
	1000					
	SKY 0	14.37				
	DEC 1000					
	960 40	8.39	68.53	17.13		
	920 80	23.08	82.59	20.65	18.89	0.4442
	880 120	36.75	82.93	20.73	20.69	1.1155
	840 160	14.71	81.44	20.36	20.55	1.7886
	820 180	6.90	67.84	16.96	18.66	0.7883
	810 190	9.48	60.06	15.02	15.99	0.4316
	800 200	28.97	66.62	16.66	15.84	0.5987
	790 210	21.27	227.58	56.90	36.78	0.7878
II	YOD 0	167.86	311.68	77.92	67.41	0.3155
	1000		379.76	94.94	86.43	1.9421
	SKY 0	93.58	489.23	122.31	108.62	0.8615
	DEC 1000					
	960 40	97.05	462.42	115.61	118.96	0.8158
	920 80	130.74	470.49	117.62	116.61	1.1211
	880 120	141.05	551.12	137.78	127.70	1.1045
	840 160	101.65	557.47	139.37	138.57	0.7335
	820 180	177.68	528.51	132.13	135.75	1.3089
	YOD 190	137.09	521.32	130.33	131.23	1.0447
	810					
	800 200	112.09	434.77	108.69	119.51	0.9379
	790 210	94.46	392.85	98.21	103.45	0.9131

Table 27 continued

III	YOD	0	91.13	352.50	88.13	93.17	0.9781
	1000						
	SKY	0	95.17	311.96	77.99	83.06	1.1458
	DEC						
	1000						
	960	40	71.74	326.05	81.51	79.75	0.8995
	920	80	53.92	346.77	86.69	84.10	0.6411
	880	120	105.22	372.48	93.12	89.91	1.1703
	840	160	115.89	408.40	102.10	97.61	1.1873
	820	180	97.45	364.79	91.20	96.65	1.0083
IV	810	190	89.84	323.47	80.87	86.03	1.0443
	800	200	61.61	254.06	63.52	72.19	0.8534
	790	210	74.57	188.80	47.20	55.36	1.3471
	YOD	0	28.04	156.18	39.05	43.12	0.6502
	1000						
	SKY	0	24.58	111.56	27.89	33.47	0.7344
	DEC						
	1000						
	960	40	28.99	112.49	28.12	28.01	1.0351
	920	80	29.95	110.70	27.68	27.90	1.0735
880	120	28.97	108.01	27.00	27.34	1.0597	
840	160	22.79	100.63	25.16	26.08	0.8738	
820	180	26.30	104.65	26.16	25.66	1.0249	
810	190	22.57	115.99	29.00	27.58	0.8183	
800	200	32.99					
790	210	34.13					

Source: Field Data 2019

a, b, c, d is the ratio to moving averages of quarter I, II, III, IV respectively as shown in table 35.

The mean ratio is calculated by finding the average of the ratio – to – moving average for the four quarters in each level.

The mean ratios for the 10 levels are then summed. Theoretically they would sum to 10.00, but due to moving and averaging, it was summed to 9.61 as shown in table 27.

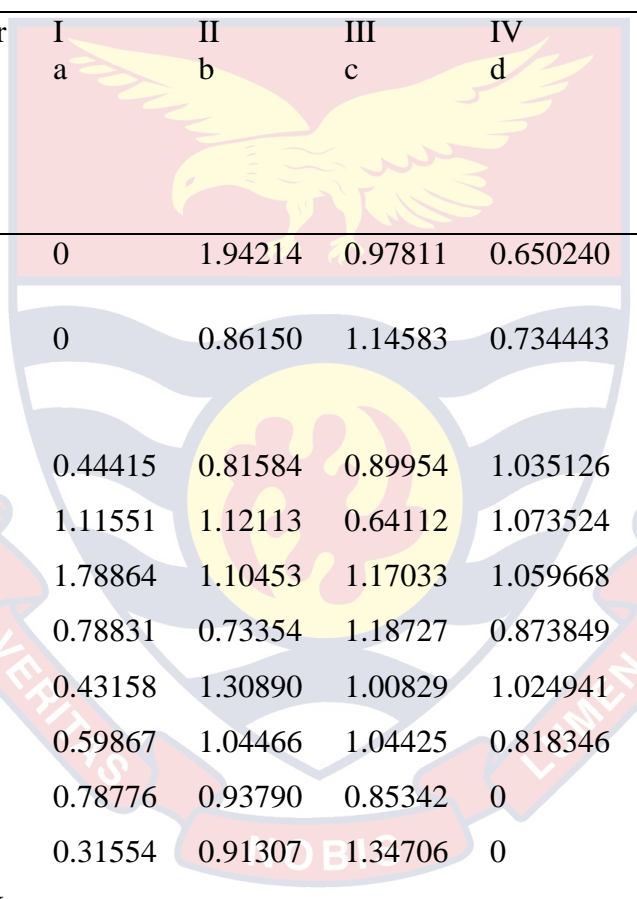
To normalize these mean ratios to get a seasonal index, the theoretical sum (10.0) is divided by the sum of the mean ratio to moving average (9.61)

$$\frac{10}{9.61} = 1.04$$

This result (1.04) is referred to as the normalization ratio or correction factor.

This normalization ratio is then multiplied to the mean ratio of each level to compute the seasonal index as shown in table 28

Table 28: Seasonal Index

Quarter	I a	II b	III c	IV d	Mean Ratio	Seasonal Index
					<i>B=average of a,b,c,d</i>	<i>normalizing ratio (1.04) ×B</i>
YOD	0	1.94214	0.97811	0.650240	1.19	1.24
1000						
SKY	0	0.86150	1.14583	0.734443	0.91	0.95
DEC						
1000						
960	0.44415	0.81584	0.89954	1.035126	0.80	0.83
920	1.11551	1.12113	0.64112	1.073524	0.99	1.03
880	1.78864	1.10453	1.17033	1.059668	1.28	1.33
840	0.78831	0.73354	1.18727	0.873849	0.90	0.94
820	0.43158	1.30890	1.00829	1.024941	0.94	0.98
810	0.59867	1.04466	1.04425	0.818346	0.88	0.92
800	0.78776	0.93790	0.85342	0	0.86	0.89
790	0.31554	0.91307	1.34706	0	0.86	0.89
TOTAL					9.61	10.00

Source: Field Data 2019

The seasonal index is divided by the measured radon concentration to obtain the Deseasonalised radon concentrations as shown in table 29.

Table 29: Deseasonalised and Radon Concentration

Levels	Distance below Reference level [1000-levels(m)]	Radon Concentration (Bq/m ³)	Seasonal Index II	De seasonalized III = I / II
YOD 1000	0	22.69	1.24	18.32
SKY DEC 1000	0	14.37	0.95	15.11
960	40	8.39	0.83	10.10
920	80	23.08	1.03	22.45
880	120	36.75	1.33	27.57
840	160	14.71	0.94	15.65
820	180	6.90	0.98	7.030
810	190	9.48	0.92	10.30
800	200	28.97	0.89	32.38
790	210	21.27	0.89	23.81
YOD 1000	0	167.86	1.24	135.54
SKY DEC 1000	0	93.58	0.95	98.40
960	40	97.05	0.83	116.77
920	80	130.74	1.03	127.19
880	120	141.05	1.33	105.83
840	160	101.65	0.93	109.05
820	180	177.68	0.98	180.99
810	190	137.09	0.91	150.31
800	200	112.09	0.89	125.30
790	210	94.46	0.89	105.73
YOD 1000	0	91.13	1.24	73.58
SKY DEC 1000	0	95.17	0.95	100.07
960	40	71.74	0.83	86.32
920	80	53.92	1.03	52.45
880	120	105.22	1.33	78.95
840	160	115.89	0.93	124.33
820	180	97.45	0.98	99.26
810	190	89.84	0.91	98.50
800	200	61.61	0.89	68.87
790	210	74.57	0.89	83.47
YOD 1000	0	28.04	1.24	22.64
SKY DEC 1000	0	24.58	0.95	25.85
960	40	28.99	0.83	34.88
920	80	29.95	1.03	29.14
880	120	28.97	1.33	21.74
840	160	22.79	0.93	24.45
820	180	26.30	0.98	26.79
810	190	22.57	0.91	24.75
800	200	32.99	0.89	36.88
790	210	34.13	0.89	38.20

Source: Field Data 2019

Modelling the trend analysis using time series analysis smoothens or reduces a lot of fluctuations in the regression equation thereby reducing a lot of errors in the model to assume a more perfect linear equation for prediction as seen in the figure 27 (thus the Deseasonalised radon concentrations were used instead of the radon concentration measured directly). The purpose of time-series analysis is to predict or forecast future values of the variable from past observations and conditions.

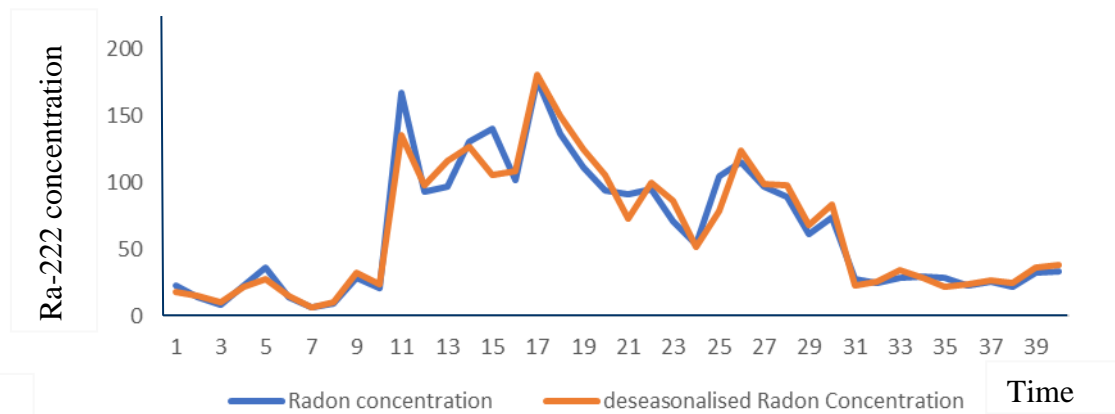


Figure 27: A Graph of Radon Concentration and Deseasonalised Radon Concentration

Source: Field Data 2019

Using the values of the independent variables (depth from reference level) in table 30 and dependent variables (Deseasonalised radon concentration) in table 31. The least square regression equation for prediction and forecasting of radon concentration at different depths is modelled using the statistical Product and Service Solutions (SPSS) version 16.0 developed by International Business Machines (IBM) Corporation, New York USA.

Table 30: Depth from Reference Level

Distance below Reference level [1000-level (m)] (X)				
0	200	180	0	40
0	210	190	40	80
40	0	200	80	120
80	0	210	120	160
120	40	0	160	180
160	80	0	180	190
180	120	40	190	200
190	160	80	200	210

Source: Field Data 2019

Table 31: Deseasonalised Radon Concentration at Various Depth.

Deseasonalized Radon Concentration (Y)				
18.32	32.38	180.99	78.95	34.88
15.11	23.81	150.31	124.33	29.14
10.10	135.54	125.30	99.26	21.74
22.45	98.40	105.73	98.50	24.45
27.57	116.77	73.58	68.87	26.79
15.65	127.19	100.07	83.47	24.75
7.03	105.83	86.32	22.64	36.88
10.30	109.05	52.45	25.85	38.20

Source: Field Data 2019

The trend equation assumes $y = \alpha + \beta x$

where α = constant value β = regression coefficient which will be computed from the SPSS output as shown in table 32.

Table 32: Trend Regression Coefficient

Model	Unstandardized Coefficients		Standardized Coefficients	t	Sig.
	B	Std. Error	Beta		
(Constant)	59.589	13.611	0.073	4.378	0.000
Distance below Reference level	0.044	0.096		0.453	0.653

a. Dependent Variable: De seasonalized Radon Conc
Source: Field Data 2019

The regression coefficient output from table 32 generated for the trend equation as shown in equation 43.

$$y = 59.6 + 0.073x \quad 43$$

Where y = Radon Concentration x = distance from reference level

Regression coefficient $R= 0.073$ explains there is a weak positive relationship between depth of the underground mine the radon concentration; thus, an increase in the depth of the underground mine will lead to an increase in radon concentration and vice versa. Thus, the deeper the underground mine the higher the radon concentration. Generally, concentration of terrestrial radionuclides is low but they tend to increase if the environment is enhanced through practices like mining and oil exploration.

Table 33: Trend Model Summary

Model	R	R Square	Adjusted R Square	Std. Error of the Estimate
1	0.073 ^a	0.005	-0.021	47.609

a. Predictors: (Constant), Distance below Reference level
Source: Field Data 2019

The $R = 0.073$ in trend model in table 33 indicates that for a 1% increase in the depth of the underground mine, radon concentration will increase by 7.3%. The adjusted $R^2 (-0.021)$ in equation shows that 2.1% variation in radon concentration is explained by the increase in depth in the underground mine and 97.9% could be due to other influencing factors that were not considered in the study.

Table 34: Trend ANOVA

Model	Sum of Squares	df	Mean Square	F	Sig.
Regression	465.661	1	465.661	0.205	0.653 ^b
Residual	86131.542	38	2266.620		
Total	86597.203	39			

a. Dependent Variable: De seasonalized Radon Concentration

b. Predictors: (Constant), Distance below Reference level

Source: Field Data 2019

The trend Analysis of Variance (ANOVA) in table 34 shows the influence of the various depths on radon concentration in the underground gold mine are not statistically significant at the 5% level of significance ($P > 0.05$), thus there is not enough statistical evidence to conclude that the increase in depth have a significant relationship with radon concentration. The negative adjusted R^2 shows that the impact of depth on radon concentration in the underground mine is negligible. The statistical insignificance and negligible effect could be due to a good ventilation measure in all the levels in the underground goldmine. Also, the weak relationship and adjusted R^2 explains that various influencing factors contribute to the radon concentration as compared to depth in the underground mine. Radon emanation levels depend on the radon concentration in the soil and the underlying rocks structure in addition

to other factors like grain size, mineralogy, porosity, permeability and moisture content.

Activity Concentration of Radionuclides in Rock and Soil Samples

The distribution of activity concentration of radionuclides in all the 10 levels in the underground goldmine are shown in table 35. Activities concentrations ranges from a minimum of $18.93 \pm 1.68 \text{ Bqm}^{-3}$ to a maximum of $45.13 \pm 3.91 \text{ Bqm}^{-3}$ for Ra-226 with a mean concentration of $32.19 \pm 6.98 \text{ Bqm}^{-3}$. The lowest activity concentration was found at level 1000 YOD and the highest activity concentration was found at level 880. The mean activity concentration of Ra-226 is above the world average value of 35 Bq kg^{-1} from the United Nations Scientific Committee on Atomic radiation as well as other measurements recorded in some mining companies in Ghana as shown in table 36.

Th-232 recorded a minimum of $17.6 \pm 2.32 \text{ Bq/kg}$ to a maximum of $51.9 \pm 3.85 \text{ Bq/kg}$ with a mean concentration of $39.08 \pm 10.66 \text{ Bq/kg}$. The lowest concentrations were found at level 1000YOD and the highest levels were found at level 880. The mean activity concentration of Th-232 is below the world average value of 40 Bq/kg from the United Nations Scientific Committee of Atomic radiation as well as other measurement recorded in some mining companies in Ghana apart from measurements recorded in Adamus mine as shown in table 36.

Table 35: Activity Concentration of Radionuclides at Various Levels

Levels	Ra-266 (Bq/kg)	Th-232 (Bq/kg)	K-40 (Bq/kg)
800	34.13±1.58	43.83±2.27	267.43±10.28
810	30.5±1.48	44.2±2.47	233.4±18.97
840	33.55±1.83	46.35±0.91	256.43±16.18
880	45.13±3.91	51.9±3.85	364±14.41
790	32.55±1.42	42.78±1.32	252.93±10.50
820	37.03±1.37	43.5±4.61	310.55±7.70
960	25.3±1.00	23.15±2.78	159.95±20.10
1000YOD	18.93±1.68	17.6±2.32	156.35±36.81
920	27.98±1.13	34.33±1.26	221.35±9.34
1000SKY DEC	35.4±1.99	44.15±2.92	239.2±8.47
Average	32.19±6.98	39.08±10.66	247.18±61.65

Source: Field Data 2019

K-40 ranges from a minimum of 156.35±36.81 Bq/kg to a maximum of 364.00±14.41 Bq/kg with a mean concentration of 247.18±61.65 Bq/kg. The lowest concentrations were found at level 1000 YOD and the highest levels were found at level 880. The mean activity concentration of K-40 is below the world average value of 400 Bq /kg from the United Nations Scientific Committee of Atomic radiation and measurements recoded in Obuasi and Adamus mine as shown in table 36.

Rock and soil samples from level 800 has to undergo further radiological test for it to be considered as a NORM free material due to the significance increase in activity concentration of radionuclides.

Table 36: Comparison of Activity Concentration Ra-226, Th-232 and K-40 in Soil and Rock Samples with Worldwide Average and other Published Work

Agency/ Country	Location	Ra-226	Th-232	K-40	Reference
United Nations Scientific Committee on Atomic Radiation (UNSCEAR)	Worldwide average	35	40	400	UNSCEAR, 2000
Ghana	Obuasi Underground mine	29.3	26.8	770.0	Darko et al., 2005
Ghana	Newmont Akyem	11.28	12.23	113.78	Wiseman et al., 2000
Ghana	Tarkwa Mine	13.61	24.22	162.18	Faanu et al., 2008
Ghana	Chirano Mines Bibiani	9.79	9.18	237.40	Faanu et al., 2008
Ghana	Adamus Mine Nzema	8.03	43.98	395.05	Awudu et al., 2016
This Study	SUG Mine Newmont Ahafo	32.19	39.08	247.18	PhD Thesis

Table 37 shows the descriptive statistics of activity concentration of Ra-226, Th-232 and K-40 distributions in the soil and rock samples.

A positive skewness of Ra-226 and K-40 shows that the radionuclide distribution in the soil was positively skewed thus the activity concentration of their mean is greater than the mode and majority of the distributed activity concentrations are clustered around the left tail of the distribution while the

right tail of the distribution is longer or their activity concentration distribution contains lower activities concentrations as compared to higher activity concentrations of Ra-226 and K-40.

Table 37: Descriptive Statistics of Activity Concentration Distribution in Soil and Rock Samples

Statistics	Ra-226	Th-232	K-40
Skewness	0.001	-0.959	0.054
Kurtosis	0.661	-0.055	0.242
Shapiro Wilk Test (P values)	0.405	0.485	0.461

A negative skewness of Th-232 in table 37 shows a negatively skewed distribution of thorium concentration in the rock and samples, thus the activity concentration of the mean is less than the mode and majority of the distributed activity concentrations are clustered around the right tail of the distribution while the left tail of the distribution is longer or the activity concentration distribution contains higher activities concentrations of Th-232 as compared to lower activity concentrations.

A leptokurtic distribution of Ra-266 and K-40 in table 37 shows that activity concentrations of the radionuclides are clustered around their mean concentration with a possibility of outliers and a platykurtic distribution of Th-232 shows that the distribution of the activity concentrations of Th-232 are scattered around the mean concentration with few outliers. The ($P > 0.05$) for Shapiro Wilk test confirms that all the data for the radionuclides are normally distributed, thus the samples collected gives a true representation of the activity concentration in the rock and soil samples in the underground mine.

Table 38 shows the external hazard indices for all the levels in the underground mine. The external hazard indices for both rooms in the house where the inhabitants live with infinitely thick walls without windows and doors (H_{EX1}) and a room with windows and doors (H_{EX2}) shows an insignificant radiological effect to inhabitants who may use the soil and rock from the underground mine.

Table 38: External Hazard Indices of Rock and Soil Samples (H_{EX})

Levels	H_{EX1}	H_{EX2}
800	0.32	0.16
810	0.30	0.15
840	0.32	0.16
880	0.40	0.20
790	0.31	0.15
820	0.33	0.17
960	0.19	0.10
1000 YOD	0.15	0.08
920	0.25	0.13
1000 SKY DEC	0.32	0.16
Average	0.29	0.14

Source: Field Data 2019

Table 39 shows the internal hazard indices for all the 10 levels in the underground mine. The internal hazard indices (H_{IN}) is the cause of harmful effects to the lungs due to the internal contact of α -particles of a higher ionization power to the sensitive tissues of the lungs and other parts of the respiratory system. Values of internal hazard indices are less than unity, rock and soil samples from the underground mine that may be used for construction of dwellings may not posse any radiological hazard.

Table 39: Internal Hazard Indices of Rock and Soil Samples (H_{IN})

Levels	H_{IN}	$I\alpha$
800	0.41	0.17
810	0.38	0.15
840	0.41	0.17
880	0.52	0.23
790	0.39	0.16
820	0.43	0.19
960	0.26	0.13
1000 YOD	0.20	0.09
920	0.33	0.14
1000 SKY DEC	0.41	0.18
Average	0.38	0.16

Source: Field Data 2019

The Internal level index ($I\alpha$) is used to access the excess alpha radiation due to radon inhalation originating from building materials (El Galy et al., 2008): Since all the values found at the 10 different levels in the underground goldmine are lower than the maximum permissible value ($I\alpha < 1$) as shown in table 40. The soil and rock samples which may be used for building material will have a radon concentration lower than 200 Bq kg^{-1} and when used for construction of buildings may not poses any radiological health to inhabitants. The internal and external hazard indices are set to limit the radiation dose to the acceptable dose limit to 1 mSvy^{-1} for the members of the public (Hewamanna, Sumithrarachchi, Mahawatte, Nanayakkara, & Ratnayake, 2001).

The radium equivalent activity (R_{aeq}) is related to exposure of both the external γ -dose and the internal γ -dose from radon and its progeny. The obtained results in table 47 shows that the radium equivalent activity (R_{aeq}) of all soil and rock samples from the underground goldmine have values less than the permissible maximum value of 370 Bq/kg (UNSCEAR, 2000) apart from

level 880 (399.62 Bq/kg) which was slightly higher. The permissible maximum value of the radium equivalent activity corresponds to an effective dose of 1mSv yr^{-1} for to the inhabitants of dwellings (Esiolo et al., 2019). Hence soil and rock samples from the underground mine are radiologically safe for construction of buildings.

Table 40: Radium Equivalent Activity and External Level in Rock and Soil Samples

Levels	Raeq (Bq/kg)	I_{γ}
800	302.71	0.42
810	273.42	0.40
840	297.28	0.43
880	399.622	0.53
790	288.4705	0.41
820	338.35	0.44
960	181.57	0.25
1000 YOD	164.48	0.20
920	247.50	0.34
1000 SKY DEC	282.72	0.42
Average	277.61	0.38

Source: Field Data 2019

The Nuclear Energy Agency (NEA) and Organisation for Economic Co-operation and Development (OECD) group of experts suggested some limits for external level index (I_{γ}) for different building materials for the members of the public to be radiologically safe. The limit for materials used in bulk amounts like bricks should be less than 1 ($I_{\gamma} < 1$) and that of superficial and other materials like tiles should be less than 6 ($I_{\gamma} < 6$). The values I_{γ} as shown in table 40 shows that soil and rock samples from the underground mine are

radiologically safe and may be used for bricks and superficial materials such tiles for construction of building.

Table 41: Annual Dose Parameters

Levels	ER mR h ⁻¹	DR mSv yr ⁻¹	Dair nGy h ⁻¹	AEDEind mSv yr ⁻¹	AEDEout mSv yr ⁻¹	AGDE μSv yr ⁻¹	ELCR %
800	63.54	5.29	54.13	0.27	0.07	297.03	0.93
810	70.87	5.90	51.27	0.25	0.06	286.33	0.88
840	71.55	5.96	54.98	0.27	0.07	305.46	0.94
880	67.14	5.59	68.26	0.34	0.08	367.81	1.17
790	63.31	5.27	52.14	0.26	0.06	287.32	0.90
820	57.88	4.82	57.07	0.28	0.07	305.99	0.98
960	20.08	1.67	32.73	0.16	0.04	179.97	0.56
1000 YOD	16.47	1.37	26.19	0.13	0.03	136.96	0.45
920	47.61	3.97	43.47	0.21	0.05	236.87	0.75
1000 SKY DEC	61.52	5.13	53.75	0.26	0.07	301.44	0.92
Average	53.99	4.50	49.40	0.24	0.06	270.52	0.85

Source: Field Data 2019

Concerning exposure rate (ER), in table 41, it was observed that all the soil and rock samples have values less than the criterion of 600 mR h⁻¹ of exposure rate to naturally occurring radioactive materials. The dose rate (DR) due to naturally occurring radioactive materials from the soil and rock samples are lower than the maximum permissible limits (50 mSv yr⁻¹) (Darwish, Abul-Nasr, & El-Khayatt, 2015).

The absorbed gamma dose rate in air 1m above the ground surface (Dair), in soil and rock samples are lower than the permissible maximum limit apart from level 880 (68.26 nGy h⁻¹) and level 820 (57.09 nGy h⁻¹), which recorded a value higher than the population-weighted value of 57 nGy h⁻¹

(Baykara et al., 2011; Hewamanna et al., 2001). However, it may not be advisable to use soil and rock samples from these levels for construction of buildings.

The annual effective dose equivalent (AEDE) measures the risk of stochastic and deterministic effects in the irradiated individuals. The recommended value of the annual effective dose equivalent is 0.48 mSv yr^{-1} and the criterion of the total annual effective dose equivalent (indoors + outdoors) should be less than 1 mSv yr^{-1} (Esiole et al., 2019). The values for both indoor and outdoor annual effective dose equivalent from soil and rock samples were less than the recommended values and the sum of the indoor and outdoor annual effective dose equivalent is less than 1 mSv yr^{-1} . Thus, there may not be any significant radiation effect on individuals who will be exposed to soil and rock samples from the underground mine.

The gonads, the active bone marrow and the bone surface cells are considered to be the organs of importance. An increase in AGDE has been known to affect the bone marrow, causing destruction of the red blood cells that are then replaced by white blood cells. The annual gonadal dose equivalent (AGDE) from soil and rock samples ranged from a minimum of $179.97 \mu\text{Sv yr}^{-1}$ in level 960 to a maximum of $367.81 \mu\text{Sv yr}^{-1}$ in level 880 with a mean of $270.52 \mu\text{Sv yr}^{-1}$ which was less than the standard UNSCEAR value for AGED of 300 mSv yr^{-1} . This shows a low probability of radiation effect on the bone marrow of individuals exposed to the rock and soil samples from the underground mine apart from rocks from level 880.

The excess lifetime cancer risk (ELCR) gives the probability of developing cancer over a lifetime at a given exposure level. The ELCR ranges

from a minimum of 0.45 at level 1000YOD to a maximum of 1.17 at level 880 with a mean of 0.85 are higher than the world's average value of 0.29×10^{-3} (Uosif et al., 2014). Thus, the chance of developing using soil and rock samples from the underground mine is higher as compared to the world average.

Table 42: Correlation Matrix Between Ra-222, Rn-226, Th-232 and K-40

Radionuclides		Ra-222	Rn-226	Th-232	K-40
Ra-222	Pearson	1	0.627	0.594	0.499
	Correlation				
	Sig. (2-tailed)		0.049	0.070	0.142
Ra-226	Pearson	0.627	1	0.911**	0.953**
	Correlation				
	Sig. (2-tailed)	0.049		0.000	0.000
Th-232	Pearson	0.594	0.911**	1	0.872**
	Correlation				
	Sig. (2-tailed)	0.070	0.000		0.001
K-40	Pearson	0.499	0.953**	0.872**	1
	Correlation				
	Sig. (2-tailed)	0.142	0.000	0.001	

** . Correlation is significant at the 0.01 level (2-tailed)

Source: Field Data 2019

The correlation matrix in table 42 describes the type and strength of relationship between the measured Ra-222, Rn-226, Th-232 and K-40 from the rock and soil samples from the underground goldmine. There is a positive correlation between Ra-222, Th-232 and K-40 but there was a moderate positive correlation ($r = 0.627$) between Rn-226 (parent radionuclide) and Ra-222 (daughter radionuclide) and the relationship was statistically significant at the 5% level of significance ($P < 0.05$). The strength of the relationship could be due to the low diffusion coefficient of radon gas in solid grains and it is assumed that the release of radon is mainly due to the recoil process (Yang, Chou, Chen, Chyi, & Jiang, 2003). The matrix also shows that there is no significant relationship between Ra-222, Th-232 and K-40.

There is a strong positive correlation between Rn-226 and Th-232 and K-40 and the relationship was statistically significant at the 1% level of significance ($P < 0.1$) but the relationship between Rn-226 and K-40 ($r = 0.953$) was stronger as compared to the relationship between Rn-226 and Th-232 ($r = 0.911$). The strong correlation between Rn-226 and K-40 explains the higher concentrations of K-40 in the soil and rock samples as compared to Th-232. Also, the strong correlation between Rn-226, Th-232 and K-40 shows that there is a probability of high concentration of Th-232 and K-40 in soils containing high concentration of Rn-226.

Chapter Summary

The radiological impact assessment in the underground mine shows that the activity concentration of radon ranges from a minimum of 2 Bqm^{-3} to a maximum of 284 Bqm^{-3} with a mean value of 58.51 Bqm^{-3} . The highest radon concentration was observed in the second quarter when the season was warm and the lowest radon concentration was observed in the first quarter when the season was colder.

The exposure rate, annual effective dose and excess lung cancer risk were below the acceptable limit.

Principal component analysis deduced three main factors that influence the indoor radon concentration, Barometric Pressure, Relative Humidity and Temperature of which wet bulb temperature was statistically significant.

The hazard indices, exposure rate, excess lung cancer risk and annual effective dose from the rock and soil samples possess no radiological hazard if used for building materials. The time series analysis revealed a positive correlation between radon concentration and depth of the underground mine.

CHAPTER FIVE

SUMMARY, CONCLUSIONS AND RECOMMENDATIONS

Overview

This section entails findings of the research study and draws conclusion. Recommendations are made based on the findings and analysis of data obtained from the field.

Summary

The radiological impact assessment of radon concentration as well as the soil and rock samples show that there is no likelihood of any immediate radiological health hazards to underground goldmine workers, final users of soil and rock samples, and the environment from the exploitation and utilization of. However, due to stochastic effect of radiation and a higher excess cancer risk recorded gives a signal of an increased risk of lung cancer among the underground goldmine workers.

Apart from a good ventilation system in the underground mine environment, one of the principles of radiation protection measures, which is time can be used to reduce the risk of stochastic effect, since some key supervisors spend majority of their time underground. The assumption of the time series model confirms that when good ventilation measures are taken into consideration, depth will cause an insignificant or negligible radon concentration in the underground goldmine.

The analysis from the principal component and factor analyses confirms that the major environmental contributors to the indoor radon concentration is Relative humidity, Barometric pressure and wet bulb temperature. Temperature,

Barometric Pressure and Relative Humidity and its changes have a critical impact on ventilation conditions in the underground workings of deep mines. Changes in pressure are particularly important because they are responsible for the transient states of ventilation conditions, therefore, assessing the scale of pressure change is essential. Keeping an eye on the barometer is critical during mining operations because situations in which the barometric pressure either rises too high or drops too low can create serious safety risks.

The statistical insignificance and low values of radon concentration could be due to the fact that ventilation at the underground goldmine is adequate but a statistical significance of temperature signals that it is a variable that must be of interest to the environmental health and safety department of the mine. It has to be closely monitored to inform if ventilation rate has to be increased to reduce radon concentration in the underground mine. Mine atmospheres contain varying amounts of moisture that can be present at varying temperatures due to prevailing conditions encountered, it then follows that their presence can have effects on a person's safety and their ability to perform hard work.

Conclusions

This study was aimed at assessing the level of indoor radon and naturally occurring radioactive materials in underground goldmine in Ghana.

Radon gas was present within the underground goldmine and the distribution of the radon concentration was positively skewed and platykurtic. The recorded values for all the four quarters are below the reference levels for both homes and workplaces. Generally, the radon soil concentrations at all the locations fall below the reference levels (1000 Bqm^{-3}) set by the international commission for radiological protection (ICRP). The measured radon

concentration will be used as part of a reference data for regulatory authorities to set reference levels for underground workers. The mean activity concentration of naturally occurring radioactive materials (Ra-226, Th-232 and K-40) were below the permissible limit of set by the United Nations Scientific Committee on Atomic Radiation (UNSCEAR) as 35 Bq kg^{-1} , 40 Bq kg^{-1} and 400 Bq kg^{-1} respectively.

The average values of exposure rate to radon daughters was lower than the derived reference level (DRL) of $1 \text{ WLM}\cdot\text{y}^{-1}$ by the international Commission for radiological protection (ICRP) and the National Institute for occupational Safety and Health (NIOSH) as well as $4 \text{ WLM}\cdot\text{y}^{-1}$ by the US Mine Safety and Health Administration regulation. The effective dose received by the underground workers is above the worldwide average dose limit (1.15 mSv y^{-1}) but lies below the suggested benchmark of ICRP (10 mSvy^{-1}) for nations developing radon management strategies but was higher than the annual effective dose of 1 mSvy^{-1} for the members of the public. The Excess Lifetime Cancer Risk (ELCR) was less as compared to the National Council for Radiation Protection and Measurement (NCRP) over the lifetime of any individual exposed to enhanced levels of radon (Pawel & Puskin, 2003). It is also less than the estimated excess lifetime lung cancer risk for continuous exposure at the United States Environmental Protection Agency (US EPA) of 2.3% for the U.S. population, 4.1% for ever-smokers, but higher than 0.73% for never smokers and the worldwide value $0.29 \times 10^{-9} \%$ from UNSCEAR.

A negative relationship was between barometric pressure, wet bulb temperature, air quantity, wet kata temperature and the radon concentration but the relationship was statistically insignificant at the 5% level of significance and

a positive relationship between dry bulb temperature, relative humidity and radon concentration but further statistical analysis using principal component revealed that out of the environmental factors considered for the study the main factors that had influence on the radon concentration in the underground goldmine were wet bulb temperature, barometric pressure and relative humidity of which the wet bulb temperature had a statistical significance at the 5% level of significance.

The trend equation used for the forecasting and prediction of the radon concentration at different depths in the underground goldmine showed a positive relationship with depth from the reference level. It was also observed that only 2.1% variation in radon concentration in the underground mine is explained by the increase in depth from the reference level of the underground mine and 97.9% could be due to other factors that were not considered in the study. Also, the statistical insignificance of the relationship between depth and radon concentration underground and a negative adjusted R^2 shows that increase in depth in the underground goldmine has an insignificant or negligible effect on radon concentration.

The radium equivalent activity, internal and external hazard indices from the soil and rock samples from the underground goldmine may not pose any significant radiological hazard if the soil and rock samples from the underground mine are used for building materials. The values of the external level index (I_{γ}) is also known as the representative level index suggest that if the rock and soil samples will not pose any radiological health effect if they are used for building materials like bricks and tiles. The values of the internal (α -radioactivity) level index (I_{α}) also suggest that when the soil and rock samples

are used for construction of buildings there wouldn't be any risk of excess alpha radiation due to radon inhalation originating from building materials. The exposure rate, dose rate and the indoor and outdoor annual effective dose rate are all below the permissible limit apart from the excess lifetime cancer risk (ELCR) which was higher than the world's average value of 0.29×10^{-3} .

Recommendations

The levels of Radon concentration at the underground gold mine appears to be low but may present a potential long-term health risk to occupationally exposed workers due to stochastic effect of radiation. Nonetheless, as a new underground goldmine, monitoring of indoor radon for deeper levels is recommended. Also, further indoor radon testing after some years would enable a determination of the indoor levels and support the implementation of additional radon gas mitigation measures, if required. This will ensure that the occupationally exposed workers at the underground work with no radon gas health hazard.

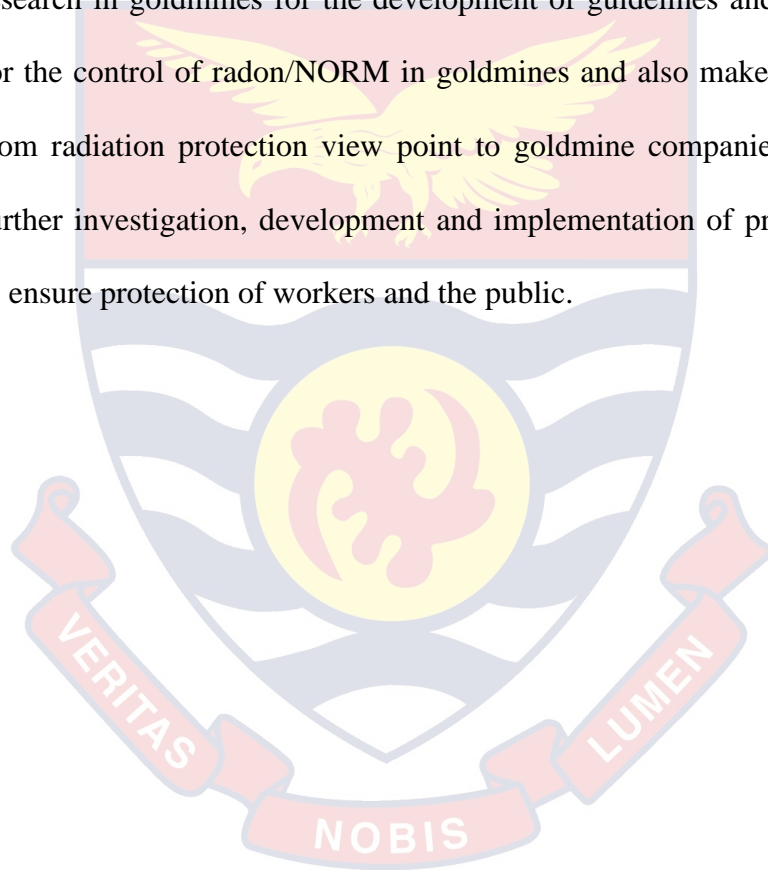
The study also recommends continuous monitoring of indoor radon concentration as well as other influencing factors that has effect on the concentration of indoor radon to help understand the behaviour of radon in the underground environment.

Ventilation rate must be increased at any level that has an elevated radon concentration and underground goldmine workers must be advised on the increased risk of lung cancer in smokers as compared with non- smokers.

Management should organise training and retraining on the health and safety in underground mine environment to help workers abreast themselves with existing and current safety issues.

The rate of ventilation that was pumped in all the 10 levels which lead to the lower concentration of radon gas must be equally considered if the mine decides to explore gold further deep in the underground mine for the radon concentration to be negligible as predicted by the adjusted R^2 in the time series model.

Lastly, Regulatory bodies must encourage Technical Support Organisations (TSO), Research institutions and Universities to conduct further research in goldmines for the development of guidelines and a national policy for the control of radon/NORM in goldmines and also make recommendations from radiation protection view point to goldmine companies on the need for further investigation, development and implementation of protection strategies to ensure protection of workers and the public.



REFERENCES

- 1, I. C. o. R. P. C. (1991). *Risks Associated with Ionising Radiations: Five Papers* (Vol. 22): International Commission on Radiological Protection.
- Adjirackor, T., Darko, E. O., & Sam, F. (2017). Naturally occurring radionuclide transfer from soil to vegetables in some farmlands in Ghana and statistical analysis. *Radiation Protection and Environment*, 40(1), 34.
- Agency, E. P. (1993). EPA 402-R-92-003 Protocols for radon and radon decay product measurements in homes: Washington DC: EPA.
- Agency, I. A. E. (2004). *Occupational radiation protection in the mining and processing of raw materials*: International Atomic Energy Agency.
- Ahmed, N. K. (2005). Measurement of natural radioactivity in building materials in Qena city, Upper Egypt. *Journal of environmental radioactivity*, 83(1), 91-99.
- Ahmed, N. K., & El-Arabi, A. G. M. (2005). Natural radioactivity in farm soil and phosphate fertilizer and its environmental implications in Qena governorate, Upper Egypt. *Journal of environmental radioactivity*, 84(1), 51-64.
- Ahn, G. H., & LEE, J.-K. (2005). Construction of an environmental radon monitoring system using CR-39 nuclear track detectors. *Nuclear Engineering and Technology*, 37(4), 395-400.
- Akhtar, N., Tufail, M., Ashraf, M., & Iqbal, M. M. (2005). Measurement of environmental radioactivity for estimation of radiation exposure from saline soil of Lahore, Pakistan. *Radiation Measurements*, 39(1), 11-14.

- Alonso, N. H., Kotsarenko, A., Yutsis, V., Silva, G. H., Perego, P., Fazio, M., . . .
.Silva, A. C. (2013). Environmental and indoor study of Radon concentration in San Joaquin area, Queretaro, Mexico, first results. *Radiation Measurements*, 50, 149-153.
- Altman, D. G., & Bland, J. M. (2005). Standard deviations and standard errors. *Bmj*, 331(7521), 903.
- Alvarez-Gallego, M., Garcia-Anton, E., Fernandez-Cortes, A., Cuezva, S., & Sanchez-Moral, S. (2015). High radon levels in subterranean environments: monitoring and technical criteria to ensure human safety (case of Castañar cave, Spain). *Journal of environmental radioactivity*, 145, 19-29.
- Appleton, J. (2005). Radon in air and water *Essentials of Medical Geology: Impacts of the Natural Environment on Public Health* ed O Selinus: Amsterdam: Elsevier.
- Appleton, J. D. (2013). Radon in air and water *Essentials of medical geology* (pp. 239-277): Springer.
- Apraku, T. B. (2013). *Soil radon mapping in selected areas of the Ashanti Region of Ghana*. MSc Thesis, Knust.edu.gh.
- Bajwa, B., & Virk, H. (1997). Environmental radon monitoring in dwellings near the radioactive sites. *Amristar-143005, india. radiation measurement*, 26(1), 457-460.
- Baykara, O., Karatepe, Ş., & Doğru, M. (2011). Assessments of natural radioactivity and radiological hazards in construction materials used in Elazig, Turkey. *Radiation Measurements*, 46(1), 153-158.

- Bekteshi, S., Kabashi, S., Ahmetaj, S., Xhafa, B., Hodolli, G., Kadiri, S., . . .
Abdullahu, B. (2017). Radon concentrations and exposure levels in the
Trepça underground mine: A comparative study. *Journal of cleaner
production*, 155, 198-203.
- Bhagwat, A. (1993). Solid state nuclear track detection: theory and applications:
Indian Society for Radiation Physics.
- Biira, S., Kisolo, A. W., & D'ujanga, F. M. (2014). Concentration levels of
radon in mines, industries and dwellings in selected areas of Tororo and
Busia districts, Eastern Uganda. *Adv Appl Sci Res*, 5(6), 31-44.
- Blaauboer, R., & Smetsers, R. (1997). Outdoor concentrations of the
equilibrium-equivalent decay products of ^{222}Rn in the Netherlands and
the effect of meteorological variables. *Radiation Protection Dosimetry*,
69(1), 7-18.
- Board, N. R. C. P. R. (1983). *Snow and Ice Research: An Assessment*: National
Academies.
- Bodansky, D., Robkin, M. A., & Stadler, D. R. (1987). Indoor radon and its
hazards. United State: University of Washington Press.
- Cember, H., Johnson, T. E., & Alaei, P. (2008). Introduction to health physics.
Medical Physics, 35(12), 5959.
- Chancellor, J. C., Blue, R. S., Cengel, K. A., Auñón-Chancellor, S. M., Rubins,
K. H., Katzgraber, H. G., & Kennedy, A. R. (2018). Limitations in
predicting the space radiation health risk for exploration astronauts. *npj
Microgravity*, 4(1), 8.
- Choppin, G., Liljenzin, J.-O., & Rydberg, J. (2002). *Radiochemistry and
nuclear chemistry*: Butterworth-Heinemann.

- Colgan, P., & Gutiérrez, J. (1996). Cost effectiveness of reducing radon exposure in Spanish dwellings. *Journal of Radiological Protection*, 16(3), 181.
- Cooper, D. R., Schindler, P. S., & Sun, J. (2006). *Business research methods* (Vol. 9): McGraw-Hill Irwin New York.
- Coskeran, T., Denman, A. R., Phillips, P. S., & Gillmore, G. K. (2002). A critical comparison of the cost-effectiveness of domestic radon remediation programmes in three counties of England. *Journal of environmental radioactivity*, 62(2), 129-144.
- Council, N. R. (1999a). *Health effects of exposure to radon: BEIR VI* (Vol. 6): National Academies Press.
- Daniels, R. D., & Schubauer-Berigan, M. K. (2017). Radon in US workplaces: a review. *Radiation Protection Dosimetry*, 176(3), 278-286.
- Darko, E., & Faanu, A. (2007). Baseline radioactivity measurements in the vicinity of a gold processing plant. *Journal of Applied Science and Technology*, 12(1), 18-24.
- Darwish, D., Abul-Nasr, K., & El-Khayatt, A. (2015). The assessment of natural radioactivity and its associated radiological hazards and dose parameters in granite samples from South Sinai, Egypt. *Journal of Radiation Research and Applied Sciences*, 8(1), 17-25.
- De Cicco, F., Pugliese, M., Roca, V., & Sabbarese, C. (2013). Track counting and thickness measurement of LR115 radon detectors using a commercial image scanner. *Radiation Protection Dosimetry*, 162(3), 388-393.

- Denman, A., Groves-Kirkby, C., Coskeran, T., Parkinson, S., Phillips, P., & Tornberg, R. (2005). Evaluating the health benefits and cost-effectiveness of the radon remediation programme in domestic properties in Northamptonshire, UK. *Health policy*, 73(2), 139-150.
- Dowdall, A., Fenton, D., & Rafferty, B. (2016). The rate of radon remediation in Ireland 2011–2015: Establishing a base line rate for Ireland's National Radon Control Strategy. *Journal of environmental radioactivity*, 162, 107-112.
- Duffy, J., Madden, J., Mackin, G., McGarry, A., & Colgan, P. (1996). A reconnaissance survey of radon in show caves in Ireland. *Environment International*, 22, 415-423.
- Durante, M., Golubev, A., Park, W.-Y., & Trautmann, C. (2019). Applied nuclear physics at the new high-energy particle accelerator facilities. *Physics Reports*. 800,1-37.
- Durrani, S. A. (1997). *Radon measurements by etched track detectors: applications in radiation protection, earth sciences and the environment*: World Scientific, Singapore, Pp.96-99.
- Durrani, S. A., & Bull, R. K. (2013). *Solid state nuclear track detection: principles, methods and applications* (Vol. 111): Elsevier.
- Eisenbud, M., & Gesell, T. F. (1997). *Environmental radioactivity from natural, industrial and military sources: from natural, industrial and military sources*: Elsevier.
- El-Gamal, A., Nasr, S., & El-Taher, A. (2007). Study of the spatial distribution of natural radioactivity in the upper Egypt Nile River sediments. *Radiation Measurements*, 42(3), 457-465.

- El Galy, M., El Mezayn, A., Said, A., El Mowafy, A., & Mohamed, M. (2008). Distribution and environmental impacts of some radionuclides in sedimentary rocks at Wadi Naseib area, southwest Sinai, Egypt. *Journal of environmental radioactivity*, 99(7), 1075-1082.
- Esiolo, S., Ibeanu, I., Garba, N., & Onoja, M. (2019). Determination of radiological hazard indices from surface soil to individuals in Angwan Kawo Gold Mining Sites, Niger state, Nigeria. *Journal of Applied Sciences and Environmental Management*, 23(8), 1541-1547.
- Faanu, A., Emi-Reynolds, G., Darko, E., Awudu, R., Glover, E., Adukpo, O., . . . Lawluvi, H. (2011). Calibration and Performance Testing of Sodium Iodide, NaI (Tl), Detector at the Food and Environmental Laboratory of the Radiation Protection Institute of the Ghana Atomic Energy Commission. *West African Journal of Applied Ecology*, 19(1).
- Fentiman, A. W., & Hajek, B. K. Joyce E. meredith (2009). *OHIO State university, What Are the Sources of Ionizing Radiation*.
- Field, M. S. (2007). Risks to cavers and cave workers from exposures to low-level ionizing a radiation from ^{222}Rn decay in caves. *Journal of Cave and Karst Studies*, 69(1), 207-228.
- Field, R. W. (1999). Radon occurrence and health risk. *Occupational and Environmental Medicine Secrets, First Edition, Philadelphia, PA, Hanley and Belfus*.
- Fijałkowska-Lichwa, L., & Przylibski, T. A. (2011). Short-term ^{222}Rn activity concentration changes in underground spaces with limited air exchange with the atmosphere. *Natural Hazards and Earth System Sciences*, 11(4), 1179-1188.

- Gazineu, M., & Hazin, C. (2008). Radium and potassium-40 in solid wastes from the oil industry. *Applied radiation and isotopes*, 66(1), 90-94.
- Gillmore, G. K., Sperrin, M., Phillips, P., & Denman, A. (2000). Radon hazards, geology, and exposure of cave users: a case study and some theoretical perspectives. *Ecotoxicology and Environmental Safety*, 46(3), 279-288.
- Gordon, S. (2006). The normal distribution. *Mathematics Learning Centre, University of Sydney. Hal*, 1-41.
- Griffith, R. V., & Tommasino, L. (1990). Etch track detectors in radiation dosimetry. *The dosimetry of ionizing radiation*, 3, 323-426.
- Guides, S. (1989) Radiation Protection Series: International Atomic Energy Agency IAEA, Vienna, Austria. Specific Safety Guide No. SSG 46.
- Guimond, R. (1988). Reducing radon risks: the approach in the United States. *Radiation Protection Dosimetry*, 24(1-4), 483-485.
- Hashim, A. K., Awad, E. I., & Mezher, H. A. (2017). Measurement of annual effective dose for Radon in Kerbala University Campus, Freiha, Iraq. *Iraqi Journal of Public Health*, 1(1), 20-25.
- Health, U. D. o., & Services, H. (1999). Agency for Toxic Substances and Disease Registry-ATSDR.
- Hewamanna, R., Sumithrarachchi, C., Mahawatte, P., Nanayakkara, H., & Ratnayake, H. (2001). Natural radioactivity and gamma dose from Sri Lankan clay bricks used in building construction. *Applied radiation and isotopes*, 54(2), 365-369.
- Hodolli, G., Bekteshi, S., Kadiri, S., Xhafa, B., & Dollani, K. (2015). Radon concentration and gamma exposure in some Kosovo underground mines. *International Journal of Radiation Research*, 13(4), 369-372.

- Hosseini, S., Hassanabadi, H., Akrawy, D., & Zarrinkamar, S. (2018). Alpha-decay half-lives for isotopes of even-even nuclei: A temperature-dependent approach with Woods-Saxon potential. *The European Physical Journal Plus*, 133(1), 7.
- Hussein, A. (2008). Radon in the environment: friend or foe? Proceedings of the 3rd Environmental Physics Conference, Aswan, Egypt.
- Kalsi, P., Ramaswami, A., & Manchanda, V. (2005). Solid state nuclear track detectors and their applications. *BARC Newsletter*, 257, 6-15.
- Kearfott, K., Metzger, R., Kraft, K., & Holbert, K. (1992). Mitigation of elevated indoor radon gas resulting from underground air return usage. *Health physics*, 63(6), 674-680.
- Keith, S., Faroon, O., Roney, N., Scinicariello, F., Wilbur, S., Ingerman, L., . . .
- Kojima, H., & Abe, S. (1988). Measurements of the total and unattached radon daughters in a house. *Radiation Protection Dosimetry*, 24(1-4), 241-244.
- Kotrappa, P., Dua, S., Gupta, P., Pimpale, N., & Khan, A. (1983). Measurement of potential alpha energy concentration of radon and thoron daughters using an electret dosimeter. *Radiation Protection Dosimetry*, 5(1), 49-56.
- Kurnaz, A., Küçükömeroğlu, B., Keser, R., Okumusoglu, N., Korkmaz, F., Karahan, G., & Çevik, U. (2007). Determination of radioactivity levels and hazards of soil and sediment samples in Fırtına Valley (Rize, Turkey). *Applied radiation and isotopes*, 65(11), 1281-1289.
- L'Annunziata, M. F. (2012). *Handbook of radioactivity analysis*: Academic press.

- Lecomte, J.-F., Solomon, S., Takala, J., Jung, T., Strand, P., Murith, C., . . . Janssens, A. (2014). ICRP Publication 126: Radiological Protection against Radon Exposure. *Annals of the ICRP*, 43(3), 5-73.
- Lilley, J. (2013). *Nuclear physics: principles and applications*: John Wiley & Sons.
- Mattsson, S., Johansson, L., & Liniecki, J. (2008). Radiation dose to patients from radiopharmaceuticals. Addendum 3 to ICRP Publication 53. ICRP Publication 106. Approved by the Commission in October 2007. *Annals of the ICRP*, 38(1-2), 1-197.
- McAdam, K., Kimpton, H., Porter, A., Liu, C., Faizi, A., Mola, M., . . . Rodu, B. (2017). Comprehensive survey of radionuclides in contemporary smokeless tobacco products. *Chemistry Central Journal*, 11(1), 131.
- Mohammed, N. (2013). Investigation of ^{238}U and ^{232}Th in rock samples selected from Touria Mountain Omdurman.
- G, Muller., S, Chikkagoudar., S, Chatterjee., DG, Thomas., & TE, Carroll. (2017). *Research Methods for Cyber Security*, 153-173
- Munyaradzi, Z., Anna, K. N., & Makondelele, T. V. (2018). Excess lifetime cancer risk due to natural radioactivity in soils: Case of Karibib town in Namibia. *African Review of Physics*, 13, 71-78.
- Murugesan, S., Mullainathan, S., Ramasamy, V., & Meenakshisundaram, V. (2011). Radioactivity and radiation hazard assessment of Cauvery River, Tamilnadu, India. *Iran J Radiat Res*, 8(4), 211-222.
- Mustafa, A., & Vasisht, C. (1987). Health effects of exposure to indoor radon and its decay products. *Radiation Protection Dosimetry*, 18(3), 179-182.

- Nazaroff, W. W., & Nero, A. V. (1988). Radon and its decay products in indoor air. Wiley, New York.
- NEA-OECD, O. (1979). for EC and D. Ex po sure to Ra di ation from the Nat u ral Ra dio ac tiv ity in Build ing Ma teri als, Re port by a Group of Ex perts of the OECD Nuclear En ergy Agency: OECD, Paris.
- Neingo, P., & Tholana, T. (2016). Trends in productivity in the South African gold mining industry. *Journal of the Southern African Institute of Mining and Metallurgy*, 116(3), 283-290.
- Nero Jr, A. (1985). What we kow about indoor radon. Testimony prepared for hearings on" Radon Contamination: Risk Assessment and Mitigation Research." held by the Subcommittee on Natural Resources. *Agricultural Research and Environmental Committee on Science and Technology, US House of Representatives (Oct. 10. 1985) USGPO. Washington. DC.*
- Nero Jr, A. V. (1990). Radon and its decay products in indoor air. Technical Report LBL-27798, Lawrence Berkeley Laboratory.
- Njinga, R., Tshivhase, V., & Elele, U. (2019). Correlation of gamma emitting radionuclides and radiological health hazards indices around Lancaster dam. *International Journal of Radiation Research*, 17(1), 151-161.
- Njinga, R. L., & Tshivhase, V. M. (2016). Lifetime cancer risk due to gamma radioactivity in soils from Tudor Shaft mine environs, South Africa. *Journal of Radiation Research and Applied Sciences*, 9(3), 310-315.
- Noz, M. E., & Maguire Jr, G. Q. (2007). *Radiation Protection in the Health Sciences:(With Problem Solutions Manual)*: World Scientific Publishing Company.

- O'Brien, K., & Sanna, R. (1976). The distribution of absorbed dose-rates in humans from exposure to environmental gamma rays. *Health physics*, 30(1), 71-78.
- O'Brien, Robert M. (2007). A Caution Regarding Rules of Thumb for Variance Inflation Factors," *Quality and Quantity* 41(5), 673-690.
- Opoku-Ntim, I., Andam, A. B., Roca, V., Fletcher, J., & Akiti, T. (2019). Indoor Radon Concentration and Risk Assessment in Some Dwellings of Obuasi, Mining Town. *Radiation Protection Dosimetry*.
- Pawel, J., & Puskin, J. (2003). EPA assessment of risks from radon in homes. Washington, DC: US Environmental Protection Agency: EPA 402-R-03-003.
- Pflitsch, A., & Piasecki, J. (2003). Detection of an airflow system in Niedzwiedzia (Bear) cave, Kletno, Poland. *Journal of Cave and Karst Studies*, 65(3), 160-173.
- Podstawczyńska, A. (2015). Interrelationship of indoor radon concentration and meteorological parameters in Łódź (Central Poland) case study- preliminary results: Recuperado el.
- Protection, N. C. o. R., & Measurements. (1993). *Limitation of exposure to ionizing radiation*. United States Nuclear Regulatory Commission
- Przylibski, T. A. (1999). Radon concentration changes in the air of two caves in Poland. *Journal of environmental radioactivity*, 45(1), 81-94.
- Quarto, M., Pugliese, M., La Verde, G., Loffredo, F., & Roca, V. (2015). Radon exposure assessment and relative effective dose estimation to inhabitants of Puglia Region, South Italy. *International journal of environmental research and public health*, 12(11), 14948-14957.

- Radvanyi, P., & Villain, J. (2017). The discovery of radioactivity. *Comptes Rendus Physique*, 18(9-10), 544-550.
- Rashed-Nizam, Q., Tafader, M., Zafar, M., Rahman, M., Bhuian AKMSI, K. R., Kamal, M., . . . Alam, M. (2016). Radiological risk analysis of sediment from Kutubdia island, Bangladesh due to natural and anthropogenic radionuclides. *Int J Radiat Res*, 14(4), 273-277.
- Righi, S., & Bruzzi, L. (2006). Natural radioactivity and radon exhalation in building materials used in Italian dwellings. *Journal of environmental radioactivity*, 88(2), 158-170.
- Rowland, R. (1993). Low-level radium retention by the human body: a modification of the ICRP publication 20 retention equation. *Health physics*, 65(5), 507-513.
- Sahu, P., Panigrahi, D.C. & Mishra, D.P. (2016). A comprehensive review on sources of radon and factors affecting radon concentration in underground uranium mines. *EnvironEarth Sci* **75**, 617. <https://doi.org/10.1007/s12665-016-5433-8>.
- Schimmack, U., & Diener, E. (1997). Affect intensity: Separating intensity and frequency in repeatedly measured affect. *Journal of Personality and Social Psychology*, 73(6), 1313.
- Shoeib, M., & Thabayneh, K. (2014). Assessment of natural radiation exposure and radon exhalation rate in various samples of Egyptian building materials. *Journal of Radiation Research and Applied Sciences*, 7(2), 174-181.
- Smith, B. T. (2010). Introduction to radioactivity and radioactive decay: Nuclear Pharmacy. Londres, Pharmaceutical Press.

- Solomon, S., Langroo, R., Lyons, R., & James, J. (1996). Radon exposure to tour guides in Australian show caves. *Environment International*, 22, 409-413.
- Sonnentag, S., & Frese, M. (2002). Performance concepts and performance theory. *Psychological management of individual performance*, 23(1), 3-25.
- Stigler, S. M. (2008). Karl Pearson's theoretical errors and the advances they inspired. *Statistical Science*, 23(2), 261-271.
- Strohmeier, R. (2011). Marie Skłodowska-Curie (1867–1934). *European Women in Chemistry*, 39.
- Taylor, J. R., Dubson, M. A., & Zafiratos, C. D. (2004). *Modern physics for scientists and engineers*: Prentice-Hall.
- Tirmarche, M., Harrison, J., Laurier, D., Paquet, F., Blanchardon, E., & Marsh, J. (2010). ICRP publication 115. *Lung cancer risk from radon and progeny and statement on radon*. *Ann ICRP*, 40(1), 1-64.
- Tufail, M., Ahmad, N., Almakky, S., Zafar, M., & Khan, H. A. (1992). Natural radioactivity in the ceramics used in dwellings as construction material. *Science of the total environment*, 127(3), 243-253.
- Turner, J. (2007). *Atoms, radiation and radiation protection*. 3. comp. rev. and enl. Pp 607; Wiley-VCH; Weinheim (Germany).
- UNSCEAR, S. (2006). *Effects of Ionizing Radiation-United Nations Scientific Committee on the Effects of Atomic Radiation*. UNSCEAR 2000 Report to the General Assembly with Scientific Annexes, United Nations, New York: United Nations Scientific Committee on the Effects of Atomic Radiation.

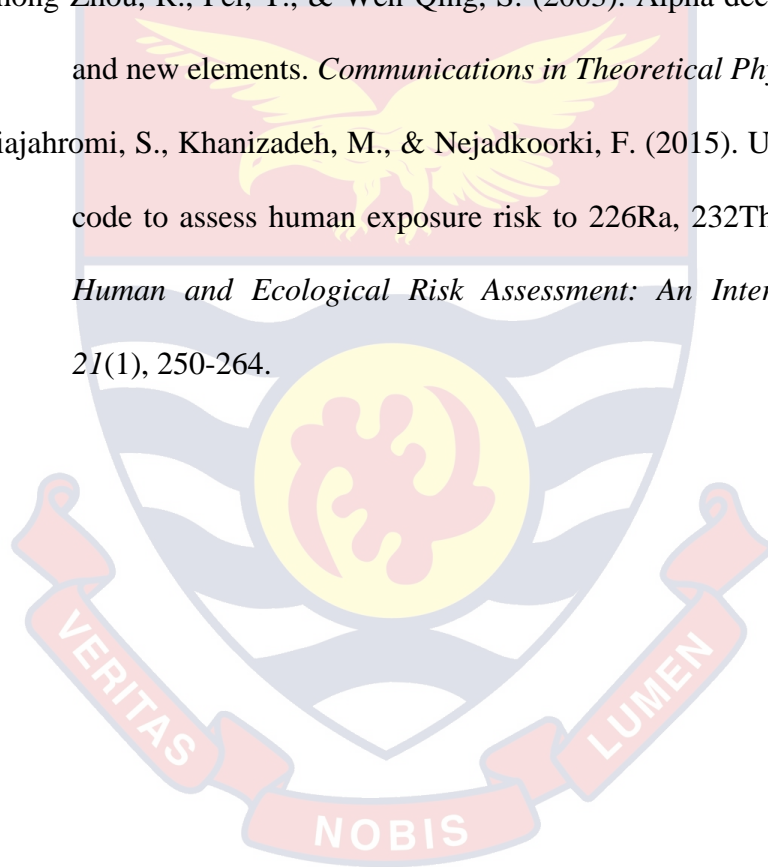
- Uosif, M., Issa, S. A., Ebrahim, A., Zahran, E. M., & Moussa, M. (2014). Determination of natural radioactivity in building raw materials from the quarries of Assiut cement company, Assiut, Egypt. *Int. J. New. Hor. Phys*, 1(1), 25-32.
- Valentin, J. (2007). The 2007 recommendations of the international commission on radiological protection. ICRP publication 103. *Ann ICRP*, 37(2), 1-332.
- Vaupoti, J., Csige, I., Radolić, V., Hunyadi, I., Planinić, J., & Kobal, I. (2001). Methodology of radon monitoring and dose estimates in Postojna Cave, Slovenia. *Health physics*, 80(2), 142-147.
- Veiga, L., Melo, V., Koifman, S., & Amaral, E. (2004). High radon exposure in a Brazilian underground coal mine. *Journal of Radiological Protection*, 24(3), 295.
- Vernon, H., & Warner, C. (1932). The influence of the humidity of the air on capacity for work at high temperatures. *Epidemiology & Infection*, 32(3), 431-462.
- Vogiannis, E. G., & Nikolopoulos, D. (2015). Radon sources and associated risk in terms of exposure and dose. *Frontiers in public health*, 2, 207.
- Wilkes, A., & Williams, D. (2018). Measurement of humidity. *Anaesthesia & Intensive Care Medicine*, 19(4), 198-201.
- Wilks, D. S. (2011). *Statistical methods in the atmospheric sciences* (Vol. 100): Academic press.

Xie, D., Liao, M., Wang, H., & Kearfott, K. J. (2017). A study of diurnal and short-term variations of indoor radon concentrations at the University of Michigan, USA and their correlations with environmental factors. *Indoor and Built Environment*, 26(8), 1051-1061.

Yu, K., Cheung, T., Guan, Z., Young, E., Mui, B., & Wong, Y. (1999). Concentrations of ^{222}Rn , ^{220}Rn and their progeny in residences in Hong Kong. *Journal of environmental radioactivity*, 45(3), 291-308.

Zhong-Zhou, R., Fei, T., & Wen-Qing, S. (2003). Alpha decay, shell structure, and new elements. *Communications in Theoretical Physics*, 40(2), 191.

Ziajahromi, S., Khanizadeh, M., & Nejadkoorki, F. (2015). Using the RESRAD code to assess human exposure risk to ^{226}Ra , ^{232}Th , and ^{40}K in soil. *Human and Ecological Risk Assessment: An International Journal*, 21(1), 250-264.



APPENDICES

APPENDIX A

RADON CONCENTRATIONS OF FIRST TO FOURTH QUARTER

Table 1: Radon Concentrations at Locations for First Quarter

Location	Level	Block	Reg. No.	Radon Concentration Min-Max (Bqm ⁻³)	Radon Concentration Mean (Bqm ⁻³)
S1	800	EMP	L800 E 03	4.25-47.73	28.97±16.22
S2	810	YOD	810-02	4.45-22.34	9.48±5.90
S3	840	YOD	L804-39	2.10-40.50	14.71±15.42
S4	880	YOD	880-04	5.58-49.25	36.75±15.67
S5	790	EMP	L790 E 02	4.49-37.76	21.27±13.62
	EXPL				
S6	820	SKY ACCN	SKY26	2.71-14.37	6.90±4.12
S7	960	YOD	960-09	2.59-12.38	8.39±3.63
S8	1000	SKY DEC	SKY-08	2.14-43.38	14.37±14.45
S9	920	YOD	920E-01	3.80-43.87	23.08±13.37
S10	1000	YOD	L100018	3.32-50.42	22.69±19.15
Average ± SD				2.10-50.42	19.08±15.49

Table 2: Radon Concentrations at Locations for Second Quarter

Location	Level	Block	Reg. No.	Radon Concentration Min-Max (Bqm ⁻³)	Radon Concentration Mean (Bqm ⁻³)
S1	800	EMP	L800 E 03	39.92-176.37	112.09±54.23
S2	810	YOD	810-02	45.77-232.27	137.09±73.50
S3	840	YOD	L804-39	24.46-143.56	101.65±41.49
S4	880	YOD	880-04	66.45-267.91	141.05±75.25
S5	790 EXPL	EMP	L790 E 02	32.68-151.84	94.46±51.08
S6	820	SKY ACCN	SKY26	175.72-182.49	177.68±3.25
S7	960	YOD	960-09	55.04-173.28	97.05±45.10
S8	1000	SKY DEC	SKY-08	55.04-147.24	93.58±38.57
S9	920	YOD	920E-01	94.63-193.87	130.74±43.01
S10	1000	YOD	L100018	112.84-238.67	167.86±57.74
Average ± SD				24.46-283.76	123.64±55.78

Table 3: Radon Concentrations at Locations for Third Quarter

Location	Level	Block	Reg. No.	Radon Concentration Min-Max (Bqm ⁻³)	Radon Concentration Mean (Bqm ⁻³)
S1	800	EMP	L800 E 03	36.00-111.00	61.61±42.71
S2	810	YOD	810-02	31.00-141.00	89.84±41.12
S3	840	YOD	L804-39	68.00-195.00	115.89±50.55
S4	880	YOD	880-04	56.00-186.00	105.22±54.62
S5	790	EMP	L790 E 02	63.00-96.00	74.57±13.90
	EXPL				
S6	820	SKY ACCN	SKY26	40.00-151.00	97.45±62.06
S7	960	YOD	960-09	41.00-127.00	71.74±41.42
S8	1000	SKY DEC	SKY-08	34.00-185.00	95.17±59.66
S9	920	YOD	920E-01	33.00-72.00	53.92±15.91
S10	1000	YOD	L100018	40.00-166.00	91.13±56.75
Average ± SD				31.00-195.00	86.60±46.03

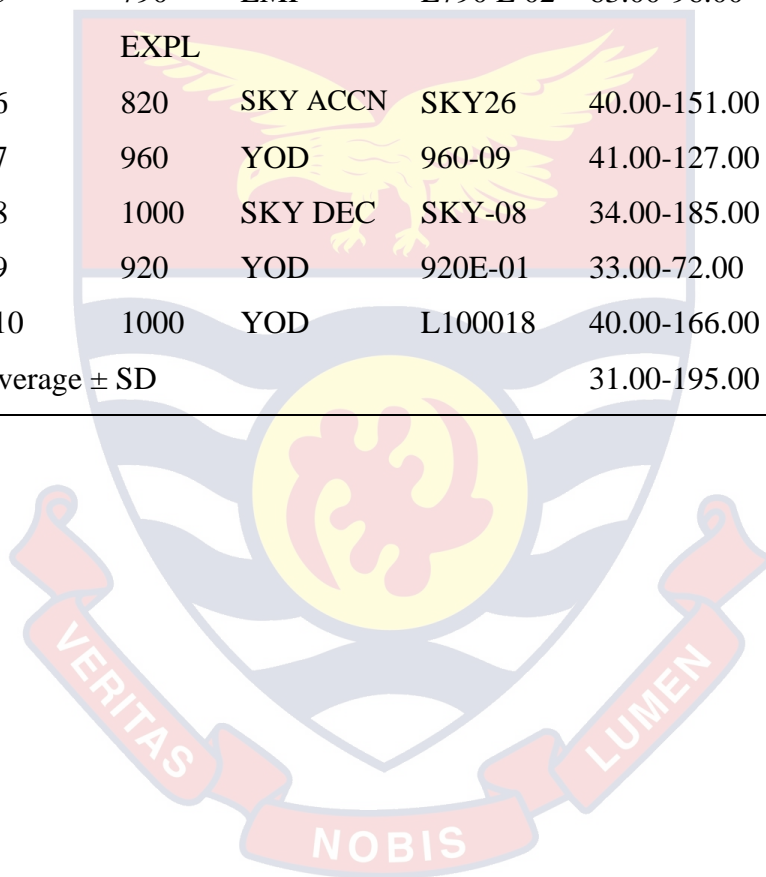
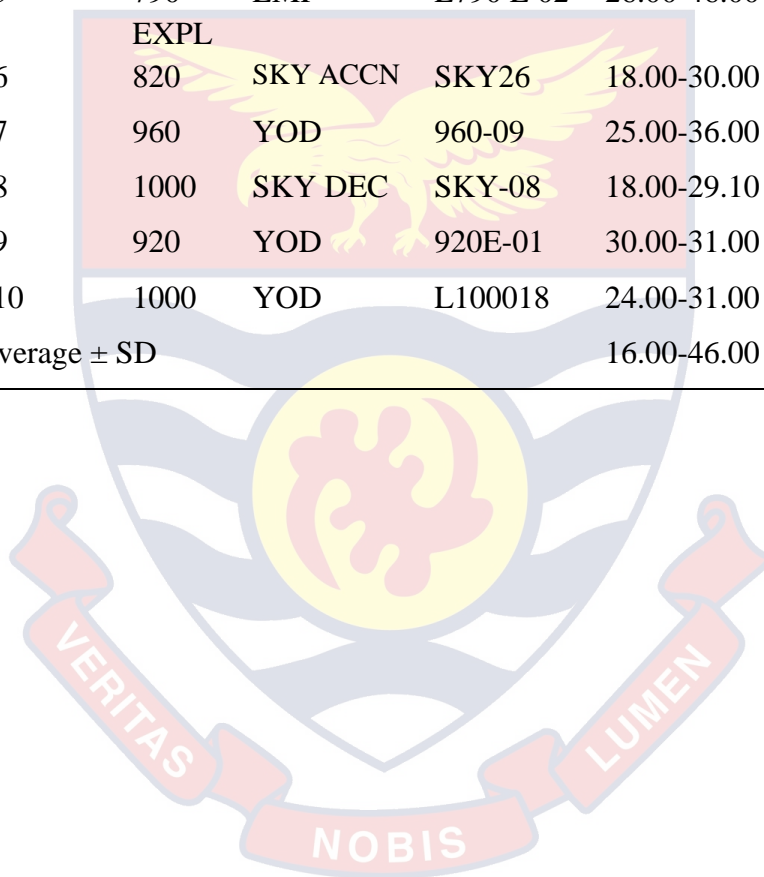


Table 4: Radon Concentrations at Locations for Fourth Quarter

Location	Level	Block	Reg. No.	Radon Concentration Min-Max (Bqm ⁻³)	Radon Concentration Mean (Bqm ⁻³)
S1	800	EMP	L800 E 03	25.00-44.00	32.99±6.30
S2	810	YOD	810-02	18.00-30.00	22.57±4.60
S3	840	YOD	L804-39	16.00-27.00	22.79±4.59
S4	880	YOD	880-04	21.00-38.00	28.97±6.10
S5	790	EMP	L790 E 02	26.00-46.00	34.13±7.68
S6	820	EXPL SKY ACCN	SKY26	18.00-30.00	26.30±3.78
S7	960	YOD	960-09	25.00-36.00	28.99±3.66
S8	1000	SKY DEC	SKY-08	18.00-29.10	24.58±3.63
S9	920	YOD	920E-01	30.00-31.00	29.95±0.40
S10	1000	YOD	L100018	24.00-31.00	28.04±2.39
Average ± SD				16.00-46.00	27.78±5.86



APPENDIX B

EFFECT OF ENVIRONMENTAL FACTORS ON RADON
CONCENTRATION

Location	Level	RC (Bqm ⁻³) Y	BP X1 (kPa)	WBT X2 (°C)	DBT X3 (°C)	RH X4 %	AQ X5 (m ³ /s)	WKT X6 (mcal/cm ² s)
S1	800	28.97	101.7	31.2	32.0	90.4	32.0	18.3
S2	810	9.48	101.6	27.9	29.4	91.5	32.1	18.3
S3	840	14.71	100.1	28.8	32.6	78.1	10.3	11.0
S4	880	36.75	100.7	28.8	32.0	85.1	7.1	8.7
S5	790	21.27	101.8	28.4	31.0	82.1	16.0	15.0
S6	820	6.90	101.5	27.9	30.3	87.6	12.0	12.7
S7	960	8.39	99.9	29.1	32.0	84.4	9.4	15.0
S8	1000	14.37	102.5	29.7	33.1	82.6	15.5	8.3
YOD								
S9	920	23.08	100.4	29.2	32.5	82.9	33.7	9.7
S10	1000	22.69	101.7	30.0	32.5	86.3	33.7	7.8
SKY								
DEC								
S1	800	112.09	101.7	29.5	30.9	92.8	2.8	8.3
S2	810	137.09	101.6	24.6	27.7	83.3	13.4	26.4
S3	840	101.65	102.3	27.7	31.7	93.8	8.3	9.6
S4	880	141.05	100.7	29.5	32.5	84.0	9.6	15.0
S5	790	94.46	101.8	27.8	30.1	88.4	3.6	9.2
S6	820	177.68	101.5	27.9	30.3	87.6	12.0	12.7
S7	960	97.05	99.9	27.5	28.3	97.9	11.5	21.1
S8	1000	93.58	99.5	26.5	28.2	90.8	5.9	9.2
YOD								
S9	920	130.74	100.4	27.4	30.7	81.9	22.2	16.5
S10	1000	167.86	99.5	25.1	27.7	90.8	31.9	16.5
SKY								
DEC								
S1	800	61.61	101.7	29.5	32.2	85.6	12.5	20.7
S2	810	89.84	101.6	24.6	27.7	83.3	13.4	26.4

S3	840	115.89	100.1	28.5	32.0	82.0	13.2	12.7
S4	880	105.22	100.7	29.5	32.5	84.0	9.6	15.0
S5	790	74.57	101.8	32.0	32.5	96.5	11.0	12.7
S6	820	97.45	101.5	29.5	32.4	84.1	12.4	18.3
S7	960	71.74	99.9	27.5	28.3	97.9	11.5	21.1
S8	1000	95.17	100.4	28.4	33.0	90.3	6.2	9.1
	YOD							
S9	920	53.92	100.4	29.8	31.3	89.1	4.1	7.5
S10	1000	91.13	99.5	25.1	27.7	90.8	31.9	16.5
	SKY							
	DEC							
S1	800	32.99	101.7	29.4	31.9	85.9	25.3	19.2
S2	810	22.57	101.6	27.8	31.3	81.1	17.6	19.2
S3	840	22.79	102.3	27.7	31.0	82.5	18.2	17.6
S4	880	28.97	100.7	29.5	32.5	84.0	9.6	15.0
S5	790	34.13	101.3	29.8	31.0	92.9	13.3	26.4
S6	820	26.30	101.5	27.9	30.3	82.1	12.0	12.7
S7	960	28.99	101.6	27.5	28.3	97.9	11.5	21.1
S8	1000	24.58	101.7	27.8	31.3	81.1	17.6	19.2
	YOD							
S9	920	29.95	100.4	30.0	31.0	94.3	5.5	8.8
S10	1000	28.04	101.8	28.0	31.8	88.2	31.8	21.1
	SKY							
	DEC							

APPENDIX C

ACTIVITY CONCENTRATION FOR ROCK AND SOIL SAMPLES

#	Sample ID	Concentration Bq/kg		
		226Ra	232Th	40K
1	S1	36.0 ± 2.5	42.6 ± 1.4	267.6 ± 6.9
2	S1	32.2 ± 1.8	41.4 ± 1.5	253.6 ± 4.7
3	S1	33.8 ± 1.8	46.5 ± 2.5	278.3 ± 3.9
4	S1	34.5 ± 1.4	44.8 ± 1.8	270.2 ± 5.1
5	S2	33.8 ± 1.8	46.0 ± 1.6	265.8 ± 2.1
6	S2	31.0 ± 1.0	40.3 ± 1.5	252.0 ± 41.9
7	S2	32.4 ± 1.5	42.2 ± 1.9	223.3 ± 3.1
8	S2	30.5 ± 1.7	44.2 ± 1.4	233.4 ± 2.4
9	S3	32.9 ± 1.8	45.4 ± 2.4	280.4 ± 5.0
10	S3	34.2 ± 1.6	45.9 ± 2.8	245.4 ± 4.6
11	S3	35.7 ± 1.8	46.6 ± 2.7	248.3 ± 5.8
12	S3	31.4 ± 1.9	47.5 ± 1.9	251.6 ± 3.5
13	S4	41.4 ± 1.5	48.6 ± 0.2	358.5 ± 10.7
14	S4	49.9 ± 2.0	54.5 ± 0.4	385.4 ± 6.2
15	S4	46.7 ± 1.2	55.9 ± 0.9	354.0 ± 1.8
16	S4	42.5 ± 1.8	48.6 ± 0.7	358.1 ± 12.5
17	S5	34.2 ± 1.4	41.2 ± 1.4	244.1 ± 2.4
18	S5	33.1 ± 1.1	44.1 ± 2.5	253.2 ± 3.1
19	S5	30.9 ± 0.9	42.2 ± 1.7	246.8 ± 5.3
20	S5	32.0 ± 1.2	43.6 ± 1.8	267.6 ± 4.9

21	S6	35.3 ± 1.0	39.1 ± 2.8	302.5 ± 3.8
22	S6	37.4 ± 1.4	45.2 ± 1.1	308.7 ± 4.4
23	S6	36.8 ± 1.2	40.5 ± 1.8	321 ± 5.1
24	S6	38.6 ± 1.6	49.2 ± 1.3	310.0 ± 2.7
25	S7	25.3 ± 1.4	21.7 ± 1.3	145.4 ± 6.5
26	S7	24.8 ± 1.9	27.1 ± 1.4	155.1 ± 3.9
27	S7	26.7 ± 1.4	20.8 ± 1.0	149.8 ± 10.3
28	S7	24.4 ± 1.3	23.0 ± 1.1	189.5 ± 9.5
29	S8	19.1 ± 0.8	20.9 ± 0.9	185.4 ± 6.2
30	S8	18.9 ± 0.5	16.3 ± 1.3	169.5 ± 2.2
31	S8	16.8 ± 1.0	17.5 ± 1.5	102.4 ± 5.2
32	S8	20.9 ± 0.5	15.7 ± 1.3	168.1 ± 7.8
33	S9	26.7 ± 0.9	35.1 ± 1.4	214.4 ± 5.6
34	S9	29.2 ± 1.1	34.5 ± 1.8	215.7 ± 4.6
35	S9	27.4 ± 1.2	32.5 ± 1.5	220.5 ± 5.1
36	S9	28.6 ± 1.4	35.2 ± 1.7	234.8 ± 6.6
37	S10	34.4 ± 1.9	40.1 ± 1.5	250.4 ± 13.1
38	S10	33.4 ± 1.4	45.8 ± 2.3	230.7 ± 1.3
39	S10	38.0 ± 1.0	46.7 ± 1.1	235.2 ± 9.3
40	S10	35.8 ± 1.6	44.0 ± 1.4	240.5 ± 3.7